TESIS DE DOCTORADO

# ENDOGENOUS SYSTEMS INVOLVED IN THE DEVELOPMENT OF PANCREATIC CANCER: ROLE OF THE OBESTATIN/GPR39 SYSTEM

Lara Sofía Estévez Pérez

**ESCUELA DE DOCTORADO INTERNACIONAL**

**PROGRAMA DE DOCTORADO EN ENDOCRINOLOGÍA**

SANTIAGO DE COMPOSTELA

2018

# DECLARACIÓN DEL AUTOR DE LA TESIS

### Endogenous systems involved in the development of pancreatic cancer: role of the obestatin/GPR39 system

**Dña.** Lara Sofía Estévez Pérez

*Presento mi tesis, siguiendo el procedimiento adecuado al Reglamento, y declaro que:*

1) *La tesis abarca los resultados de la elaboración de mi trabajo.*
2) *En su caso, en la tesis se hace referencia a las colaboraciones que tuvo este trabajo.*
3) *La tesis es la versión definitiva presentada para su defensa y coincide con la versión enviada en formato electrónico.*
4) *Confirmo que la tesis no incurre en ningún tipo de plagio de otros autores ni de trabajos presentados por mí para la obtención de otros títulos.*

En Santiago de Compostela, Octubre de 2018

Fdo. Lara Sofía Estévez Pérez

# AUTORIZACIÓN DEL DIRECTOR / TUTOR DE LA TESIS
## Endogenous systems involved in the development of pancreatic cancer: role of the obestatin/GPR39 system

Dña. Yolanda Pazos Randulfe
D. Juan Enrique Domínguez Muñoz
Dña. Rosalía Gallego Gómez

INFORMAN:

*Que la presente tesis, corresponde con el trabajo realizado por Dña.* **Lara Sofía Estévez Pérez**, *bajo mi dirección, y autorizo su presentación, considerando que reúne los requisitos exigidos en el Reglamento de Estudios de Doctorado de la USC, y que como director de ésta no incurre en las causas de abstención establecidas en Ley 40/2015.*

*En Santiago de Compostela, Octubre de 2018*

Fdo. Dra. Yolanda Pazos Randulfe             Fdo. Dra. Rosalía Gallego Gómez

Fdo. Dr. J. Enrique Domínguez Muñoz

La doctoranda Lara Sofía Estévez Pérez declara no tener ningún conflicto de interés en relación con la tesis de doctorado.

Santiago de Compostela, Octubre de 2018.

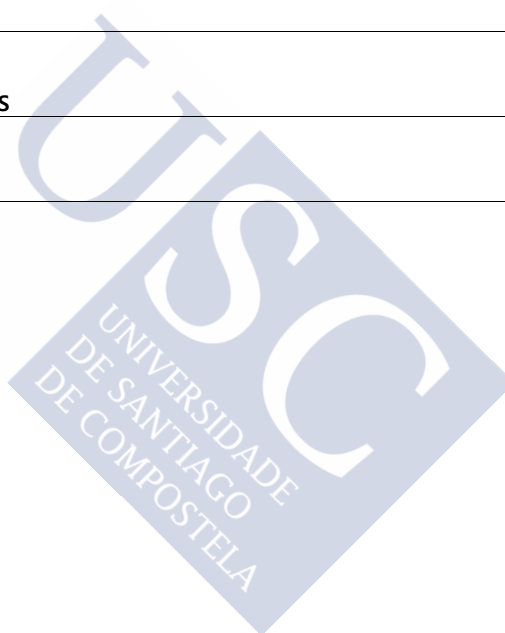Fdo. Lara Sofía Estévez Pérez

A mis padres
Magdalena y Moncho

# INDEX

# ABSTRACT

ABSTRACT

Pancreatic cancer is one of the most aggressive neoplasms due to its rapid spread and late diagnosis. The objective of this thesis is to elucidate the obestatin/GPR39 potential as a therapeutic target in chronic pancreatitis and pancreatic cancer. The expression of GPR39 found in normal pancreas indicates a possible regulatory and regenerative role for the obestatin/GPR39 system in the human pancreas. Likewise, the expression found in premalignant lesions could involve this system in the pathogenesis and progression to pancreatic adenocarcinoma. In addition, this system favours proliferative, invasive and tumoral settlement processes in immortalized cancer cell lines. These facts prompted us to postulate the use of GPR39 as a marker of tumoral progression and its applicability to antagonize the fundamental mechanisms associated with the development of pancreatic cancer.

Keywords: obestatin, GPR39, pancreatic cancer, chronic pancreatitis, regeneration.

RESUMO

O cancro de páncreas é un dos neoplasmas máis agresivos debido á súa rápida difusión e diagnose tardía. O obxectivo desta tese é esclarecer o papel do sistema obestatina/GPR39 como potencial marcador prognose e axente terapéutico en pancreatite crónica e cancro de páncreas. A expresión de GPR39 achada no páncreas normal, indica un posible papel regulador e rexenerativo do sistema obestatina/GPR39 no páncreas humano. Así mesmo, a expresión atopada nas lesións premalignas podería implicar a este sistema na patoxénese e progresión cara ao

adenocarcinoma pancreático. Por outra banda, o devandito sistema favorece procesos proliferativos, invasivos e de asentamento tumoral en liñas canceríxenas inmortalizadas. Isto lévanos a postular o uso de GPR39 como un marcador de progresión tumoral e a súa aplicabilidade para antagonizar os procesos básicos asociados ao desenvolvemento do cancro de páncreas.

Palabras chave: obestatina, GPR39, cancro de páncreas, pancreatite crónica, rexeneración.

RESUMEN

El cáncer de páncreas es una de las neoplasias más agresivas debido a su rápida difusión y diagnóstico tardío. El objetivo de esta tesis es dilucidar el papel del sistema obestatina/GPR39 como potencial marcador diagnóstico y agente terapéutico en pancreatitis crónica y cáncer de páncreas. La expresión de GPR39 hallada en el páncreas normal, indica un posible papel regulador y regenerativo del sistema obestatina/GPR39 en el páncreas humano. Asimismo, la expresión hallada en lesiones premalignas podría implicar a este sistema en la patogénesis y progresión hacia el adenocarcinoma pancreático. Además, este sistema favorece procesos proliferativos, invasivos y de asentamiento tumoral en líneas cancerígenas inmortalizadas. Ello nos lleva a postular el uso de GPR39 como un marcador de progresión tumoral y su aplicabilidad para antagonizar los procesos básicos asociados al desarrollo del cáncer de páncreas.

Palabras clave: obestatina, GPR39, cáncer de páncreas, pancreatitis crónica, regeneración.

# ABBREVIATIONS

**7TM:** 7 transmembrane
**ABC:** ATP-binding cassette
**ABCG2:** ATP-binding cassette sub-family G member 2
**ADRP:** Adipose differentiation-related protein
**Akt:** Serine/threonine kinase (protein kinase B)
**ALK:** Anaplastic lymphoma kinase
**Alpha4GNT:** Alpha1,4-N-acetylglucosaminyltransferase
**AMP:** Adenosine monophosphate
**ANOVA:** Analysis of variance
**aPSCs:** Activated pancreatic stellate cells
**ATCC:** American type culture collection
**Bcrp1:** Breakpoint cluster region pseudogene 1
**BrdU:** Bromodeoxiuridine
**BSA:** Bovine serum albumin
**CA19-9:** Carbohydrate antigen 19-9
**CAF:** Cancer-associated fibroblast
**CC2:** Chamber slides covered with cell conditioning solution 2
**cDNA:** Complementary DNA
**CEACAM-1:** Carcinoembryonic antigen related cell adhesion molecule 1
**CK:** Cytokeratins
**CM:** Conditioned medium
**CP:** Chronic pancreatitis
**CREB:** cAMP response element-binding
**DAB:** 3,3'-Diaminobenzidine
**DA-OB:** Deamidated obestatin
**DAPI:** 4 ',6-diamino-2-fenilindol
**DNA:** Deoxyribonucleic acid
**DUPAN-2:** Duke pancreatic monoclonal antigen type 2
**Dvl2:** Dishevelled segment polarity protein 2
**ECACC:** European collection of authenticated cell cultures
**ECM:** Extracellular matrix components
**EGF:** Epidermal growth factor
**EGFR:** Epidermal growth factor receptor

**EGFRvIII:** Epidermal growth factor receptor variant III
**ELISA:** Enzyme-linked immunosorbent assay
**EMA:** Epithelial membrane antigen
**EMP:** Epithelial-mesenchymal plasticity
**EMT:** Epithelial-mesenchymal transition
**ERAD:** Endoplasmic reticulum-associated degradation
**ERK1/2:** Extracellular signal-regulated kinase-1/2
**ESCC:** Esophageal squamous cell carcinoma
**FAK:** Focal adhesion kinase
**FBS:** Foetal bovine serum
**FFPE:** Formalin-fixed paraffin-embedded
**FGFR2:** Fibroblast growth factor receptor 2
**Flk1/VEGF:** Receptor for vascular endothelial growth factor
**FRK:** Fyn-related kinase
**GAPDH:** Glyceraldehyde-3-phosphate dehydrogenase
**GAS6:** Growth arrest-specific factor 6
**GFAP:** Glial fibrillary acidic protein
**GHS-R:** Growth hormone secretagogue receptor
**GPCR:** G protein-coupled receptors
**GPR39:** G protein-coupled receptor 39
**GSK-3:** Glycogen synthase kinase 3
**Hck:** Hemopoietic cell kinase
**HGFR:** Hepatocyte growth factor receptor
**HHS:** Harris haematoxylin solution
**HIF-1α:** Hypoxia-inducible factor 1-α
**HM:** Hydrophobic motif
**HRP:** Horseradish peroxidase
**hRPE:** Human retinal pigment epithelial
**HSCs:** Hepatic stellate cells
**HSP 27:** Heat shock protein 27
**HSP47:** Heat shock protein 47
**IF:** Immunofluorescence
**IGF-1R:** Insulin-like growth factor 1 (IGF-1)

**IgG:** Immunoglobulin G
**IHC:** Immunohistochemistry
**IPMN:** Intraductal papillary mucinous neoplasm
**ISCs:** Islet stellate cells
**ITK:** Interleukin-2-inducible T-cell kinase
**JAK:** Janus kinase
**JNK:** c-Jun N-terminal kinases
**LC3:** Microtubule-associated protein 1A/1B-light chain 3
**LCK:** Lymphocyte-specific *protein* tyrosine kinase
**LTK:** Leukocyte tyrosine kinase
**MAPK:** Mitogen-activated protein kinase
**MATK:** Megakaryocyte-associated tyrosine kinase
**MCN:** Mucinous cystic neoplasm
**M-CSF1R:** Macrophage colony stimulating factor 1 receptor
**MD:** Moderately differentiated
**MEK:** Mitogen-activated protein kinases
**MET:** Mesenchymal-epithelial transition
**Mhrt:** Myosin heavy chain associated RNA transcript
**MIC-1:** Macrophage inhibitory cytokine 1
**MKK:** Mitogen-activated protein kinase kinase
**mLST8:** Mammalian lethal with SEC13 protein 8
**MMPs:** Matrix metalloproteinases
**mRNA:** Messenger RNA
**mSin1:** Mitogen-activated protein kinase associated protein 1
**MTOC:** Microtubule-organizing centre
**mTOR:** Mammalian target of rapamycin
**mTORC2:** Mammalian target of rapamycin complex 2
**MUSK:** Muscle-specific kinase
**Neg:** Negative
**NGFR:** Nerve growth factor receptor
**NMR:** Nuclear magnetic resonance
**Nrf2:** NF-E2-related factor 2
**ON:** Overnight
**PanIN:** Pancreatic intraepithelial neoplasia
**PARD3:** Partitioning defective 3 homolog

**PBS:** Phosphate buffered saline
**PBST:** BSA in PBS containing Tween-20
**PC:** Pancreatic cancer
**PCR:** Polymerase chain reaction
**PCP:** Planar cell polarity
**PD:** Poorly differentiated
**PDAC:** Pancreatic ductal adenocarcinoma
**PDK1:** 3-phosphoinositide-dependent protein kinase-1
**PEDF:** Pigment epithelium-derived factor
**PFA-PBS:** Paraformaldehyde buffered with PBS
**PI3K:** Phosphatidylinositol-4,5-bisphosphate 3-kinase
**PKC-δ:** Protein kinase C delta type
**PKC-ε:** Protein kinase C epsilon type
**POS:** Position
**PPY:** Pancreatic polypeptide
**PSCs:** Pancreatic stellate cells
**qPCR:** Quantitative polymerase chain reaction
**qPSC:** Quiescent pancreatic stellate cells
**RICTOR:** Rapamycin-insensitive companion of mammalian target of rapamycin
**RNA:** Ribonucleic acid
**ROR:** receptor tyrosine kinase-like orphan receptor
**ROR-1:** Receptor tyrosine kinase-like orphan receptor 1
**RSK:** Ribosomal s6 kinase
**RT:** Room temperature
**RTK:** Receptor tyrosine kinase
**RT-PCR:** Real time PCR
**RTU:** Ready to use
**RYK:** Related to receptor tyrosine kinase
**S/Ser:** Serine
**SCFR:** Recombinant stem cell factor receptor
**SDS:** Sodium dodecyl sulphate
**sEGFR:** Soluble epidermal growth factor receptor
**SEM:** Standard error of mean
**SFKs:** Src family kinases
**siRNA:** Small interfering RNA
**SQSTM1:** Sequestosome-1

**SRMS:** Src-related kinase lacking C-terminal regulatory tyrosine and N-terminal myristylation sites
**SS:** Somatostatin
**SYK:** Spleen tyrosine kinase
**TIE1:** Tyrosine kinase with immunoglobulin-like and EGF-like domains 1
**TIMPs:** Tissue inhibitors of metalloproteinases
**TNK1:** Tyrosine kinase non receptor 1
**TNM:** Tumour, node and metastasis cancer classification

**TOR:** Target of rapamycin
**TrkB:** Tropomyosin receptor kinase B
**TYRO10/DDR2**: Discoidin domain-containing receptor 2 precursor
**VA-lip:** Vitamin A-coupled liposomes
**VEGF:** Vascular endothelial growth factor
**VEGFR2:** Vascular endothelial growth factor receptor 2
**WB:** Western blot
**WD:** Well differentiated
**α-SMA:** α smooth muscle actin

# INTRODUCTION

# THE HUMAN PANCREAS

The pancreas is an unpaired organ located in the left superior retroperitoneum that includes an exocrine and an endocrine portion. The exocrine pancreas makes and secretes digestive enzymes into the duodenum, this includes acinar and duct cells with associated connective tissue, vessels, and nerves. The endocrine unit is composed by the Langerhans islets. The human pancreatic tissue is rarely resected thus are few opportunities for pathologists to observe the normal histology. The gland quickly autolysis, and the non-neoplastic parenchyma adjacent to resected neoplasms usually has substantial obstructive changes. For this reason, minor histologic alterations or even normal structures may not be accurately recognized[1].

## MACROSCOPIC FEATURES

The human adult pancreas measures around 15 to 20 cm in length, 4 to 5 cm in width and is composed by four anatomic regions (the head, neck, body, and tail) which are grossly indistinct (**Diagram 1**). The bulk of the organ is composed of the head. The neck of the pancreas is the short constricted area that rests anterior to the mesenteric vessels. The neck and body are somewhat triangular in cross section, whereas the tail flattens out as it approaches the spleen[2].

---

[1] Klimstra DS, Hruban RH & Pitman MB. (2012). Pancreas. In Mills, Stacey E. (Ed.), *Histology for Pathologists*. (4th ed., pp. 778-816). PA: Philadelphia. Lippincott Williams & Wilkins.
[2] Moore KL. (1980). *Clinically oriented anatomy*. Baltimore. MD: Williams & Wilkins.
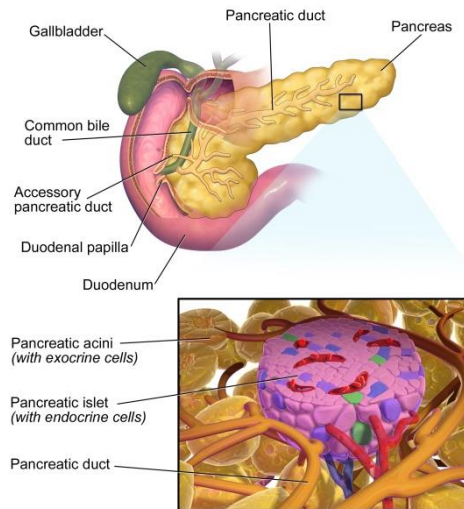
**Diagram 1.** Schematic diagram of the pancreas showing the major ducts and a detail of exocrine and endocrine pancreas. The pancreatic exocrine function involves the acinar cells secreting digestive enzymes. The endocrine function involves the secretion of hormones within the pancreatic islets.

## MICROSCOPIC FEATURES

Microscopically the human pancreas is arranged in 1 to 10 mm lobules. The parenchyma consists almost entirely of the epithelial elements, including, mostly, the acini, the ducts, and the islets of Langerhans[1].

**Acini.** Acinar cells make up approximately 85% of the mass of the pancreas and constitute the main exocrine secretory component of the gland. The prototypical architectural of the acinus appears to be a single layer of polygonal cells surrounding a minute central lumen. Not all acini are located at the terminal end of ductules. Thus, the secretions of a given acinus may pass through a number of different pathways to reach

the ductal system [3]. The exocrine cells show a strongly basophilic cytoplasm that represents the area occupied by the rough endoplasmic reticulum. The eosinophilic apical side of the cells is filled with zymogen granules that contain a variety of digestive such trypsin, chymotrypsin, lipase, amylase, and elastase[1].

**Ducts.** The ductal system of the pancreas transports the acinar cell secretions to the duodenum. The ductal epithelial cells secrete water, chloride, and bicarbonate to buffer the acidity of the pancreatic juices and stabilize the proenzymes until they become activated within the duodenum. The ductal system is subdivided into five continuous segments: Centroacinar cells, intercalated ducts, intralobular ducts, interlobular ducts (large and small), and main ducts[4]. The ductal system begins with the centroacinar cells, which are small, relatively inconspicuous, and flat to cuboidal cells with pale or lightly eosinophilic cytoplasm and central oval nuclei. Centroacinar cells are located in the middle of the acini, where they partially border the acinar lumina along with the acinar cells[1].

**Islet of Langerhans.** The islets of Langerhans are the endocrine component of the pancreas and constitute the 1 to 2% of the volume of the gland in adults[1]. Islets of Langerhans are distributed heterogeneously along the whole organ, being more numerous in the tail[5]. Two types of islets are found. Most (90%) are the compact islets between 75 to 225 μm [6] founded predominantly in the body and tail of the gland. The

---

[3] Akao S, Bockman DE, Lechene de la Porte P, *et al.* Three-dimensional pattern of ductuloacinar associations in normal and pathological human pancreas. Gastroenterology. 1986;90:661-8.

[4] Kodama T. A light and electron microscopic study on the pancreatic ductal system. Acta Pathol Jpn. 1983;33:297-321.

[5] Wittingen J, Frey CF. Islet concentration in the head, body, tail and uncinate process of the pancreas. Ann Surg. 1974;179:412-14.

[6] Grube D, Bohn R. The microanatomy of human islets of Langerhans, with special reference to somatostatin (D-) cells. Arch Histol Jpn. 1983;46:327-53.

second type of islet, the diffuse islet, is essentially restricted to the posteroinferior head[7].

Each endocrine cell produces only one specific peptide hormone. The major peptides produced by islet cells are insulin (β-cells around 60-70% of total islet cells), glucagon (α-cells, around 15-20%), somatostatin (SS) (δ-cells <10%), pancreatic polypeptide (PPY) (γ or PP-cells, <5%) and epsilon cells ghrelin (ε-cells <1%). The presence of these cell types depends of the area of the pancreas in which we are as well as the type of islet[1].

## HUMAN PANCREAS VS. MOUSE PANCREAS: TWO VERY DIFFERENT ORGANS

As we mentioned above, human pancreatic islets have different cell types with different percentages according to the secreted hormone. These percentages hide great variations between regions of the pancreas, genders and species. During the development of the pancreas two buds are generated and results in two distinct regions with different islet types[8]. In humans we designate as head, neck, body and tail regions of the organ from proximal to distal, while in rodents the pancreatic tissue presents a less defined shape[9]. The pancreatic ventral bud comprises a tenth of the entire organ mass and contains islets with different cell composition. In mouse pancreas this region only presents 20% of cells PP+[10] versus 80% in human pancreas[8], and they become the dominant

---

[7] Stefan Y, Grasso S, Perrelet A, *et al*. The pancreatic polypeptide-rich lobe of the human pancreas: Definitive identification of its derivation from the ventral pancreatic primordium. Diabetologia. 1982;23:141-2.

[8] Stefan Y, Orci L, Malaisse-Lagaeet F, *et al*. Quantitation of endocrine cell content in the pancreas of nondiabetic and diabetic humans. Diabetes. 1982;31:694-700.

[9] Slack JMW. Developmental biology of the pancreas. Development. 1995;121:1569-80.

[10] Baetens D, Malaisse-Lagae F, Perrelet A, *et al*. Endocrine pancreas: three-dimensional reconstruction shows two types of islets of langerhans. Science. 1979;206:1323-5.

cell. Also differences between species were also observed. The mice have more β-cells and fewer α-cells compared to the human islet. In addition, the distribution of the different cell types is different between both species. In mice the β-cells are distributed in the core of the islet surrounded by α-cells whereas in humans this distribution seems to be more randomized. Also an enrichment of PP cells has been observed in males compared to females[8].

## CAN THE HUMAN PANCREAS REGENERATE ITSELF?

It is widely known that the rodent pancreas is capable of undergoing regeneration, like the liver, although to a lesser extent[11,12].

The human pancreas is not an organ readily available to carry out studies *in vitro* studies such as *in vivo*. In the last decades, the diabetic epidemic has unleashed new research in the development, homeostasis, and pancreatic regeneration. Indeed, it remains unclear whether the adult human pancreas can spontaneously regenerate β-cells in any physiologically meaningful way[13]. Learning how to enhance or induce the intrinsic regenerative ability of endocrine and exocrine cells will have profound implications for developing therapeutic treatment for diabetes, chronic pancreatitis (CP)[14] or pancreatic ductal adenocarcinoma (PDAC).

The bibliography describes various mechanisms responsible for pancreatic regeneration. 1) Neogenesis, which includes differentiation of

---

[11] Lehv M, Fitzgerald PJ. Pancreatic acinar cell regeneration. IV. Regeneration after resection. Am J Pathol. 1968;53:513-35.
[12] Pearson KW, Scott D, Torrance B. Effects of partial surgical pancreatectomy in rats. I. Pancreatic regeneration. Gastroenterology. 1997;72:469-73.
[13] Zhou Q, Melton DA, *et al*. Pancreas regeneration. Nature. 2018;557:351-8.
[14] The English acronym will be used.

mature cells to mature cellular components[15,16,17,18,19,20,21,22,23], or trans-differentiation of mature cells into other mature cells type; and 2) self-replication of pre-existing endocrine and exocrine cells and/or endocrine cells[24].

Such diversity in the proposed mechanism may be due to the differences in the experimental models or the methodologies employed, which generates greater discrepancies; although the numerous experiments conducted so far in animals assure the plasticity and the regeneration of both the exocrine and the endocrine pancreas[25]. However, in both animals and humans, the investigations were mainly focused on the sources of cells which underwent regeneration, and little has been studied on the molecular mechanisms by which regeneration is triggered by extracellular stimuli, although intracellular genetic events, expression of transcription factors which facilitate neogenesis, have been explored[26,27].

[15] Bonner-Weir S, Baxter LA, Schuppin GT, *et al*. A second pathway for regeneration of adult exocrine and endocrine pancreas. A possible recapitulation of embryonic development. Diabetes. 1993;42:1715-20.

[16] Xu X, D'Hoker J, Stangé G, *et al*. Beta cells can be generated from endogenous progenitors in injured adult mouse pancreas. Cell. 2008;132:197-207.

[17] Inada A, Nienaber C, Katsuta H, *et al*. Carbonic anhydrase II-positive pancreatic cells are progenitors for both endocrine and exocrine pancreas after birth. Proc Natl Acad Sci US A. 2008;105:19915-19.

[18] Criscimanna A, Speicher JA, Houshmand G, *et al*. Duct cells contribute to regeneration of endocrine and acinar cells following pancreatic damage in adult mice. Gastroenterology. 2011;141:1451-62.

[19] Smukler SR, Arntfield ME, Razavi R, *et al*. The adult mouse and human pancreas contain rare multipotent stem cells that express insulin. Cell Stem Cell. 2011;8:281-93.

[20] Li WC, Rukstalis JM, Nishimura W, *et al*. Activation of pancreatic-duct-derived progenitor cells during pancreas regeneration in adult rats. J Cell Sci. 2010;123:2792-802.

[21] Zhou Q, Brown J, Kanarek A, *et al*. *In vivo* reprogramming of adult pancreatic exocrine cells to beta-cells. Nature. 2008;455:627-32.

[22] Pan FC, Bankaitis ED, Boyer D, *et al*. Spatiotemporal patterns of multipotentiality in Ptf1a-expressing cells during pancreas organogenesis and injury-induced facultative restoration. Development. 2013;40:751-64.

[23] Thorel F, NeÂpote V, Avril I, *et al*. Conversion of adult pancreatic alpha cells to beta-cells after extreme beta-cell loss. Nature. 2010;464:1149-54.

[24] Dor Y, Brown J, Martinez OI, *et al*. Adult pancreatic beta-cells are formed by self-duplication rather than stem-cell differentiation. Nature. 2004;429:41-6.

[25] Ota S, Nishimura M, Murakami Y, *et al*. Involvement of Pancreatic Stellate Cells in Regeneration of Remnant Pancreas after Partial Pancreatectomy. PLoS ONE. 2016;11:e0165747.

[26] Ziv O, Glaser B, Dor Y. The plastic pancreas. Dev Cell. 2013;26:3-7.

[27] Migliorini A, Bader E, Lickert H. Islet cell plasticity and regeneration. Mol Metab. 2014;3:268-74.

## THE PANCREATIC STELLATE CELLS

The pancreatic stellate cells (PSCs) are a type of vitamin A-storing fibroblast-like stromal cell which presents pluripotent cell characteristics. PSCs are found mainly in the exocrine pancreas but also in the endocrine pancreas named, in this case, islet stellate cells (ISCs)[28] and compose 4-7% of the total cell mass in the gland[8]. The PSCs have two phenotypes, quiescent and activated. When suffering from chronic inflammation or oxidative stress, PSCs will be activated and turned into myofibroblast cells, losing their vitamin A-storing lipid droplets, expressing (α smooth muscle actin) α-SMA, vimentin, and glial fibrillary acidic protein (GFAP), extracellular matrix components (ECM), producing cytokines and chemokines, connective tissue, matrix metalloproteinases (MMPs) and tissue inhibitors of metalloproteinases (TIMPs) as well as having higher proliferation and migration activities[29,30,31,32]. Recent studies show that the origin of activated PSCs may be in the stem/progenitor cells of bone marrow **(Diagram 2)**[33].

---

[28] Zha M, Xu W, Jones PM, *et al.* Isolation and characterization of human islet stellate cells. Exp Cell Res. 2016;34:61-6.

[29] Lee E, Ryu GR, Ko SH, *et al.* Antioxidant treatment may protect pancreatic beta cells through the attenuation of islet fibrosis in an animal model of type 2 diabetes. BBRC. 2011;414:397-402.

[30] Saito R, Yamada S, Yamamoto Y, *et al.* Conophyllin suppresses pancreatic stellate cells and improves islet fibrosis in Goto-Kakizaki rats. Endocrinology. 2012;153:621-30.

[31] Datar SP, and Bhonde RR. Islet-derived stellate-like cells as a novel source for islet neogenesis in chicks. Poultry Science. 2009;88:654-60.

[32] Yang J, Waldron RT, Su HY, *et al.* Insulin promotes proliferation and fibrosing responses in activated pancreatic stellate cells. AJP Gastrointestinal and Liver Physiology. 2016;311: G675-G687.

[33] Habisch H, Zhou S, Siech M, *et al.* Interaction of Stellate Cells with Pancreatic Carcinoma Cells. Cancers. 2010;2:1661-82.

**Diagram 2.** Characteristics of quiescent (fat-storing phenotype) and activated PSC (myofibroblast-like phenotype). Habisch H, *et al*. Cancers;2:1661-82. Licensed under Creative Commons.

PSCs are associated with diseases such as CP, PDAC, and fibrosis[34,35] this association could have its origin in the ignorance of the different types of cells that are being hidden under the name of PSCs. Cancer-associated fibroblast (CAF) is a subpopulation that produce desmoplastic stroma, thereby modulating disease progression and therapeutic response in PADC [36] . Characterizing the membrane markers, in these subpopulations, is essential to know exactly which cell type we are working with. Several publications point to the capacity of PSCs as regenerating cells of the pancreas[25,37,38]. The first work to describe the capacity of early regeneration of these cells after acute necrotizing pancreatitis in humans was in 2002. Zimmermann *et al*. affirm that PSCs

---

[34] Phillips PA, McCarroll JA, Park S, *et al*. Rat pancreatic stellate cells secrete matrix metalloproteinases: implications for extracellular matrix turnover. Gut. 2003;52:275-82.

[35] Omary MB, Lugea A, Lowe AW, *et al*. The pancreatic stellate cell: a star on the rise in pancreatic diseases. J Clin Invest. 2007;117:50-59.

[36] Öhlund D, Handly-Santana A, Biffi G, *et al*. Distinct populations of inflammatory fibroblasts and myofibroblasts in pancreatic cancer. J Exp Med. 2017;214:579-96.

[37] Mato E, Lucas M, Petriz L, *et al*. Identification of pancreatic stellate cell population with properties of progenitor cells: new role for stellate cells in the pancreas. Biochem J. 2009;421:181-91.

[38] Zimmermann A, Gloor B, Kappeler A, *et al*. Pancreatic stellate cells contribute to regeneration early after acute necrotising pancreatitis in humans. Gut. 2002;51:574-8.

and their activated myofibroblastic offspring may participate in the regeneration after acute necrotizing pancreatitis in humans[38].

Mato *et al.* identified a population of PSCs in adult pancreas positive for ABCG2 transporter, a stem cell marker, where ABC is ATP binding cassette, which have the capacity to transdifferentiate into insulin-producing cells[37]. Also in 2015 Bayan *et al.* data suggested that that these mesenchymal cells may support the regeneration of the islets[39].

In 2016 Shigenori Ota *et al.* reported that after pancreatectomy, the acinar and islet cell proliferation was increased, this increase is closely related to PSCs HSP47^{+}. The acinar cells was augmented by co-culturing with activated PSCS (aPSCs) HSP47^{+} and the augmentation was nullified by siRNA HSP47. HSP47 in addition to be an activated PSCs marker is a key-regulator for the correct collagen biosynthesis and pancreatic regeneration, which makes it an important therapeutic target in pancreatic regeneration[25].

In addition to the aforementioned, we have learned recently from animal models, that part of the activated PSCs originates from stem/progenitor cells of bone marrow. In the last decade it has been demonstrated that certain PSCs isolated from the rat and human pancreatic tissue express markers of stem/progenitor markers such as CD34, Nestin, CD271, GFAP, Bcrp1, Aldh, Notch and are able to differentiate into other pancreatic cell types[35,39,40].

---

[39] Bayan JA, Peng Z, Zeng N, *et al.* Crosstalk between activated myofibroblasts and β-cells in injured mouse pancreas. Pancreas. 2015;44:1111-20.
[40] Fujiwara K, Ohuchida K, Mizumoto K, *et al.* CD271^{+} subpopulation of pancreatic stellate cells correlates with prognosis of pancreatic cancer and is regulated by interaction with cancer cells. PLoS One. 2012;7:e52682.

## CP: CRONIC PANCREATITIS

CP is characterized by chronic inflammation of the pancreas that results in progressive loss of pancreatic acinar and islet cells, atrophy of the pancreatic tissue, pain, maldigestion (exocrine insufficiency), diabetes mellitus (endocrine insufficiency) and increased risk of pancreatic cancer (PC)[41]. The chronic inflammation triggers necrosis or apoptosis, chronic secondary inflammatory infiltration of the pancreatic parenchyma, and activation of PSCs for the repair of pancreatic damage by the synthesis of ECM proteins.

**Epidemiology and aetiology.** In Spain the estimated incidence of CP was 4.66 cases per $10^5$ in habitants/year. Incidence was heterogeneous between influence areas, with a range of 0.13 to 26.7 cases per $10^5$ in habitants/year. Tobacco use and alcohol use appear as associated risk factors[42].

## PDAC: PANCREATIC DUCTAL ADENOCARCINOMA

PDAC is an infiltrating epithelial neoplasm with glandular (ductal) differentiation, usually demonstrating luminal and/or intracellular production of mucin, and without a predominant component of any other histological type. An abundant desmoplasic stromal response is a typical feature of neoplasm[43].

---

[41] Hammad AY, Ditillo M, Castanon L. Pancreatitis. Surg Clin North Am. 2018;98:895-913.

[42] Domínguez Muñoz JE, Lucendo Villarín AJ, Carballo Álvarez LF, *et al*. Spanish multicenter study to estimate the incidence of chronic pancreatitis. Rev Esp Enferm Dig. 2016;108:411-6.

[43] Bosman FT, Carneiro F, Hruban RH & Theise ND. (2010). World Health Organization & International Agency for Research on Cancer. (4th ed.,). *WHO classification of tumours of the digestive system*. Lyon: International Agency for Research on Cancer.

**Epidemiology and aetiology.** The epidemiological study of this disease is complicated by significant geographical and temporal variations in the sensitivity and specificity of the clinical diagnosis and in the proportion of cases that are histologically verified. Differences in the access to health care (e.g. for different social classes or age groups) can affect the reported incidence and mortality rates. Given the very poor survival, mortality rates closely parallel incidence rates[43]. Most patients are between 60 and 80 years age. Incidence is about 50% higher in men than in women which may be due to consumption habits. Although the predictive values for the year 2017 in Europe show a stabilization of the growth rate for men, in the case of women it reaches values of $5.6/10^5$ in habitants and year, representing the second cancer with worse predictions after the lung. These increases are especially important in countries such as France and Spain, where tobacco consumption became common among women in the 1970s[44]. The best-known risk factor is tobacco smoking. The risk in smokers is two to three times greater than in non-smokers, there is a dose-response relationship, and smoking cessation has been shown to lower the risk in many populations[45]. In addition, heavy drinking of alcohol can also be a risk factor[46].

Moreover has been suggested that PC is associated with nutritional and dietary factors, including obesity and low physical activity, high intake of fats, especially saturated fats, and low intake of vegetables and fruits[47].

---

[44] Levi F, Bosetti C, Fernandez E, *et al.* Trends in lung cancer among young European women: the rising epidemic in France and Spain. Int J Cancer. 2007;121:462-5.

[45] Iodice S, Gandini S, Maisonneuve P, *et al.* Tobacco and the risk of pancreatic cancer: a review and meta-analysis. Langenbecks Arch Surg. 2008;393:535-45.

[46] Tramacere I, Scotti L, Jenab M, *et al.* Alcohol drinking and pancreatic cancer risk: a metaanalysis of the dose-risk relation. Int J Cancer. 2009;126:1474-86.

[47] World Cancer Research Fund / American Institute for Cancer Research. Food, Nutrition, Physical Activity and the Prevention of Cancer: A global Perspective. Washington, DC: AICR, 2007.

Other medical conditions, including history of CP, hereditary pancreatitis, diabetes mellitus and gastrectomized patients, has also been associated with an increased risk of PC[43,48].

**Localization:** Most of PDACs (60-70%) arise in the head of the gland, and the remainder in the body (5-15%) or tail (10-15%). The vast majority of PCs are solitary, but the multifocal disease can occur[49,50].

**Signs and symptoms.** The clinical features include back pain, unexplained weight loss, jaundice, and pruritus[51]. Diabetes mellitus is present in 70% of patients and new-onset diabetes may be the first manifestation of PC[52]. Later symptoms are related to liver metastasis and/or invasion of adjacent organs (duodenum) or involvement of the peritoneal cavity (ascites)[53].

**Tumour spread and staging.** At diagnosis, the vast majority of PC has spread beyond the pancreatic parenchyma[54]. Carcinomas of the head commonly extend into the duodenum and the ampulla of Vater, the intrapancreatic portion of the common bile duct, and into peripancreatic or retroperitoneal adipose tissue. Perineural invasion is also a common mechanism by which PC reach these structures and may proceed the development of peripancreatic lymph-node metastases[55,56].

---

[48] Lowenfels AB, Maisonneuve P, Dimagno, *et al.* Hereditary pancreatitis and the risk of pancreatic cancer. International Herediary Pancreatitis Study Group. J Natl Cancer Inst. 1997;89:442-6.

[49] Hruban RH, Pitman MB & Klimstra DS eds. (2007). *Tumors of the Pancreas.* Armed Forces Institute of Pathology: Washington, DC.

[50] Solcia E, Capella C, & Klöppel G eds. (1997). *Tumours of the Pancreas.* Armed Forces Institute of Pathology: Washington, DC.

[51] Holly EA, Chaliha I, Bracci PM, *et al.* Signs and symptoms of pancreatic cancer: a population-based case-control study in the San Francisco Bay area. Clin Gastroenterol Hepatol. 2004;2:510-17.

[52] Chari ST, Leibson CL, Rabe KG, *et al.* Probability of pancreatic cancer following diabetes: a population-based study. Gastroenetrology. 2005;129:504-11.

[53] Greenberg RE, Bank S, Stark B. Adenocarcinoma of the pancreas producing pancreatitis and pancreatic abscess. Pancreas. 1990;5:108-13.

[54] Sohn TA, Yeo CJ, Cameron JL, *et al.* Resected adenocarcinoma of the pancreas-616 patients: results, outcomes, and prognostic indicators. J Gastrointest Surg. 2000;4:567-79.

[55] Kayahara M, Nakagawara H, Kitagawa H, *et al.* The nature of neural invasion by pancreatic cancer. Pancreas. 2007;35:218-23.

Hepatic blood-borne metastases are frequent. Metastases to lung, pleura and bone are seen only in advanced tumour stages, particularly with tumours of the body or tail; however, cerebral metastases are uncommon[57].

The pathologic staging of PDAC is based on the TNM classification[58]. It takes into account the size and extent of invasion of the primary tumour (pT1-pT4) and the presence or absence of regional metastatic lymph nodes (pN1a, or pN1b if multiple regional lymph nodes are involved), as well as of distant metastases (pM).

**Histopathology.** Most ductal adenocarcinomas are composed of well-to moderately develop glandular and duct-like structures, which infiltrate the pancreatic parenchyma, grow in a haphazard pattern, are associated with a desmoplastic stroma and produce sialo-type and sulfated acid mucins. Poorly differentiated PDAC form small, poorly formed glands composed of cells with pleomorphic nuclei, individual infiltrating cells, and solid cellular areas. Those produce much less mucin than more differentiated carcinomas[43].

The currently available grading schemes for ductal adenocarcinomas both follow a three-tiered system (**Table 1**)[59].

**TNM Classification of PDACs**[60]**.** The classification is based in size and spread of the pancreas tumour (T), in the nearness lymph nodes involved (N) and the distant metastasis (M).

---

[56] Nagakawa T, Kayahara M, Ueno K, *et al.* Clinicopathological study on neural invasion to the extrapancreatic nerve plexus in pancreatic cancer. Hepatogastroenterology. 1992;39:51-5.

[57] Fletcher CDM. (2013) *Diagnostic Histopathology of Tumors* (Volume 1) 4th ed. Philadelphia, US: Elsevier.

[58] Edge BN, Byrd DR, Carducc MA, *et al.* (2010) *AJCC Cancer Staging Manual*, 7th ed. New York, US: Springer.

[59] Klöppel G, Hruban RH, Longnecker DS, *et al.* (2000). Pathology and genetics of tumours of the digestive system. In: Hamilton SR, Aaltonen LA (Eds.). *Ductal adenocarcinoma of the pancreas*. (pp. 221-30). World Health Organization classification of tumours. Lyon, France: IARC Press.

**Primary Tumour (T)**

TX. Primary tumor cannot be assessed

T0. No evidence of primary tumour

Tis. Carcinoma in situ*

T1 Tumour 2 cm or less in greatest dimension

T1a Tumour 0.5 cm or less in greatest dimension

T1b Tumour greater than 0.5 cm and less than 1 cm in greatest dimension

T1c Tumour greater than 1 cm but no more than 2 cm in greatest dimension

T2 Tumour more than 2 cm but no more than 4 cm in greatest dimension

T3 Tumour and more than 4 cm in greatest dimension

T4 Tumour involves coeliac axis, superior mesenteric artery and/or common hepatic artery

*Tis also includes the "PanIN–III" classification, intraductal papillary mucinous neoplasm with high-grade dysplasia, intraductal tubulopapillary neoplasm with high-grade dysplasia and mucinous cystic neoplasm with high grade dysplasia.

**Regional Lymph Nodes (N)**

NX Regional lymph nodes cannot be assessed

N0 No regional lymph node metastasis

N1 Metastases in 1 to 3 regional lymph node

N2 Metastases in 4 or more regional lymph node

**Distant Metastases (M)**

cM0 No distant metastasis

cM1 Distant metastasis

pM1 Distant metastasis, microscopically confirmed

## Histologic Grade (G)

**Table 1:** Histologic grade and definition

| Grade | G Definition |
|---|---|
| GX | Grade cannot be assessed |
| G1 | Well differentiated |
| G2 | Moderately differentiated |
| G3 | Poorly differentiated |

---

[60] Amin, MB, Edge SB, Greene FL, *et al.* (Eds.). (2017) *AJCC Cancer Staging Manual.* 8th ed. NY, US: Springer.

**Immunohistochemistry.** At present, there is no sufficiently sensitive and specific biomarker for clinical use in diagnosis. Although the CA19.9 antigen has been used in some studies and has rates of sensitivity and specificity between 70-92% and 68-92%, respectively, its use is not recommended systematized for several reasons. First, CA19.9 is not expressed in about 5% of the population (individuals who do not possess the Lewis antigen). Second, the sensitivity of CA19.9 is dependent on the size of the tumour. This fact and the low prevalence of the disease, makes CA19.9 antigen a biomarker with little predictive value is not recommended for screening PDAC, especially in asymptomatic population and a high number of false positives would be obtained. Finally, CA19.9 is also altered in other pathologies such as cirrhosis, CP, cholangitis, or other gastrointestinal cancers. However, CA19-9 is very useful in the follow-up of patients who, after surgery, are receiving chemotherapy treatment where their elevation is indicative of recurrence. Other recently researched markers are MIC-1 (macrophage inhibitory cytokine 1) CEACAM-1 (carcinoembryonic antigen related cell adhesion molecule 1), SPAN1, DUPAN, Alpha4GNT (alpha1,4-N-acetylglucosaminyltransferase) and PAM4, but none is validated for routine clinical use. It has also been shown that high levels of fasting glucose are associated with sporadic PDAC, and a European registry uses these levels of glucose monitoring individuals at high risk of PC, along with mutational analysis of pancreatic juice and status methylation of the p16 promoter[61].

**Prognosis:** Most (80-90%) ductal carcinomas are not resectable at the time of diagnosis, and these patients rarely live longer than 6 months. Of the patients with resectable tumours, approximately 80 to 90% survive

---

[61] Urayama S. Pancreatic cáncer early detection: expanding higher-risk group with clinical and metabolomics parameters. World J Gastroenterol. 2015;21:1707-17.

no longer than 3 years, and just between 5% to 20% have 5-year survival rate[62,63,64].
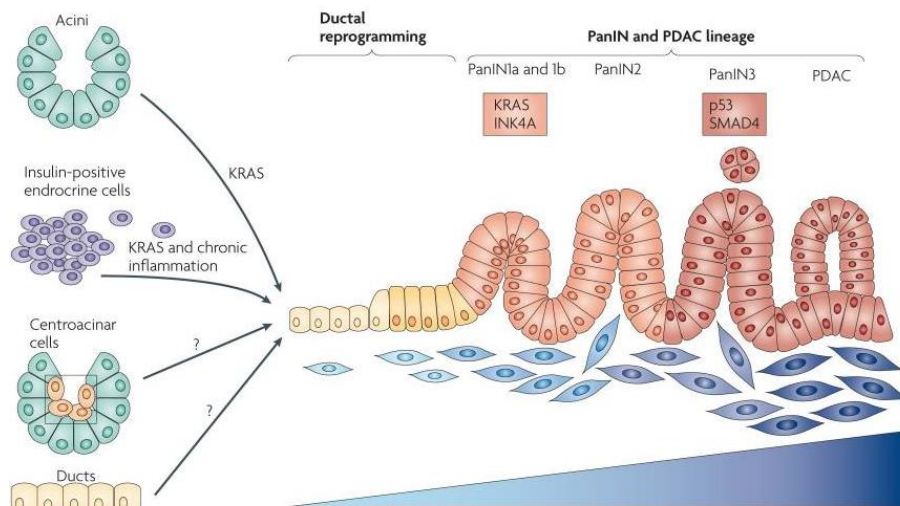


**Diagram 3.** Development of PanIN and PDAC. Modified from Morris J *et al.* Nat Rev Cancer; 2010;10:683-95. With permission from Springer Nature.

**Precursory lesions.** Mucinous cystic neoplasm (MCN), intraductal papillary mucinous neoplasm (IPMN) and pancreatic intraepithelial neoplasia (PanIN) are thought to represent precursor stages for PDAC[65] (**Diagram 3**). PanIN is the most common precursory lesion of PDAC. PanIN was described for the first time in 1998, it is characterized by presenting, noninvasive epithelial neoplasms confined to pancreatic ducts;

---

[62] Makhlouf HR, Almeida JL, Sobin LH. Carcinoma in jejunal pancreatic heterotropia. Arch Pathol Lab Med. 1999;123:707-11.

[63] Carpelan-Holmström M, Nordling S, Pukkala E, *et al.* Does anyone survive pancreatic ductal adenocarcinoma? A nationwide study re-evaluating the data of the Finnish Cancer Registry. Gut. 2005;54:385-7.

[64] Nagakawa T, Nagamori M, Futakami F, *et al.* Results of extensive surgery for pancreatic carcinoma. Cancer. 1996;77:640-5.

[65] Morris JP, Wang SC, Hebrok M. KRAS, Hedgehog, Wnt and the twisted developmental biology of pancreatic ductal adenocarcinoma. Nat Rev Cancer. 2010;10:683-95.

composed of columnar to cuboidal cells with variable mucin and divided into three different grades according to degree of cytological and architectural atypia (PanIN-1(PanIN-1A, PanIN-1B), PanIN-2 and PanIN-3)[66].

PanIN-1 and PanIN-2 are now to be categorized as low-grade and PanIN-3 as high grade. It has been shown that two-tiered systems improve concordance and uniformity over three-tiered systems. In this way, the stages with more advanced dysplasia are determined, to ensure a careful clinical attention and treatment[67].

## OBESTATIN/GPR39 SYSTEM

### OBESTATIN

Obestatin is an amidated peptide of 23 amino acids derived from the preproghrelin precursor encoded by the ghrelin gene [68]. The human ghrelin gene is located on the chromosome position 3p25-26 and comprises five exons and three introns [69,70]. Three main peptides are derived from the preproghrelin gene: ghrelin (acylated ghrelin), des-acyl ghrelin and obestatin[71].

**Structure of human obestatin**. Obestatin originates from post-translational modifications of the ghrelin prepropeptide composed of 117

---

[66] Brat DJ, Lillemoe KD, Yeo CJ, *et al*. Progression of pancreatic intraductal neoplasias to infiltrating adenocarcinoma of the pancreas. Am J Surg Pathol. 1998;22:163-9.

[67] Basturk O, Hong SM, Wood LD, *et al*. A revised classification system and recommendations from the Baltimore consensus meeting for neoplastic precursor lesions in the pancreas. Am J Surg Pathol. 2015;39:1730-41.

[68] Li JB, Asakawa A, Cheng KC, *et al*. Biological effects of obestatin. Endocr. 2011;39:205-11.

[69] Camina JP. Cell biology of the ghrelin receptor. J Neuroendocrinol. 2006;18:65-76.

[70] McKee KK, Palyha OC, Feighner SD, *et al*. Molecular analysis of rat pituitary and hypothalamic growth hormone secretagogue receptors. Mol Endocrinol. 1997;11:415-23.

[71] Ma X, Lin L, Qin G, *et al*. Ablations of Ghrelin and Ghrelin Receptor Exhibit Differential Metabolic Phenotypes and Thermogenic Capacity during Aging. PLoS ONE. 2011;6:e16391.

residues whose cleavage leads to the synthesis of two peptides, ghrelin (segment of peptide 76-98) and obestatin (segment of peptide 24-51)[72].

Obestatin is principally produced in the gastric mucosa but it can be found throughout the gastrointestinal tract, has a molecular weight of 2516.3 and is structurally characterized by having the well-conserved C-terminal end flanked by glycine residues[73] suggesting that this peptide is functionally important[74].

Human obestatin presents a three-dimensional structure of α-helical conformations (**Diagram 4**) and the amidation at the C-terminus is necessary for their bioactivity through GPR39 receptor. The truncate peptide (11-23)-obestatin is also synthesized in the stomach and is able to induce selective coupling to the β-arrestin-dependent signalling[75].
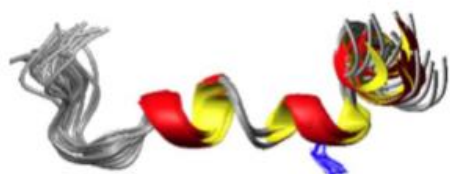


**Diagram 4.** Superimposition of the 20 best human obestatin representative structures of peptides as calculated from the NMR data for the peptides in SDS micelles. The Tyr16 side chain is shown in blue. Modified from: Alén BO *et al.* PLoS One. 2012;7:e45434. Licensed under Creative Commons.

**Obestatin: its physiological functions.** The first physiological function attributed to the obestatin was the intake reduction. This issue was controversial because the trials to demonstrate the anorexigenic

---

[72] Zhang JV, Ren PG, Avsian-Kretchmer O, *et al*. Obestatin, a peptide encoded by the ghrelin gen, opposes ghrelin´s effects on food intake. Science. 2005;310:996-9.

[73] Tang SQ, Jiang QY, Zhang YL, *et al*. Obestatin: Its physicochemical characteristics and physiological functions. Peptides. 2008;29:639-45.

[74] Green BD, Grieve DJ. Biochemical properties and biological actions of obestatin and its relevance in type 2 diabetes. Peptides. 2018;100:249-59.

[75] Alén BO, Nieto L, Gurriarán-Rodríguez U, *et al*. The NMR structure of human obestatin in membrane-like environments: insights into the structure-bioactivity relationship of obestatin. PLoS ONE. 2012;7:e45434.

effect were not reproducible by other laboratories [76, 77]. Sibilia *et al.* examined various factors related to energy metabolism such as food intake, body weight, body composition, energy expenditure, locomotor activity, respiratory quotient, or hypothalamic neuropeptides involved in energy balance regulation with long-term obestatin administration, but failed to observe any effects[78]. In fasting conditions obestatin levels in plasma differed between men and women, obestatin levels (pg/mL) was higher in women (130.9 ± 45.1) compared to men (111.0 ± 36.9). In addition, differences have been observed between normal weights and obese. The individuals with overweight and obesity had obestatin concentrations that were 12.6 and 25.4 pg/mL respectively lower compared to normal weight[79]. Also has been observed that in patients with anorexia nervosa, submitted to the oral glucose tolerance test, the obestatin, acyl ghrelin, and des-acyl ghrelin levels in plasma are increased. The obestatin differences are the most important, suggesting that this hormone could be a diagnostic marker reflecting both acute and chronic changes of the nutritional state, in anorexia nerviosa patients[80].

Numerous biological functions have been described for it in both central and peripheral tissues (**Diagram 5**).

---

[76] Seoane LM, Al-Massadi O, Pazos Y, *et al.* Central obestatin administration does not modify either spontaneous or ghrelin-induced food intake in rats. J Endocrinol Invest. 2006;29:RC13-5.

[77] Nogueiras R, Pfluher P, Tovar S, *et al.* Effects of obestatin on energy balance and growth hormone secretion in rodents. Endocrinology. 2007;148:21-6.

[78] Sibilia V, Bresciani E, Lattuada N, *et al.* Intracerebroventricular acute and chronic administration of obestatin minimally affect food intake but not weight gain in the rat. J Endocrinol Invest. 2006;29:RC31-4.

[79] Beasley MJ, Ange BA, Anderson CAM *et al.* Characteristics associated with fasting appetite hormones (obestatin, ghrelin, and leptin). Obesity (Silver Spring). 2009;17:349-54.

[80] Harada T, Nakahara T, Yasuhara D, *et al.* Obestatin, acyl ghrelin, and des-acyl ghrelin responses to an oral glucose tolerance test in the restricting type of anorexia nervosa. Biol Psychiatry. 2008;63:245-7.

**BRAIN**
↓ Growth hormone secretion
↑ Proliferation and survival of rat hippocampal
progenitor cells
↓ Oxidative brain damage

**PANCREAS**
↑ β-cell viability
↑ Islet vascularisation
↓ Apoptosis and inflammation
Modulation of insulin secretion
↑ Protective against acute pancreatitis
Pancreatic development/regeneration

**WHITE ADIPOSE TISSUE**
↑ Preadipocyte differentiation
and adipocyte proliferation

**METABOLISM**
Changes the circulating levels of
phospholipids, and amino acids.
Modulation of
lipogenesis/lipolysis
Modulation glucose metabolism

**STOMACH**
Pepsinogen and lipase secretion
stimulation
Regulates proliferation and
invasion of gastric cancer cells
Diminish GI inflammation

**HEART**
↓ Ischaemia-reperfusion injury
and contractile dysfunction
↑ Plasma levels in heart failure

**MUSCLE**
↑ Muscle regeneration after injury
↑ Number of activated satellite cell

**Diagram 5.** Pathophysiological effects of obestatin. Obestatin reportedly exerts general actions on metabolism but also acts on several tissues, including the gastrointestinal system, pancreas, white adipose tissue, the heart, vasculature, and brain. Author original.

Camiña *et al.* showed that this peptide induced cell proliferation, in primary cultures of hRPE cells, in a dose-dependent manner with MEK/ERK1/2 phosphorylation [81]. Also, the same group determined obestatin/GPR39 signalling stimulates skeletal muscle repair by inducing the expansion of satellite stem cells as well as myofiber hypertrophy. Obestatin/GPR39 system acts as an autocrine/paracrine factor on human myogenesis regulating myoblast proliferation, cell cycle exit, differentiation and recruitment to fuse and form multinucleated

---

[81] Camiña JP, Campos JF, Caminos JE, *et al.* Obestatin-mediated proliferation of human retinal pigment epithelial cells: regulatory mechanisms. J Cell Physiol. 2007;211:1-9.

hypertrophic myotubes [82]. More they demonstrated that obestatin promotes engraftment of primary human myoblast into host skeletal muscle thereby highlighting potential benefits for tissue regeneration[83].

In cardiac muscle, obestatin protect against *ex vivo* myocardial ischemia-reperfusion injury and dysfunction via specific reduction of cell death mediated by activation of ERK1/2, PKC-δ, PKC-ε and PI3K[84]. These data were recently confirmed in the same *in vivo* model by two independent studies [85, 86, 87]. Obestatin is also reported to attenuate cardiotoxicity both *in vivo* and *in vitro* via Mhrt and Nrf2-mediated reduction of cardiomyocyte apoptosis[88]. In addition to these apparent cardioprotective actions, obestatin has been found to directly modulate cardiac contractility, Sazdova *et al.* observed a positive inotropic effect of obestatin on the *in vitro* heart preparations of the *Rana ridibunda* frog[89].

Obestatin is a multi-functional peptide which exerts a variety of functions in diverse tissues. In addition, recently, it has been described the possible physiological role of the obestatin/GPR39 system. Exogenous

---

[82] Santos-Zas I, Gurriarán-Rodríguez U, Cid-Díaz T, *et al.* β-Arrestin scaffolds and signalling elements essential for the obestatin/GPR39 system that determine the myogenic program in human myoblast cells. Cell Mol Life Sci. 2016;73:617-35.

[83] Santos-Zas I, Negroni E, Mamchaoui K, *et al.* Obestatin increases the regenerative capacity of human myoblasts transplanted intramuscularly in an immunodeficient mouse model. Mol Ther. 2017;25:345-59.

[84] Alloatti G, Arnoletti E, Bassino E, *et al.* Obestatin affords cardioprotection to the ischemic-reperfused isolated rat heart and inhibits apoptosis in cultures of similarly stressed cardiomyocytes. Am J Physiol Heart Circ Physiol. 2010;299:H470-81.

[85] Zhang MY, Li F, Wang JP. Correlation analysis of serum obestatin expression with insulin resistance in childhood obesity. Genet Mol Res. 2017;16(2) gmr16029210.

[86] Zhang Q, Dong XW, Xia JY, *et al.* Obestatin plays beneficial role in cardiomyocyte injury induced by ischemia-reperfusion *in vivo* and *in vitro*. Med Sci Monit. 2017;23:2127-36.

[87] Penna C, Tullio F, Femminò S, *et al.* Obestatin regulates cardiovascular function and promotes cardioprotection through the nitric oxide pathway. J Cell Mol Med. 2017;21:3670-8.

[88] Li HQ, Wu YB, Yin CS, *et al.* Obestatin attenuated doxorubicin-induced cardiomyopathy via enhancing long noncoding Mhrt RNA expression. Biomed Pharmacother. 2016;81:474-81.

[89] Sazdova IV, Ilieva BM, Minkov IB, *et al.* Obestatin as contractile mediator of excised frog heart. Cent Eur J Biol. 2009;4:327-34.

administration of obestatin increased pepsinogen [90] and gastric lipase release[91] in an *in vitro* system of human stomach explants.

**Obestatin and pancreatic tissue.** Obestatin expression was found in foetal and neonatal rat pancreas and its immunoreactivity positively correlated with insulin secretion suggesting that pancreatic obestatin would contribute to β-cell function[92]. However, the reported effects of obestatin on insulin secretion are quite unclear with both *in vitro* and *in vivo* investigations producing inconsistent results[93,94,95,96,97]. Furthermore, Pradhan *et al.* recently demonstrated that obestatin is a potent insulin secretagogue, but only under hyperglycemic conditions whilst implicating the ghrelin receptor, GHS-R, as a key mediator[94]. Interestingly, Egido *et al.* found that in rodent islets incubated in high glucose obestatin had differential effects on insulin release, with low obestatin concentrations exerting a stimulatory effect whilst high concentrations were inhibitory, which may appear to suggest that β-cells may become less responsive to obestatin in diabetes[98]. However, it is worth noting that obestatin has

[90] Unpublished results. Digestive Disease Week (DDW). Chicago, IL, US. MAY 06-09, 2017. Otero-Alen B, Leal-Lopez S, Estévez LS, *et al.*. The Obestatin/G Protein-Coupled Receptor 39 (GPR39) System in Human Stomach: Its Role on Pepsinogen I Secretion. Gastroenterology. 2017;152(5-S1):S911.

[91] Unpublished results. Semana de las Enfermedades Digestivas. Valencia, Spain, 2018. Leal-Lopez S, Otero-Alen B, Estévez LS, *et al*. Papel del sistema obestatina/receptor acoplado a proteínas G 39 (GPR39) en la secreción de lipasa gástrica en estómago humano. Rev Esp Enferm Dig. 2018;110(Supl.1):239-240.

[92] Chanoine JP, Wong AC, Barrios V: Obestatin, acylated and total ghrelin concentrations in the perinatal rat pancreas. Horm Res. 2006;66:81-88.

[93] Granata R, Settanni F, Gallo D, *et al*. Obestatin promotes survival of pancreatic beta-cells and human islets and induces expression of genes involved in the regulation of beta-cell mass and function. Diabetes. 2008;57:967-79.

[94] Pradhan G, Wu CS, Han Lee J, *et al*. Obestatin stimulates glucose-induced insulin secretion through ghrelin receptor GHS-R. Sci Rep. 2017;7:979.

[95] Green BD, Irwin N, Flatt PR, et al. Direct and indirect effects of obestatin peptides on food intake and the regulation of glucose homeostasis and insulin secretion in mice. Peptides. 2007;28:981-7.

[96] Qader SS, Håkanson R, Rehfeld, JF, *et al*. Proghrelin-derived peptides influence the secretion of insulin glucagon, pancreatic polypeptide and somatostatin: a study on isolated islets from mouse and rat pancreas. Regul Pept. 2008;146:230-7

[97] Ren A, Guo Z, Wang YK, *et al*. Inhibitory effect of obestatin on glucose-induced insulin secretion in rats. Biochem Biophys Res Commun. 2008;369:969-72.

[98] Egido EM, Hernández R, Marco J, *et al*. Effect of obestatin on insulin: glucagon and somatostatin secretion in the perfused rat pancreas. Regul Pept. 2009;152:61-6.

been reported to regulate the secretion of other pancreatic hormones such as glucagon, PPY, and SS in isolated rodent islets[96], whilst it also increases pancreatic protein output in rats via vagal activation[99].

Other effects on islets and β-cells were showed last years. Granata *et al.* report that obestatin promotes proliferation, survival and reduced apoptosis in β-cells and human pancreatic islets cultured in either absence of serum or presence of cytokines, both conditions to induce apoptosis[93]. Moreover, obestatin activates signalling pathways and induces expression of genes that regulate β-cell growth, differentiation, insulin biosynthesis and glucose metabolism[93]. In the rat exocrine pancreas Kapica *et al.* also observed effects, obestatin intravenous and intraduodenal boluses (30, 100 and 300 nmol/kg body weight) increased the protein output and trypsin activity and did not affect the pancreatic-biliary juice volume[100]. More recent work suggest that obestatin has a role in pancreatic development and regeneration, specifically enhancing the generation of pancreatic islet-like clusters and increasing insulin gene expression during endocrine pancreatic precursor cell selection and differentiation. These effects appear to involve fibroblast growth factor receptors, notch receptors and neurogenin 3[101]. Indeed, patients with acute pancreatitis have increased circulating levels of obestatin[102], highlighting a potential protective function, which is supported by experimental rat studies in which obestatin is reported to reduce acute

---

[99] Favaro E, Granata R, Miceli I, *et al.* The ghrelin gene products and exendin-4 promote survival of human pancreatic islet endothelial cells in hyperglycaemic conditions, through phosphoinositide 3-kinase/ Akt, extracellular signal-related kinase (ERK)1/2 and cAMP/protein kinase A (PKA) signalling pathways. Diabetologia. 2012;55:1058-70.

[100] Kapica M, Zabielska M, Puzio I, *et al.* Obestatin stimulates the secretion of pancreatic juice enzymes through a vagal pathway in anaesthetized rats - preliminary results. J Physiol Pharmacol. 2007;58:123-30.

[101] Baragli L, Grande C, Gesmundo I, *et al.* Obestatin enhances *in vitro* generation of pancreatic islets through regulation of developmental pathways. PLoS One. 2013;8:e64374.

[102] Kanat BH, Ayten R, Aydin S, *et al.* Significance of appetite hormone ghrelin and obestatin levels in the assessment of the severity of acute pancreatitis. Turk J Gastroenterol. 2014;25:309-13.

pancreatitis induced by cerulein or ischaemia/reperfusion[103,104]. Treatment with obestatin ameliorated morphological signs of pancreatic damage including edema, vacuolization of acinar cells, haemorrhages, acinar necrosis, and leukocyte infiltration of the gland, leading to early pancreatic regeneration. The involved mechanisms are likely to be multifactorial and are mediated, at least in part, by anti-inflammatory properties of obestatin[105].

**Obestatin signalling.** Pazos´s group dilucidated the transmembrane signalling pathway responsible for obestatin induced-Akt activation in human gastric carcinoma cells; KATO III and AGS[106]. They carried out an analysis of the sequential transmembrane signalling pathway of obestatin to characterize the intracellular mechanisms responsible for the activation of Akt, a serine/threonine kinase that acts as a key molecule of apoptosis, transcription and cell cycle, in addition to his role on the regulation of metabolism [107] . Results showed that Akt activation requires the phosphorylation of T308 in the A-loop by the phosphoinositide-dependent kinase 1 (PDK1) and S473 within the HM by the mTOR kinase complex 2 (mTORC2: RICTOR, mLST8, mSin1, mTOR kinase) with participation neither of Gi/o-protein nor Gβ dimers. Obestatin induces the association of the GPR39/β-arrestin1/Src signalling complex leading to the transactivation of the epidermal growth factor receptor (EGFR) and subsequently to the activation of Akt (**Diagram 6**). After administration of

[103] Ceranowicz P, Warzecha Z, A. Dembinski A, *et al.* Pretreatment with obestatin inhibits the development of cerulean induced pancreatitis. J PhysioL Pharmacol. 2009;60:95-101.

[104] Bukowczan J, Warzecha Z, Ceranowicz P, *et al.* Pretreatment with obestatin reduces the severity of ischemia/reperfusion- induced acute pancreatitis in rats. Eur J Pharmacol. 2015;760:113-21.

[105] Bukowczan J, Warzecha Z, Ceranowicz P, *et al.* Obestatin accelerates the recovery in the course of ischemia/reperfusion- induced acute pancreatitis in rats. PLoS ONE. 2015;10:E0134380.

[106] Álvarez CJ, Lodeiro M, Theodoropoulou M, *et al.* Obestatin stimulates Akt signalling in gastric cancer cells through b-arrestin-mediated epidermal growth factor receptor transactivation. Endocr-Relat Cancer. 2009;16:599-611.

[107] Manning BD, Cantley LC. Akt/PKB signalling: navigating downstream. Cell. 2007;129:1261-74.

obestatin, phosphorylation of both mTOR (S2448) as p70S6K1 (T389) increases with a time course in parallel to the activation of Akt. Apart from the obvious complexity and specificity of cellular signalling pathways of EGFR transactivation, in KATO III cells they found that the signalling routes of ERK1/2 and Akt act in parallel. Based on the experimental data obtained, a signalling pathway involving a beta-arrestin 1 scaffolding complex and EGFR to activate Akt signalling is proposed (**Diagram 6**)[106].
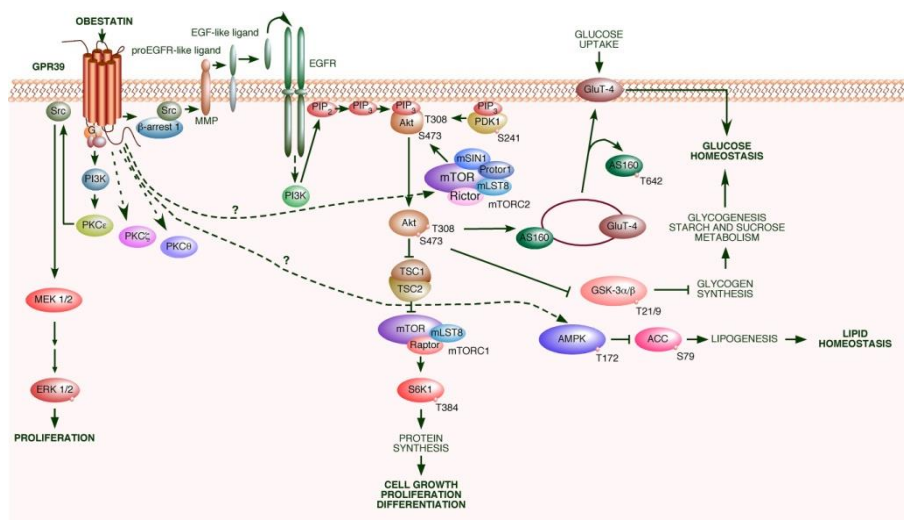
**Diagram 6.** Proposed model of signalling pathway for Akt and ERK1/2 activation in response to obestatin. Translocation of β-arrestins 1 to obestatin receptor (GPR39) allows its association with Src. β-arrestin 1 activates Src (phosphorylation at Y416) triggering the transactivation of EGFR and the subsequent downstream Akt signalling. Alvarez CJ *et al.* Endocr-Relat Cancer. 2009;16:599-611. With permissions from Bioscientifica Limited.

## OBESTATIN RECEPTOR

**GPR39 receptor:** The G-protein coupled receptor 39 (GPR39) is a seven trans-membrane-spanning proteins, member of the ghrelin receptor family comprising of the ghrelin receptor, neurotensin receptors, and motilin receptor[108]. GPR39 exists in two isoforms: the full-length active receptor (GPR39-1a) containing 7 transmembrane (7TM) domains and the truncate form which is biologically inactive (GPR39-1b)[109] containing 5 transmembrane domains.

---

[108] Tremblay F, Perreault M, Klaman LD, *et al.* Normal food intake and body weight in mice lacking the G protein-coupled receptor GPR39. Endocrinology. 2007;148:501-6.
[109] Egerod KL, Holst B, Petersen PS, *et al.* GPR39 splice variants versus antisense gene LYPD1: expression and regulation in gastrointestinal tract, endocrine pancreas, liver and white adipose tissue. Mol Endocrinol. 2007;21:1685-98.

The endogenous ligand of GPR39 was unknown until Zhang *et al.* based on the data of radiolabelled ligand binding assay identified obestatin as a GPR39 ligand[72]. Subsequent studies on bone metabolism[110] and term pregnancy[111] have shown the correlation of both receptor and ligand. Other studies tested the influence of the acute GPR39 deficiency by siRNA showing that observed obestatin effects were mediated by GPR39 receptor in several cell lines (healthy and pathological)[112,113]. Recently, Camiña's group demonstrated that obestatin coimmunoprecipitated specifically with GPR39, validating the binding of obestatin to this receptor in cultured C2C12 myoblast cells[114].

**GPR39 structure.** The human GPR39 is a single copy gene mapped to chromosome 2 at q21-q22, encoding the 453 amino acid. Analysis of the genomic structure revealed that it consists of two exons separated by a very large intron of approximately 200 kb. Importantly, the fact that that GPR39 is a 7TM receptor, which is known to be highly drugable proteins, directly makes it an interesting target for the development of drugs (**Diagram 7**)[115].

---

[110] Pacheco-Pantoja EL, Ranganath LR, Gallagher JA, *et al.* Receptors and effects of gut hormones in three osteoblastic cell lines. BMC Physiol. 2011;11:12-52.

[111] Fontenot E, DeVente JE, Seidel ER. Obestatin and ghrelin in obese and in pregnant women. Peptides. 2007;28:1937-44.

[112] Gurriarán-Rodríguez U, Al-Massadi O, Crujeiras AB, *et al.* Preproghrelin expression is a key target for insulin action on adipogenesis. J Endocrinol. 2011;210:R1-7.

[113] Gurriarán-Rodríguez U, Santos-Zas I, Al-Massadi O, *et al.* The obestatin/GPR39 system is up-regulated by muscle injury and functions as an autocrine regenerative system. J Biol Chem. 2012;287:38379-89.

[114] Gurriarán-Rodríguez U, Santos-Zas I, González-Sánchez J, *et al.* Action of obestatin in skeletal muscle repair: stem cell expansion, muscle growth, and microenvironment remodeling. Mol Ther. 2015;23:1003-21.

[115] Holst B, Egerod KL, Jin C, *et al.* G-protein-coupled receptor 39 deficency is associated with pancreatic islet dysfunction. Endocrinology. 2009;150:2477-585.

**Diagram 7.** Shows a serpentine model of GPR39 in which residues highlighted in black indicate residues that are most highly conserved within the family and residues highlighted in gray indicate residues that are generally conserved. The position of the intron, which is conserved throughout the ghrelin receptor family, is indicated by an orange line. Egerod *et al*. Mol Endocrinol. 2007;21:1685-98. With permission from Oxford Univeristy Press.

**GPR39 expression.** GPR39-1a, the full-length biologically active form, GPR39 expression has been determined in mouse by specific qPCR, in tissues such as the liver, gastrointestinal mucosa, white adipose tissue, kidney, the pituitary gland, the kidney, the white adipose tissue, the muscle, the heart, the brain, the spleen, the thyroid and the lung[109,116]. In recent years an extensive immunohistochemical characterization of GPR39

[116] McKee KK , Tan CP, Palyha OC, *et al*. Cloning and characterization of two human G protein-coupled receptor genes (GPR38 and GPR39) related to the growth hormone secretagogue and neurotensin receptors. Genomics. 1997;46:426-34.

has been defined in human tissues such as stomach[117] and muscle[114]. GPR39 is strongly expressed in muscular tissue as well as in stellate cells (muscle stem cells) and is a key therapeutic target in human muscle regeneration[83,113,114]. Also in mice sebaceous glands GPR39 colocalizes with the stem cell marker, Blimp1, in a specific cell population[118]. In human stomach, GPR39 presents a strong immunohistochemical staining for chief cells, located at the base of the oxyntic glands. In addition to normal tissue, GPR39 is expressed in human gastric adenocarcinomas where the expression presents a correlation with tumour degree[117]. Until now the bibliography only describes the detection of GPR39 in mouse by RT-PCR[109].

## OBESTATIN/GPR39 SYSTEM IN CANCER

After the discovery of obestatin, numerous papers agree that this hormone or the receptor also have a pathophysiological role in cancer. In humans Volante´s group suggested that obestatin expression is reduced in thyroid and neuroendocrine pancreatic tumour because obestatin may be specifically downregulated by these tumour types in order to circumvent the inhibition of proliferation demonstrated *in vitro*[119]. In 2009 Markowska *et al.* report that blood concentrations of obestatin both in women with benign ovarian tumours and those with ovarian cancer were higher than in the control group[120]. Similar observations have been made

---

[117] Alén BO, Leal-López S, Otero Alén M, *et al*. The role of the obestatin/GPR39 system in human gastric adenocarcinomas. Oncotarget. 2015;7:5957-71.

[118] Zhao H, Qiao J, Zhang S. GPR39 marks specific cells within the sebaceous gland and contributes to skin wound healing. Mol Endocr. 2007;7:1685-98.

[119] Volante M, Rosas R, Ceppi P, *et al*. Obestatin in human neuroendocrine tissues and tumours: expression and effect on tumour growth. J Pathol. 2009;218:458-66.

[120] Markowska A, Ziółkowska A, Jaszczyńska-Nowinka K, *et al*. Elevated blood plasma concentrations of active ghrelin and obestatin in benign ovarian neoplasms and ovarian cancers. Eur J Gynaecol Oncol. 2009;30:518-22.

in prostate cancer, where obestatin blood serum concentration was higher than in benign prostate hyperplasia and control[121]. In human esophageal squamous cell carcinoma (ESCC) found that GPR39 was frequently overexpressed in primary ESCC which was significantly associated with the lymph node metastasis. Moreover, depletion of endogenous GPR39 by siRNA could effectively decrease the oncogenicity of ESCC cells[122]. Also in human gastric adenocarcinomas was found an aberrant pattern of GPR39 expression, correlating to the dedifferentiation of the tumour and highlight the usefulness of GPR39 as a prognostic marker of these tumours[117].

---

[121] Malendowicz W, Ziolkowska A, Szyszka M, *et al.* Elevated blood active ghrelin and unaltered total ghrelin and obestatin concentrations in prostate carcinoma. Urol Int. 2009;83:471-5.

[122] Xie F, Liu H, Zhu YH, *et al.* Overexpression of GPR39 contributes to malignant development of human esophageal squamous cell carcinoma. BMC Cancer. 2011;11:86.

# OBJECTIVES

The fact that the obestatin/GPR39 system regulates the expression of distinctive proteins of EMT and angiogenesis, causing phenotypic changes, increasing the proliferation, migration and invasion of gastric cancer cells, together with the enhancing effect of obestatin on proliferation, the capacity of invasion and the reorganization of the cytoskeleton observed in the PANC-1 pancreatic tumour line, leads us to postulate its applicability to antagonize the fundamental mechanisms associated with the development of pancreatic cancer. However, it is necessary to deepen the mode of action of the obestatin/GPR39 system to define its potential as a therapeutic target in the treatment of pancreatic cancer.

The objective of this project is to define the potential of the obestatin/GPR39 system as a therapeutic target in the treatment of pancreatic cancer and chronic pancreatitis.

This objective is subdivided into the following sub-objectives:

1. Study of the expression of the obestatin/GPR39 system in the pancreatic systems of the study.

2. Study of the functionality of the obestatin/GPR39 system in the pancreatic systems of the study.

# MATERIAL AND METHODS

## MATERIALS

### PEPTIDES

Human obestatin peptide and non amidated obestatin was obtained from California Peptide Research Inc. (Napa, CA, US) and Biomedal (Sevilla, ES) respectively listed in the **Table 2**.

**Table 2:** Peptides. Relation of the peptides used in the different analyses performed in this work.

| Materials | Code | Manufacturer |
|---|---|---|
| Human obestatin | 471-97 | California Peptide Research Inc. |
| Human deamidated obestatin | SE-4764 | Biomedal |

### HUMAN SAMPLES

The study protocol was approved by the local ethical committee (CAEI Galicia, 2017/294) and carried according to the Declaration of Helsinki. All of the FFPE (formalin-fixed paraffin-embedded) human pancreas samples were obtained from the Biobank of the University Clinical Hospital of Santiago de Compostela, Spain. Pathological tissue was obtained from patients with pancreatic adenocarcinoma. The pathological tissue samples were from pancreatic adenocarcinomas located in pancreas area. CP samples corresponded to patients who have undergone surgery for complications secondary to CP as abdominal pain refractory to medical treatment, duodenal stenosis, biliary stenosis and persistence of inflammatory mass in the pancreatic head, stenosis of the main pancreatic duct with retrograde dilation, or compression of the portal vein. The surgical control specimens were located at least 3 cm from the adenocarcinoma. All of the examined control tissues originated

from macro and microscopically normal pancreatic tissue. The samples histological classification was assesed by three independent pathologists from the Pathology Department of the University Clinical Hospital of Santiago de Compostela, Spain. Grading of pancreatic adenocarcinomas was performed according to the 7th edition of the American Joint Committee Cancer staging manual[123].

A total of 36 patients were selected, of which six corresponded CP, five to PanIN, and 24 to PDAC. In the case of PDAC, three levels of differentiation were used to classify the grading as follows: well (WD) in seven samples, moderately (MD) in ten samples, and poorly differentiated (PD) in seven samples. Also, in five cases, the same patient provided PDAC samples with two degrees differentiation.

## CELL LINES

The following human PDAC cells lines were used in this work: PANC-1 obtained from ATCC (ECACC, Wiltshire, UK). The RWP-1 and BxPC-3 cell lines were kindly provided by Dr Real (Epithelial Carcinogenesis Group, Cancer Cell Biology Programme, Spanish National Cancer Research Centre-CNIO, Madrid, Spain).

The human PSCs immortalized line (RLT-PSC) was a gift from Dr Jesnowski (German Cancer Research Centre; Heidelberg, GE) and Dr Löhr (Karolinska Institutet, Stockholm, Sweden).

All cell lines were maintained as recommended by the supplier (**Table 3**) with 100 U/mL penicillin G, 100 mg/mL streptomycin sulphate and with 5% $CO_2$ at 37 °C. PDAC cell lines were also cultured with 2.5

---

[123] Edge SB, Byrd DR, Compton CC, *et al.*, editors. AJCC cancer staging manual. 7th ed. New York: Springer-Verlag; 2009; 117-126.

mM L-glutamine. Cells were passaged at 85-90% confluence using Accutase® (Sigma-Aldrich, St. Louis, MO, US).

**Table 3:** Cells. Relation of human cell lines and its growth medium used in this work. FBS: foetal bovine serum.

| Cell line | Growth medium (v/v) |
|---|---|
| RLT-PSC: Pancreatic stellate cells immortalized line | DMEM + 10% FBS |
| PANC-1: Pancreatic carcinoma | DMEM + 10% FBS |
| RWP-1: Pancreatic carcinoma | DMEM + 10% FBS + 1% Pyruvate 100 mM |
| BxPC3: Pancreatic carcinoma | DMEM + 10% FBS + 1% Pyruvate 100 mM |

## ANTIBODIES

The details of primary antibodies used in this work are summarized at the end of this section in the **Table 4.** The relation of secondary antibodies is listed in the **Table 5.** Preabsorption tests were performed with control peptides which are listed in the **Table 6**. The Human MAPKs and tyrosine kinase receptors (RTKs) included in the array are listed in the **Tables 7** and **8** respectively.

## METHODS

### IMMUNOHISTOCHEMISTRY

Immunohistochemistry was performed according to the protocol used by Raghay *et al*[124]. The samples were immersion-fixed in 10% buffered formalin for 24 h, dehydrated and embedded in paraffin by a

---

[124] Raghay K, Garcia-Caballero T, Bravo S, *et al*. Ghrelin localization in the medulla of rat and human adrenal gland and in pheochromocytomas. Histol Histopathol. 2008;23:57-65.

standard procedure. The 3 µm-thick sections were mounted on Histobond adhesion microslides (Marienfeld, Lauda-Königshofen, DE), dewaxed and rehydrated. The immunohistochemical technique was automatically performed using an AutostainerLink 48 instrument (Dako Agilent Technologies, Glostrup, DK). Anti GPR39 primary antibody was used (**Table 4**). EnVision™ peroxidase FLEX/HRP (Dako Agilent Technologies, Glostrup, DK) was employed as a detection system. Briefly, the procedure comprised the following steps: 1) epitope retrieval in 10 mM citrate buffer (pH 6.0) using a microwave (750 W, 10 min); 2) incubation with peroxidase-blocking agent (5 min); 3) incubation with primary antibody (30 min); 4) incubation with labelled polymer-horseradish peroxidase (HRP, dextran polymer conjugated with HRP and affinity-isolated immunoglobulins; 30 min); 5) incubation with 3,3'-diaminobenzidine (DAB)-tetrahydrochloride (Dako Liquid DAB + Substrate-chromogen system; 10 min); and 6) counterstaining with Harris haematoxylin solution (HHS) (9 min). The preadsorption control for GPR39 was performed applying the primary antibody plus GPR39 control peptide to positive samples. For obestatin, GFAP, α-SMA, adipophilin (ADRP), and KI67, the immunohistochemical protocol has been performed manually with the following modifications: 1) epitope retrieval in 10 mM citrate buffer (pH 6.0) using a microwave (750 W, 20 min; then to room temperature, 20 min); 2) incubation with primary antibody in EnVision FLEX Antibody Diluent (overnight, room temperature); 3) incubation with peroxidase-blocking agent (10 min); 4) incubation with HRP (60 min); 5) incubation with DAB-tetrahydrochloride (10 min); and 6) counterstaining with HHS (9 min). PBS replacement of the primary antibody was used as control. Photographs were taken using a Zeiss Observer Z1 microscope and the Axiovision software (Carl Zeiss, Göttingen, GE). For GPR39 expression quantification in the PDAC samples, ten fields of the tumour

representative DAB images were quantified by using the Image-J (Fiji-64 bit) software.

## IMMUNOHISTOFLUORESCENCE

The corresponding primary antibodies were incubated diluted in EnVision FLEX Antibody Diluent (**Table 4**) at room temperature for 16h. After three washes with PBS, samples were incubated with the secondary antibody (Alexa 488 anti-rabbit and Alexa 594 anti-mouse antibody) in PBS at room temperature for 1h. DAPI (4 ',6-Diamidino-2-Phenylindole Dihydrochloride; Invitrogen Carlsbad, CA, US) was used to counterstain the cell nuclei. Digital images of tissues were acquired with a Zeiss Axio Vert.A1 fluorescence microscope (Carl Zeiss AG, Oberkochen, Germany).

## IMMUNOCITOCHEMISTRY

Immunocitochemistry detection of RLT-PSC activation marker proteins and GPR39, obestatin in BxPC-3, RWP-1 and RLT-PSC: Cells were cultured at a density of 4-5 x $10^3$ cells per well in the culture medium described above on 8-well Lab-Tek II chamber slides covered with cell conditioning solution 2 (CC2) glass slide coverslips. At the next day the intact cells were fixed in formol 4% for 20 min and overnight 4 °C in ethanol 70°. 1) the cells were pre-treated with Dako cytomation Target Retrieval Solution pH 6.0 1x for 20 min by microwave incubation at 750 W cooled at RT for 20 min; 2) and incubated with primary antibody (1:500) overnight RT; incubation with peroxidase-blocking agent (10 min); 3) incubation with labelled polymer-horseradish peroxidase (HRP, dextran polymer conjugated with HRP and affinity-isolated immunoglobulins) 30 min; 4) incubation with 3,3′-diaminobenzidine (DAB)-tetra hydrochloride

(Dako Liquid DAB + Substrate-chromogen system) (10 min or until the immune reaction was visible); and finally 5) counterstaining with Harris haematoxylin solution (HHS) (30 s).

For PDAC cells obestatin immunohistochemistry is described above, without pre-treatment with Dako cytomation Target Retrieval Solution pH 6.0, and permeabilized with 0,25% Triton X-100 in PBS for 10 min antibody concentration is described at **Table 4**.

For RLT-PSC obestatin was permeabilized for 40 min with 0.25% Triton X-100 in PBS. The preadsorption control for obestatin was performed applying the primary antibody plus obestatin to positive samples. For RLT-PSC GPR39 is not permeabilized. The preadsorption control for GPR39 was performed applying the GPR39 control peptide plus the primary antibody to positive samples.

In all cases, triplicate dishes were used for each experimental point.

## IMMUNOCITOFLUORESCENCE

Immunofluorescence detection of F-actin, E-cadherin, Vimentin, pp38 α/β/γ, and PARD3. Cells were cultured at a density of 4-6 x $10^3$ cells per well in the culture mediums described above on 8-well Nunc® Lab-Tek® II chamber slides covered with CC2 glass slide coverslips. For polarity markers in RLT-PSC cells were cultured at a density of 50 x $10^3$ cells per microscope glass slide. The next day, the medium was renewed, and the cells were cultured in a serum-free medium (300 µL) for 24 h. Serum-starved cells were stimulated or not with obestatin and FBS at 37 °C, time and concentration indicated in corresponded figure. Intact cells were fixed with 3.7% paraformaldehyde buffered with PBS (PFA-PBS) for 30 min, washed, permeabilized with 0.25% Triton X-100 in PBS for 45 min in PANC-1 and for 15 min in RLT-PSC, and blocked with 1% BSA in PBS

containing 0.2% Tween-20 (PBST) for 30 min and then incubated with anti-E-cadherin mouse antibody diluted in 1% BSA in PBST (1:500) or anti-vimentin (1:1,000) for 1 h at RT. After that cells were incubated with the secondary antibody (Alexa 488 anti-mouse antibody (1:1,000)) and Phalloidin CruzFluor 594 in 1% BSA in PBST (1:1,000) for 1 h at RT. DAPI was used to counterstain the cell nuclei. Digital images of cells were acquired with a Zeiss Axio Vert.A1 fluorescence microscope (Carl Zeiss AG, Oberkochen, Germany).

**Aggresome and E-Cadherin detection.** Aggresome detection was performed using the ProteoStat Aggresome detection kit (Enzo Life Sciences, Farmingdale, NY, US) according to the manufacturer's instructions.

Cells were seeded directly on the glass slides, to 80% confluence. The next day, the medium was renewed, and the cells were cultured in a serum-free medium for 24 h. Serum-starved cells were stimulated or not with obestatin (100 nM 48 h) at 37 °C and negative control with vehicle only. Control positive cells were incubated with Proteasome Inhibitor (MG-132) 5 μM 18 h. After 48 h, intact cells were fixed with 4% buffered PFA-PBS for 30 min at TA, washed, permeabilized with Permeabilizing Solution for 30 min. Dispense Dual Detection Reagent, samples were protected from light and incubated 30 min at RT. To mark with E-cadherin together, then proceed bathed the samples in blocking solution (BSA 1% in PBST) for 1 h RT protected from light and incubated with anti-E-cadherin mouse antibody diluted in 1% BSA in PBST (1:500) for 1 h at RT. Cells were rinsed, air dried and mounted with DAPI in Prolonged Gold Anti-fade mounting media (Invitrogen, OR, US).

## MIGRATION, INVASION, ADHESION

**Wound healing assay (migration assay).** PANC-1 and activated RLT-PSC cells (aRLT-PSCs) were seeded on 6-well plates, grown to 100% confluence and serumdeprivate for 24 h. Then wounded with a sterile pipette tip to remove cells by linear scratches. RWP-1 and BxPC-3 cells were analysed in a wound healing assay using IBIDI culture inserts (IBIDI GmbH, Martinsried, Germany) according to the manufacturer's protocol. The cells were washed and maintained in culture medium, at the indicated concentrations of obestatin, FBS or both. The progress of migration was photographed immediately after injury and until indicated time after wounding, near the crossing point. The wound was calculated by tracing along the border of the scratch using the ImageJ64 analysis software and using the following equation:

%wound closure= [[wound area (0 h)-wound area (x h)]/ wound area (0 h)] x 100[113].

*In vitro* **invasion assay**: The migration and invasion assays were carried out using a Transwell chamber (Corning, NY, US). The inserts contained an 8 µm pore size polycarbonate membrane. Cells were seeding into the upper chambers at a density of 5-7x10$^4$ in starved medium and stimulated with obestatin, FBS or both for the indicated doses at 37 °C and the cells were allowed to migrate and invade. After 16-21 h incubation at 37 °C, non-invasive cells were scrubbed off the upper surface of the membrane using a moist cotton-tipped swab. Invasive cells on the lower surface of the membrane, which had invaded the ECM and migrated through the polycarbonate membrane, were stained by 4 µmol/L calcein-acetoxymethyl ester (Invitrogen-Thermo Fisher, Carlsbad, CA, US). The number of invading cells was counted in 10 random high-powered fields per filter by Zeiss Axio Vert.A1 fluorescence

microscope (Carl Zeiss AG, Oberkochen, Germany) using a ×10 objective. The invasion was calculated using the ImageJ64 analysis software[125].

***In vitro* adhesion assay:** aRLT-PSC cells were serum-starved for 24 hours in DMEM, detached using Acutasse® and washed twice with serum-free DMEM before treatment. The cells were treated with obestatin 100 nM and incubated at 37°C for 1 h in plates coated with collagen I. Unattached cells were removed by washing twice with PBS and fixed with 3.7% paraformaldehyde in PBS for 10 min and stained with trypan blue. The attached cells were counted, and the percentage of adherent cells in each group was calculated using the following equation:

% adhesion = number of adherent cells in treatment group/number of adherent cells in non-treatment group x 100[126].

The adhesion assays were repeated three times.

## PROLIFERATION ASSAY

**Cell proliferation assays.** The cell proliferation was measured using a bromodeoxiuridine (BrdU) cell proliferation enzyme-linked immunosorbent assay (ELISA) kit (Roche Diagnostics, Mannheim, DE). The BrdU assay was performed according to the manufacturer's protocol. Cells were cultured in a 96-well multiplate at a density of 2.5-5 x $10^3$ cells per well in the culture medium described above for 24 h. The procedure comprised the following steps: 1) 0% FBS for 24 h; 2) stimulation with conditioned medium, 10% FBS, human and no amidated obestatin for the indicated time period and doses; 3) incubation with BrdU-labeling

---

[125] Gao Z, Wang X, Wu K, *et al.* Pancreatic stellate cells increase the invasion of human pancreatic cancer cells through the stromal cell-derived factor-1/CXCR4 axis. Pancreatology. 2010;10:186-193.

[126] Almahariq M, Tsalkova T, Me F.C *et al.* A novel EPAC-specific inhibitor suppresses pancreatic cancer cell migration and invasion. Mol. Pharmacol. 83:122-128.

solution (10 µL, 16 h, 37 °C); 4) removal of labelling solution and fixing with FixDenat solution (200 µL, 30 min, 25 °C); 5) incubation with anti-BrdU-peroxidase (POD) antibody solution (100 µL, 90 min, 25 °C); and, 6) washing followed by the addition of substrate solution (100 µL, 30 min). The BrdU incorporation was quantified using the spectrophotometric absorbance at 370 nm (reference wavelength at 492 nm) measured with an the mean absorbance of the control cells represented 100% cell proliferation, and the mean absorbance of the EPOCH 2 Microplate Spectrophotometer (BioTek, Winooski, VT, US) treated cells was related to the control values to determine sensitivity. In all cases, each experiment point was replicated eight times.

**IMMUNOBLOT ANALYSIS**

**Immunoblot analysis in cells.** Serum-starved cells were stimulated with obestatin for the indicated time period and doses at 37 °C. The medium was then aspirated, and cells were lysed in ice-cold lysis buffer [RIPA buffer: 50 mM Tris-HCl pH 7.2, 150 mM NaCl, 1 mM EDTA, 1% (v/v) NP-40, 0.25% (w/v) Na-deoxycholate, protease inhibitor cocktail (1:100, Sigma Chemical Co., St. Luis, MO, US), phosphatase inhibitor cocktail (1:100, Sigma Chemical Co., St. Luis, MO, US)]. The soluble cell lysates were pre-cleared by centrifuging at 14,000 rpm for 15 min. The protein concentration was evaluated with the QuantiPro™ BCA Assay kit (Sigma Chemical Co., St. Luis, MO, US). The same amount of protein for each sample was separated on 10% SDS/polyacrylamide gels and transferred to nitrocellulose membranes (Bio-Rad, Hercules, CA, US). The blots were then incubated with the corresponding antibodies and processed as described above. The blots shown are representative of six experiments. The image processing was performed using the NIH Image Software

ImageJ 1.49 (National Institutes of Health, Bethesda, MD, US).

## RNA EXTRACTION, CDNA SYNTHESIS AND REAL-TIME PCR

**RNA extraction, cDNA synthesis and real-time PCR**. Adherent cells ($3x10^5$) were solubilized in 1 mL of TRI Reagent® (Molecular Research Centre, Inc. Cincinnati, US) and total cellular RNA was isolate according to manufacturer´s instructions.

After DNase I treatment (Thermo Fisher Scientific, Waltham, MA), 1 µg of total RNA was reverse transcribed using High-Capacity cDNA Reverse Transcription Kits (Applied Biosistems, Thermo Fisher Scientific, Waltham, MA). Real-time PCR (RT-PCR) was carried out in Applied Biosystems StepOnePlusTM RT-PCR System (Applied Biosystems/Ambion, TX, US) using Luminaris HiGreen qPCR (quantitative PCR) Master Mix (Thermo Fisher Scientific). The 2−ΔΔCt method was used to analyse the relative changes in each gene's expression normalized against B2M (mRNA) expression. Sequences of the primers used in this study were as follows:
B2M
Fw 5´-ACTGAATTCACCCCCACTGA-3´
Rv 5´-CCTCCATGATGCTGCTTACA-3´
NM23H1
Fw 5´-CAGCCGGAGTTCAAACCTA-3´
Rv 5´-GTATAATGTTCCTGTCAACTTGT-3´

## HUMAN ARRAY

**Human Phospho-MAPKs and Phospho-RTKs Array and analysis.** To analyse the activation profiles of MAPKs or RTKs the Proteome

Profiler™ Human Phospho-MAPK Array Kit and Human Phospho-RTKs Array Kit (R&D Systems, Minneapolis, MN, US) was used according to the manufacturer's instructions. This method allows simultaneous detection of the relative levels of phosphorylation of 26 Mitogen-Activated Protein Kinases (MAPKs) and other serine/threonine kinases or detection of the relative tyrosine phosphorylation levels of 49 different phospho-RTKs. Each array contained duplicate validated control and capture antibodies for specific MAPKs or RTKs respectively. RLT-PSC or PANC-1 serum-starved cells were stimulated with obestatin 100-200 nM respectively for the indicated time period (5 min) at 37 °C. The medium was then aspirated, and cells were lysed in ice-cold array lysis buffer with protease inhibitor cocktail and phosphatase inhibitor cocktail (1:100, Sigma Chemical Co., St. Louis, MO, US). After 30 min in ice-cold, samples were centrifuged at 14,000 xg for 5 min at 4 °C and the supernatant was transferred into a clean tube. Total protein concentration was quantified using the QuantiPro™ BCA Assay kit (Sigma Chemical Co., St. Luis, MO, US). The membranes were incubated with 200 or 300 µg of protein. Briefly, phospho-MAPK array membranes were blocked with Block Buffer (1 h) and incubated O/N with 1.5 mL of cell and tissue lysate after normalization for equal amounts of protein. After extensive washing with Wash Buffer the membranes were incubated with Streptavidin-HRP (RT, 30 min). The unbound Streptavidin-HRP antibody was washed with Wash Buffer. Each array was then incubated with Chemi Reagent Mix, and exposed to X-ray film (1-10 min). Dot blot densitometric analysis of the immunoblots was performed in duplicate, using NIH ImageJ software 1.49 (National Institutes of Health, Bethesda, MD, US). The relative phosphorylation profiles in 2 groups were normalized by using mean of positive control spots that are located in all 3 corners of the array. Fold

changes were calculated by dividing untreated phosphorylation profile to treated profile accordingly[127].

**Human Phospho-RTKs Array and analysis.** To analyze the activation profiles of RTKs the Abcams´s human RTK Phosphorylation Antibody Array was used according to the manufacturer's instructions. This method allows simultaneous detection of the relative tyrosine phosphorylation levels of 71 different phospho-RTKs. Each array contained duplicate validated control and capture antibodies for specific RTKs. Serum-starved cells were stimulated with obestatin 100 nM for the indicated time period (10 min) at 37 °C. The medium was then aspirated and washed with 1x PBS before add Lysis Buffer. The PANC-1 cell line was lysed in lysis buffer with protease and phosphatase inhibitor cocktail set II. After 30 min in ice-cold, samples were centrifuged at 14,000 xg for 10 min at 4 °C and the supernatant was transferred into a clean tube. Total protein concentration was quantified using the QuantiPro™ BCA Assay kit (Sigma Chemical Co., St. Luis, MO, US). The membranes were incubated with 200 µg of protein. Briefly, phospho-RTK array membranes were blocked with Block Buffer (30 min) and incubated O/N with 1 mL of cell and tissue lysate after normalization for equal amounts of protein. After extensive washing with Wash Buffer the membranes were incubated with Biotinylated Anti-Phosphotyrosine Antibody (RT, 2 h). After extensive washing with Wash Buffer the membranes were incubated with HRP-Conjugated Streptavidin (RT, 2 h). Each array was then incubated with equal volumes (1:1) of Detection Buffer C and Detection Buffer D, and exposed to X-ray film (1-10 min). Dot blot densitometric analysis of the immunoblots was performed in duplicate, using NIH ImageJ software 1.49

---

[127] Gur S, Sikka SC, Abdel-Mageed AB, *et al.* Imatinib mesylate (Gleevec) induces human corpus cavernosum relaxation by inhibiting receptor tyrosine kinases (RTKs): identification of new RTK targets. Urology. 2013;82:745.

(National Institutes of Health, Bethesda, MD, US). The relative phosphorylation profiles in 2 groups were normalized by using mean of positive control spots that are located in all 4 corners of the array. Fold changes were calculated by dividing untreated phosphorylation profile to treated profile accordingly[127].

## INDUCTION AND QUANTIFICATION OF ACTIVATION/QUIESCENCE IN RLT-PSC

**Activated PSCs (aRLT-PSC) culture.** To maintain activate state, RLT-PSC cell line was culture in DMEM (Dulbecco's Modified Eagle Medium. Lonza) 4.5 g/L glucose concentration supplemented with 10% fetal bovine serum (FBS, GE Healthcare Hyclone) and with 100 U/mL penicillin G, 100 mg/mL streptomycin sulphate (Sigma-Aldrich, St. Louis, MO, US). Cells were cultured at 37 °C atmosphere containing 5% $CO_2$ and 95% of relative humidity. Cells were passaged at 85-90% confluence using Accutase® (Sigma-Aldrich, St. Louis, MO, US) until passage number 20[128].

**Quiescent PSCs (qRLT-PSC) culture:** To induce a quiescent phenotype, 80% confluent aRTL-PSCs were treated with Accutase®, resuspended in serum-free DMEM 4.5 g/L glucose supplemented with 100 U/mL penicillin G, 100 mg/mL streptomycin sulphate (Sigma-Aldrich) and 2.5 mM N-acetyl cysteine (Sigma-Aldrich), then plated at a concentration of 20,000 cells /$cm^2$ on collagen I, 0.1 g/L coated plates (Corning®), and incubated at 37 °C for 24 h[129].

---

[128] Jesnowski R, Fürst D, Ringel J, *et al.* Immortalization of pancreatic stellate cells as an *in vitro* model of pancreatic fibrosis: deactivation is induced by matrigel and N-acetylcysteine. Lab Invest. 2005;85:1276-91.
[129] Wehr AY, Furth EE, Sangar V, *et al.* Analysis of the human pancreatic stellate cell secreted proteome. Pancreas. 2011;40:557-66.

The quiescent state can also be achieved by seeding the cells in 5% FBS (GE Healthcare Hyclone) for up to 7 days under the same conditions described above[128].

**Rat tail collagen type I extraction and plate coating.** Tails were collected from Sprague Dawley rats, and stored at -80 °C until use. Skins of tails were removed exposing tendons. Tendons were extracted using fine tweezers, washed with phosphate saline buffer (PBS; Sigma-Aldrich, St. Louis, MO, US), and 70% ethanol (Montplet, Barcelona, Spain). Tendons were kept in 0.1% acetic acid, at 4 °C under stirring, until dissolved. 250 mL of 0.1% acetic acid was used for each g of tendons. The tendons/acetic acid mix were then centrifuged at 3,200 g at 4 °C for 90 min. The supernatant (collagen extract) was collected and transferred to a glass bottom with screw cap. Cloroform (1/10 of collagen volume) was added and the mixture was allowed to settle overnight at 4 °C. The upper collagen solution was aseptically removed and stored at 4 °C.

Collagen solution was quantified using QuantiPro™ BCA Assay Kit (Sigma-Aldrich, St. Louis, MO, US), and concentration was adjusted to a 0,5 g/L stock solution. Stock solution was diluted to a 0.1 g/L working solution in sterile water suitable for cell culture (Sigma-Aldrich, St. Louis, MO, US). The plates were treated with collagen working solution for 1 h at room temperature (RT). Working solution was removed and the plate was allowed to dry up to 1 h under laminar flow and UV light.

**Assay for Oil Red O (Sigma) staining and up take Oil Red O quantification.** Cells were cultured at a density of $900 \times 10^3$ cells per 10 cm plate in quiescent medium with collagen I coating or activated medium described above. As soon as the cells attach (around 5 h) add Cytarabine (Pfizer, Inc.) 50 µM to avoid proliferation of activated RLT-PSC and incubated at 37 °C for 24 h.

The cells were rinsed with PBS and fixed in 4% buffered formalin for at least 1 h until 2 h at RT. Cells were washed twice with ddH$_2$O. Wash cells with 60% isopropanol for 5 min at RT and stained with 0.2% Oil Red O for 10 min at RT. The plates were washed with ddH$_2$O and the cells were photographed.

For Oil Red O quantification all water was removed and plate was dried, 1 mL of 100% isopropanol was added and incubated for 10 min with gently shaking, mix the isopropanol with Oil Red O pipetting up and down and transfer the solution to a 1.5 mL Eppendorf® tube; and measure OD at 520 nm using 100% isopropanol as blank on EPOCH 2 Microplate Spectrophotometer (BioTek, Winooski, VT, US).

**Vitamin A autofluorescence**. Another procedure for the determination of retinol (vitamin A alcohol) consists of direct measurement of the fluorescence of retinol (excitation 328 nm; emission 475 nm)[130] using a Zeiss Axio Vert.A1 fluorescence microscope (Carl Zeiss AG, Oberkochen, DE).

## DATA ANALYSIS

All of the data are reported as the mean ± SEM. A Shapiro-Wilk normality test was performed for each data set. T-tests were carried out for comparisons between two samples. Unpaired t-test was used to assess the statistical significance of one-way or two-way analysis when the test statistic followed a normal distribution. Mann-Whitney test was employed to assess the statistical significance of one-way or two-way analysis when the test statistic did not follow a normal distribution. For

---

[130] Futterman S, Swanson D, Kalina RE. A new, rapid fluorometric determination of retinol in serum. Invest Ophthalmol. 1975;14:125.

multiple comparisons, a statistical ANOVA analysis was performed using an analysis of variance with the Bonferroni post hoc test. Values of $P<0.05$ or $P<0.01$ were considered to be statistically significant and are marked with an asterisks (*, **, ***; **** respectively).

## ETHICAL GUIDELINES

The development of the project was done respecting the Declaration of Helsinki of the World Medical Association 1964 and successive ratifications on ethical principles for medical research on human beings, the Convention for the protection of human rights and the dignity of the human being with respect to the Applications of Biology and Medicine, done in Oviedo on April 4, 1997, ratified by Spain on July 23, 1999 (Official State Gazette of 2000) and successive updates.

The essential documents will be conserved according to the applicable regulations. The Research Ethics Committee (REC) reviewed all relevant study documentation in order to safeguard the rights, safety and well-being of patients. The study only was performed in the centre where the REC authorization was obtained.

The access to the samples and the clinical data of the patients was made from the database of diagnoses coded in the Pathological Anatomy Service.

The researchers participating in this study have committed to respect the Law on Protection of Personal Data (Organic Law 15/1999, of December 13), RB 1720/2007 of December 21, for which the Regulations for the development of Organic Law 15/1999 are approved, to Law 41/2002, of November 14, as well as Law 3/2001, of May 28, (regulator of the informed consent and of the clinical history of the patients), the law 3/2005, of March 7, of modification of the law 3/2001 and the Decree

29/2009 of February 5, by which the access to the history is regulated electronic clinic and Order SSI/81/2017 by which the right to privacy of the patient is regulated and access to the medical record by students and residents in Health Sciences. The clinical data of the patients were collected by the researcher with link to the Sergas in the Data Collection Notebook (CRD). Each CRD is encrypted, protecting the patient's identity. Only the research team have access to all the data collected for the study.

The handling of samples was carried out in accordance with the provisions of Law 14/2007 of July 3 on Biomedical Research and RD 1716/2011, of November 18, which establishes the basic requirements for authorization and operation of biobanks for biomedical research and the treatment of biological samples of human origin, and regulates the operation and organization of the National Biobank Registry for biomedical research. The samples from this study (paraffin blocks) were stored in pathological anatomy services. Once the study is completed, the immunohistochemical preparations are preserved anonymized.

Human cell lines were obtained from:

RLT-PSC. This human immortalized cell line has been developed and provided by Dr. M. Löhr (Karolinska Universitetssjukhuset, Stockholm, SW) and Dr. R. Jessenofsky (German Cancer Research Center, Heidelberg, GE) and possess the necessary permits of the corresponding Ethical Committees in their institutions.

Both the pancreatic ductal adenocarcinoma cell line PANC-1 (purchased from SIGMA) and the pancreatic cancer cell lines BxPC-3 and RWP-1 (provided by Dr. F. Real of the CNIO, Madrid), are commercial human cell lines.

**Table 4: Primary antibodies**. Relation of the primary antibodies used in the different analyses performed in this work. *RTU: Ready to use.

| Antibodies | Use | Dilution | Code | Manufacturer |
|---|---|---|---|---|
| Anti-Active beta Catenin Antibody | WB | 1:1,000 | ab32572 | Abcam |
| Anti-Active beta Catenin Antibody | WB | 1:1,000 | 05-665 | Millipore |
| ADRP (B-6) Antibody | WB | 1:200 | sc-377429 | Santa Cruz Biotech., Inc. |
| Anti-Akt Antibody | WB | 1:1,000 | 9272S | Cell Signalling Tech. |
| Anti-Cathepsin L Antibody | WB | 1:1,000 | ab133641 | Abcam |
| Anti-Collagen I Antibody | ICC | 1:100 | ab34710 | Abcam |
| Anti-Desmin Antibody | ICC | 1:100 | ab15200 | Abcam |
| Anti-Dvl2 (30 D2) Antibody | WB | 1:1,000 | 3224s | Cell Signalling Tech. |
| Anti-E-Cadherin (M168) Antibody | WB | 1:1,000 | ab76055 | Abcam |
|  | IF | 1:500 |  |  |
| Flk1 (C-1158) Antibody | WB | 1:500 | sc-504 | Santa Cruz Biotech., Inc. |
| Anti-GFAP (GF5) Antibody | ICC | 1:100 | ab10062 | Abcam |
|  | WB | 1:500 |  |  |
|  | IHC | 1:100 |  |  |
|  | IF | 1:100 |  |  |
| Anti-GAPDH Antibody | WB | 1:2,000 | ab9485 | Abcam |
| Glucagon (4j80) Antibody | IF | 1:100 | sc-71152 | Santa Cruz Biotech., Inc. |
| Hsp47(G-12) Antibody | IF | 1:250 | sc-5293 | Santa Cruz Biotech., Inc. |
| Anti-Insulin (HB125) Antibody | IF | 1:800 | MU029 | BioGenex |
| Anti-Ki67 (MIB-1) Antibody | IHC/IF | RTU | MIB-1 | DAKO |

**Table 4: *(Continuation)* Primary antibodies**. Relation of the primary antibodies used in the different analyses performed in this work. *RTU: Ready to use.

| Antibodies | Use | Dilution | Code | Manufacturer |
|---|---|---|---|---|
| Anti-Ki67 Antibody | WB | 1:1,000 | ab15580 | Abcam |
| Anti-LC3A/B (D3U4C) Antibody | WB | 1:1,000 | 12741S | Cell Signalling Tech. |
| Anti-N-Cadherin (EPR1791-4) Antibody | WB | 1:1,000 | ab76011 | Abcam |
| Anti-Human NM23-H1 Antibody | WB | 1:1,000 | MAB6256 | R&D Systems |
| Mouse/rat/human Obestatin Antibody | ICC IHQ | 1:100 1:500 | OBSN11-A | Alpha Diagnostic International |
| Anti-Obestatin (Human, Monkey) Purified IgG Antibody | Block | 10 µg/mL | G-031-92 | Phoenix Pharmaceuticals, Inc. |
| Anti-Partitioning-defective 3 Antibody | IF | 1:100 | 07-330 | MERK KGaA, Darmstadt, Germany |
| Anti-Somatostatin antibody [M09204] | IF | 1:100 | ab30788 | Abcam |
| PEDF (H-125) Antibody | WB | 1:500 | sc-25594 | Santa Cruz Biotech., Inc. |
| Pancreatic Polypeptide Anticuerpo (B-2) | IF | 1:100 | sc-514155 | Santa Cruz Biotech., Inc. |
| PDX-1 Antibody (B-11) | IF | 1:100 | sc-390792 | Santa Cruz Biotech., |
| Anti-CD271/NGF R Antibody | IHC | 1:100 | MAB367 | R&D Systems |
| p44/42 MAPK (ERK1/2) Antibody | WB | 1:2,000 | 9102S | Cell Signalling Tech. |
| SQSTM1/p62 Antibody | WB | 1:1,000 | 5114S | Cell Signalling Tech. |
| P-Akt (Ser473) Antibody | WB | 1:1,000 | 9271S | Cell Signalling Tech. |
| P-c-Jun (Ser73) (D47G9)Antibody | WB | 1:1,000 | 3270 | Cell Signalling Tech. |
| p-EGFR Tyr845 Antibody | WB | 1:1,000 | sc-23420R | Santa Cruz Biotech., Inc. |

**Table 4:** *(Continuation)* **Primary antibodies**. Relation of the primary antibodies used in the different analyses performed in this work. *RTU: Ready to use.

| Antibodies | Use | Dilution | Code | Manufacturer |
|---|---|---|---|---|
| P-GSK-3α/β (Ser21/9) Antibody | WB | 1:1,000 | 9331S | Cell Signalling Tech. |
| P-EGF Receptor (Tyr1068) (D7A5) Antibody | WB | 1:1,000 | 3777 | Cell Signalling Tech. |
| P-EGF Receptor (Tyr992) Antibody | WB | 1:1,000 | 2235 | Cell Signalling Tech. |
| p-HSP 27 (B-3) Antibody | WB | 1:100 | sc-166693 | Santa Cruz Biotech., Inc. |
| p-JNK (G-7) Antibody | WB | 1:200 | sc-6254 | Santa Cruz Biotech., Inc. |
| p-MEK-3/6 (B-9) Antibody | WB | 1:200 | sc-8407 | Santa Cruz Biotech., Inc. |
| p-p38 (D-8) Antibody | IF | 1:50 | sc-7973 | Santa Cruz Biotech., Inc. |
| P-p38 MAPK (Thr180/Tyr182) Antibody | WB | 1:1,000 | 9211 | Cell Signalling Tech. |
| P-p44/42 MAPK (ERK1/2) (Thr202/Tyr204) Antibody | WB | 1:2,000 | 9101s | Cell Signalling Tech. |
| P-p53 (Ser15) Antibody | WB | 1:100 | 9284S | Cell Signalling Tech. |
| P-p70 S6 Kinase (Thr389) (108D2) Antibody | WB | 1:1,000 | 9234S | Cell Signalling Tech. |
| P-RSK (C-5) Antibody | WB | 1:100 | sc-377526 | Santa Cruz Biotech., Inc. |
| P-S6 Ribosomal Protein (Ser240/244) Antibody | WB | 1:1,000 | 2215S | Cell Signalling Tech. |

**Table 4:** *(Continuation)* **Primary antibodies**. Relation of the primary antibodies used in the different analyses performed in this work. *RTU: Ready to use.

| Antibodies | Use | Dilution | Code | Manufacturer |
|---|---|---|---|---|
| P-Src Family (Tyr416) Antibody | WB | 1:1,000 | 2101S | Cell Signalling Tech. |
| p-EGFR (Tyr 845)-R Antibody | WB | 1:100 | sc-23420R | Santa Cruz Biotech., Inc. |
| EGFRvIII antibody | WB | 1:500 | orb191506 | Biorbyt Ltd. |
| S-100 Antibody | ICC | RTU* | IR504 | Dako Aligent |
| Anti-Smooth Muscle Actin Antibody | ICC IHC | RTU | IR611 | Dako Aligent |
| Smooth Muscle Actin (CGA7) Antibody | IF/WB | 1:200 | sc-53015 | Santa Cruz Biotech., Inc. |
| Anti-GPR39 Antibody | ICC IF IHQ | 1:500/1:1,000 1:500 1:1,000 | SAB4200185 | Sigma Chemical |
| Anti-GPCR GPR39 Antibody | WB | 1:1,000 | ab213716 | Abcam |
| Anti-GPR39 Antibody | WB | 1:1,000 | NLS139 | Novus Biologicals |
| Anti-Mouse/rat/ human Obestatin Antibody | ICC IHQ | 1:100 1:500 | OBSN11-A | Alpha Diagnostic International |
| Anti-Obestatin (Human, Monkey) Purified IgG Antibody | Block | 10 μg/mL | G-031-92 | Phoenix Pharmaceuticals, Inc. |

**Table 5: Secondary antibodies**. Relation of the secondary antibodies used in the different analyses performed in this work.

| Secondary antibodies | Use | Dilution | Code | Manufacturer |
|---|---|---|---|---|
| Peroxidase-AffiniPure Goat Anti-Rabbit IgG (H+L) | WB | 1:10,000 | 111-035-003 | Jackson ImmunoResearch Europe |
| Peroxidase-AffiniPure Rabbit Anti-Goat IgG (H+L) | WB | 1:10,000 | 305-035-003 | Jackson ImmunoResearch Europe |
| Peroxidase-AffiniPure Goat Anti-Mouse IgG (H+L) | WB | 1:10,000 | 115-035-003 | Jackson ImmunoResearch Europe |
| Goat Anti-Rabbit IgG Fc  (Alexa Fluor®488) | IF | 1:250 | ab150089 | Abcam |
| Goat Anti-Mouse IgG H&L (Alexa Fluor®594) | IF | 1:250 | ab150160 | Abcam |
| Goat anti-Mouse IgM (Heavy chain) Cross-Adsorbed Secondary Antibody, Alexa Fluor 488 | IF | 1:250 | A21042 | ThermoFisher Scientific |
| Goat anti-Rabbit IgG (H+L) Cross-Adsorbed Secondary Antibody, Alexa Fluor 594 | IF | 1:250 | A 11012 | ThermoFisher Scientific |

**Table 6: Control peptides**. Relation of the peptides used in the preabsorption performed in this work.

| Peptides | Use | Dilution | Code | Manufacturer |
|---|---|---|---|---|
| Obestatin Control Peptide | IF | 1:3 | OBSN11-P | Alpha Diagnostic International |
| GPR39 Control Peptide | WB | 1:3 | ab39283 | Abcam |
| Human GPR39 Control Antigen Peptide | IC | 1:3 | GPR392-P | Alpha Diagnostic International |

## Protein Arrays

### Human phospho-MAPK array

**Table 7. MAPKs**. Human MAPKs included in the array and the correspondent coordinates. R&D Systems (Minneapolis, MN, US).

| Coordinate | Target/Control | Alternate nomenclature | Phosphotylation Site Detected |
|---|---|---|---|
| A1,A2 | Reference Spot | ---- | ---- |
| A21,A22 | Reference Spot | ---- | ---- |
| B3,B4 | Akt1 | PKBα, RACα | S473 |
| B5,B6 | Akt2 | PKBβ, RACβ | S474 |
| B7, B8 | Akt3 | PKBγ, RACγ | S472 |
| B9, B10 | Akt pan | ---- | S473, S474, S472 |
| B11, B12 | CREB | ---- | S133 |
| B13, B14 | ERK1 | MAPK3, p44 MAPK | T202/Y204 |
| B15, B16 | ERK2 | MAPK1, p42 MAPK | T185/Y187 |
| B17, B18 | GSK-3α/β | GSK3A/GSK3B | S21/S9 |
| C3, C4 | HSP27 | HSPB1, SRP27 | S78/S82 |
| C5, C6 | JNK1 | MAPK8, SAPK1γ | T183/Y185 |
| C7, C8 | JNK2 | MAPK9, SAPK1α | T183/Y185 |

**Table 7. _(Continuation)_ MAPKs.** Human MAPKs included in the array and the correspondent coordinates. R&D Systems (Minneapolis, MN, US).

| Coordinate | Target/Control | Alternate nomenclature | Phosphotylation Site Detected |
|---|---|---|---|
| C9, C10 | JNK3 | MAPK10, SAPK1β | T221/Y223 |
| C11, C12 | JNK pan | ---- | T183/Y185, T221/Y223 |
| C13, C14 | MKK3 | MEK3, MAP2K3 | S218/T222 |
| C15, C16 | MKK6 | MEK6, MAP2K6 | S207/T211 |
| C17, C18 | MSK2 | RSKβ, RPS6KA4 | S360 |
| D3, D4 | p38α | MAPK14, SAPK2A, CSBP1 | T180/Y182 |
| D5, D6 | p38β | MAPK11, SAPK2B, p38-2 | T180/Y182 |
| D7, D8 | p38δ | MAPK13, SAPK4 | T180/Y182 |
| D9, D10 | p38γ | MAPK12, SAPK3, ERK6 | T183/Y185 |
| D11, D12 | p53 | ---- | S46 |
| D13, D14 | p70 S6 Kinase | S6K1, p70α, RPS6KB1 | T421/S424 |
| D15, D16 | RSK1 | MAPKAPK1α, RPS6KA1 | S380 |
| D17, D18 | RSK2 | ISPK-1, RPS6KA3 | S386 |
| D19, D20 | TOR | ---- | S2448 |
| E19, E20 | PBS | Control (-) | ---- |
| F1, F2 | Reference Spots | ---- | ---- |

## Human phospho-RTK array

**Table 8. RTKs.** Human RTKs included in the array and the correspondent coordinates.
Abcam (Cambridge, UK).

| Coordinate | Target/Control | Coordinate | Target/Control |
|---|---|---|---|
| A1, B1 | POS 1 | C1, D1 | POS 2 |
| E3, F3 | POS 3 | G1, H1 | ABL1 |
| I1, J1 | ACK1 | K1,L1 | ALK |
| A2, B2 | NEG | C2, D2 | NEG |
| E2, F2 | Axl | G2, H2 | Blk |
| I2, J2 | BMX | K2, L2 | Btk |
| A3, B3 | Csk | C3,D3 | Dtk |
| E3, F3 | EGF R | G3, H3 | Eph A1 |
| I3, J3 | Eph A2 | K3, L3 | Eph A3 |
| A4, B4 | Eph A4 | C4, D4 | Eph A5 |
| E4, F4 | Eph A6 | G4, H4 | Eph A7 |
| I4, J4 | Eph A8 | K4, L4 | Eph B1 |
| A5, B5 | Eph B2 | C5,D5 | Eph B3 |
| E5, F5 | Eph B4 | G5, H5 | EphB6 |
| I5, J5 | EerB2 | K5, L5 | EerB3 |
| A6, B6 | EerB4 | C6, D6 | FAK |
| E6, F6 | FER | G6, H6 | FGF R1 |
| I6, J6 | FGF R2 | K6, L6 | FGF R2 (α isoform) |
| A7, B7 | Fgr | C7, D7 | FRK |
| E7, F7 | Fyn | G7, H7 | Hck |
| I7, J7 | HGF R | K7, L7 | IGF IR |
| A8, B8 | Insulin R | C8,D8 | Itk |
| E8, F8 | JAK1 | G8, H8 | JAK2 |
| I8, J8 | JAK2 | K8, L8 | LCK |
| A9, B9 | LTK | C9, D9 | Lyn |
| E9, F9 | MAT K | G9, H9 | M-CSFR |
| I9, J9 | MUSK | K9, L9 | NGFR |

**Table 8.** *(Continuation)* **RTKs.** Human RTKs included in the array and the correspondent coordinates. Abcam (Cambridge, UK).

| Coordinate | Target/Control | Coordinate | Target/Control |
|---|---|---|---|
| A10, B10 | PDGFR-α | C10, D10 | PDGFR-β |
| E10, F10 | PYK2 | G10, H10 | RET |
| I10, J10 | ROR 1 | K10, L10 | ROR 2 |
| A11, B11 | ROS | C11, D11 | RYK |
| E11, F11 | SCFR | G11, H11 | SRMS |
| I11, J11 | SYK | K11, L11 | Tec |
| A12, B12 | Tie-1 | C12, D12 | Tei-2 |
| E12, F12 | TNK-1 | G12, H12 | TRK B |
| I12, J12 | TXK | K12, L12 | NEG |
| A13, B13 | Tyk 2 | C13, D13 | TYRO10 |
| E13, F13 | VEGFR 2 | G13, H13 | VEGFR 3 |
| I13, J13 | ZAP70 | K13, L13 | POS 4 |
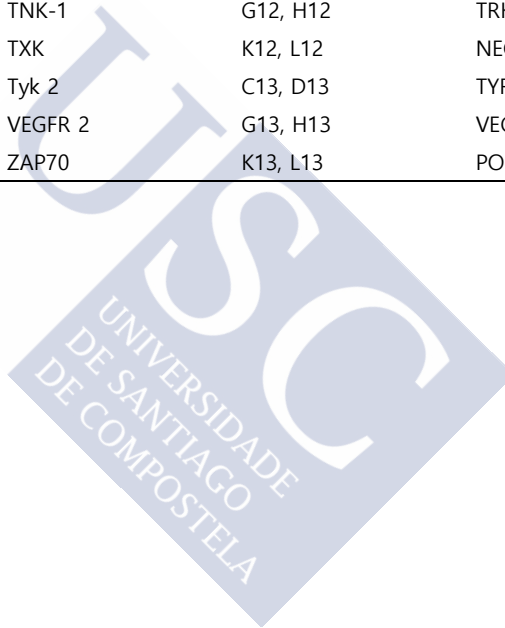
**RESULTS**

# CHAPTER 1. OBESTATIN/GPR39 IN HUMAN PANCREATIC TISSUES

Obestatin/GPR39 system was reported to be involved in the proliferation control of different cancer cell lines as well as the relationship between the obestatin/GPR39 system and human gastric cancer progression[117,142]. In the present study, we determined the expression levels of the obestatin/GPR39 system in healthy pancreas, CP, PC and premalignant conditions and explored their potential functional roles.

A total of 36 patients were selected, of which six corresponded to CP, six to PanIN, and 24 to PDAC. In the case of PDAC, three levels of differentiation were used to classify the grading as follows: WD in seven samples, MD in 10 samples, and PD in seven samples. Also, in five cases, the same patient provided PDAC samples with two degrees differentiation. The surgical control specimens were located at least 3 cm from the adenocarcinoma. All of the examined control tissues originated from macro and microscopically normal pancreatic tissue.

## GPR39 AND OBESTATIN EXPRESSION IN HUMAN NORMAL/HEALTHY PANCREAS TISSUE

As shown in **Figure 1.1**, obestatin expression was exclusively observed in single cells belonging to the endocrine pancreas **(Figure 1.1A and 1.1B).** These cells were described to be the ghrelin producing cells, the epsilon cells[131]. No expression was observed in the exocrine

---

[131] Gronberg M, Tsolakis AV, Magnusson L, *et al.* Distribution of obestatin and ghrelin in human tissues: immunoreactive cells in the gastrointestinal tract, pancreas, and mammary glands. Journal of Histochemistry and Cytochemistry. 2008;56:793-801.

pancreas. GPR39 expression was also detected in the human healthy pancreas tissue. Strong positivity was observed in the exocrine pancreas, the acini, specifically in the acinar cells, although the centroacinar cells were negative for GPR39 (**Figure 1.1C** and **1.1D**). Regarding the endocrine pancreas, stippling staining was observed in the vast majority of the islet cells; however, some cells presented a stronger positivity for GPR39 (**Figure 1.1E** and **1.1F**). **Figure 1.1G** and **1.1H** shows the negative staining in the ductal cells.

In order to identify the GPR39 positive cell type in the islet of Langerhans, several double immunofluorescences were performed. **Figure 1.2** shows the expression of GPR39 together with insulin, glucagon, SS, PPY and PDX1. Some dotted GPR39 positive cells were also positive for insulin; however, the intense GPR39 positive cells in the islet were not β-cells. When double IF was performed with glucagon, which labels the α-cells, the most intense GPR39 positive cells colocalized completely with the glucagon positive cells. Regarding SS (δ-cells) and PPY (P-cells) positive cells, no colocalization was observed for GPR39 in these subgroups of islet cells. However, when comparing to the pancreatic and duodenal homebox 1 (PDX-1), a marker for progenitor cells in the pancreas, specific GPR39-expressing cells were also immunoreactive for PDX-1, indicating a possible function for GPR39 in this cells.
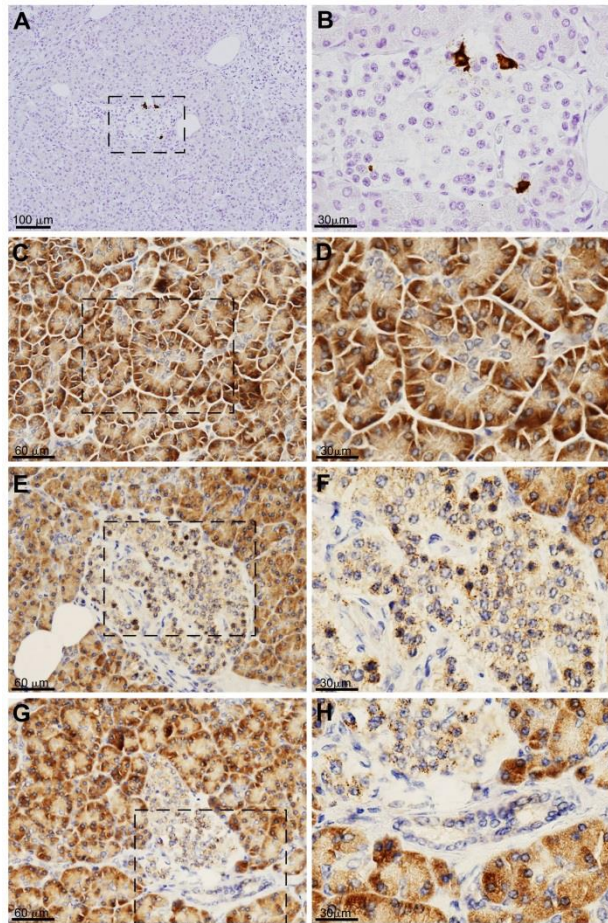
**Figure 1.1. Immmunohistochemical expression of GPR39 and obestatin in human normal pancreas. A.** An intense obestatin immunostaining was present only in the epsilon cells located at the border of the islet of Langerhans. Scale bar= 100 µm. **B.** Magnification view of the obestatin intense immunostaining. Scale bar= 30 µm. **C.** General view of GPR39 expression in the exocrine pancreas. Scale bar= 60 µm **D**. At higher magnification, GPR39 positive cells were clearly recognized with brownish staining in the basal area of the acinar cells. Centroacinar cells were negative for GPR39. Scale bar= 30 µm. **E.** General view of GPR39 expression in the endocrine pancreas. Scale bar= 60 µm. **F.** At higher magnification, the intense positivity for GPR39 was observed in a group cells in the islet. Scale bar= 30 µm. The majority of the cells of the islet presented stippling staining for GPR39. **G.** The ductal cells were negative for GPR39. Scale bar= 60 µm. **H**. Magnification view of the GPR39 negative ducts. Scale bar= 30 µm.
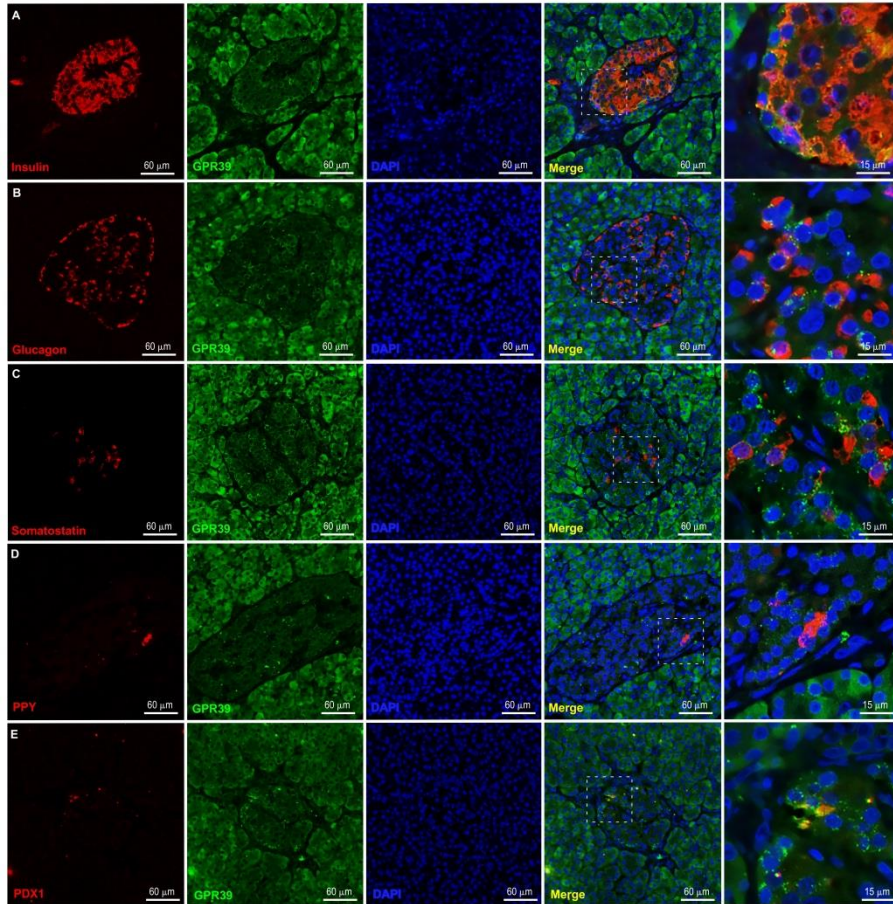
**Figure 1.2. Immunofluorescence characterization of GPR39 positive cells in the islet of Langerhans in human normal pancreas**. The figure shows the immunofluorescence detection of insulin (**A**), glucagon (**B**), SS (**C**), PPY (**D**) and PDX1 (**E**; red) and GPR39 (green) in the islets of normal pancreas. Scale bar= 60 µm. Pictures at the right side show magnifications of the positive cells. Scale bar= 15 µm. DAPI (blue) was used to counterstain nuclei.

## GPR39 EXPRESSION IN HUMAN DISEASED PANCREAS TISSUE

### GPR39 expression in human chronic pancreatitis

As a precursor condition of the PC, the expression of GPR39 was studied in serial sections of tissues affected of CP (**Figure 1.3**). **Figure 1.3A and 1.3B** shows the GPR39 expression pattern in this disease. This expression is concentrated mainly in the remaining acinar cells presented in the tissues. However, some enlarged cells appeared to be positive also for GPR39. These cells might correspond to the PSCs. In order to determine this cell type, four serial sections were stained with haematoxylin-eosin (HE), GPR39, the adipose differentiation-related protein [perilipin 2 (PLIN2) or ADRP], and GFAP (**Figure 1.3C, 1.3D, 1.3E, and 1.3F**; respectively). Some GPR39 positive cells were also ADRP and GFAP immunoreactives; these cells were part of the remaining GPR39 positive acinar cells observed in the preparations. ADRP was selected as it has been recently described to stain specifically the quiescent PSCs due to their lipid content and, therefore, the lipid droplet associate proteins, which are able to remain after FFPE tissues processing; however, its staining depends strongly on the preanalytical time interval from removal of the tissue to formalin fixation[132]. In our hands, only positive acinar cells were observed (**Figure 1.3E**). Respect to GFAP, it has been also described as a marker for quiescent PSCs[133] but some differences in expression were found between murine models and human tissues[132]. Conversely, the GFAP positive cells observed both in endocrine and exocrine pancreas,

---

[132] Nielsen MFB, Mortensen MB, Detlefsen S. Identification of markers for quiescent pancreatic stellate cells in the normal human pancreas. Histochem Cell Biol. 2017;148:359-380.

[133] Apte MV, Haber PS, Applegate TL, *et al*. Periacinar stellate shaped cells in rat pancreas: identification, isolation, and culture. Gut. 1998;43:128-33.

presented an activated-like phenotype (data not shown). α -smooth muscle actin (α-SMA) is another commonly used marker for activated stellate cells[134]. In serial sections of CP, GPR39 (**Figure 1.3G**) and α-SMA (**Figure 1.3H**) were expressed, but α-SMA was not specific enough to elucidate whether GPR39 was also expressed in the PSCs. However, when using GFAP a few of elongated cells were immunoreactive for both GPR39 and this marker (**Figure 1.3I and 1.3J**, respectively).

Heat shock protein 47 (HSP47), a collagen-specific molecular chaperone, plays a critical role in collagen synthesis. Initially, it has been reported that HSP47 was expressed in hepatic stellate cells both in normal and diseased liver[135]. More recently, HSP47 was used to identify the stellate cells in the pancreas[25]. **Figure 1.4** shows the identification of the HSP47 positive cells coexpressing GPR39 in normal pancreas. The presence of these cells was observed in the islets of Langerhans (**Figure 1.4 line A**), in a niche inserted in the acinar area (**Figure 1.4 line B**) and in periacinar sections of the sample (**Figure 1.4 line C**). **Figure 1.4 line D** presents a magnification view of one of this periacinar cells, where is patent the colocalization of both proteins.

---

[134] Xu Z, Vonlaufen A, Phillips PA, *et al*. Role of Pancreatic Stellate Cells in Pancreatic Cancer Metastasis. Am J Pathol. 2010;177:2585-96.

[135] Brown KE, Broadhurst KA, Mathahs MM, *et al*. Expression of HSP47, a collagen-specific chaperone, in normal and diseased human liver. Lab Invest. 2005;85:789-97.
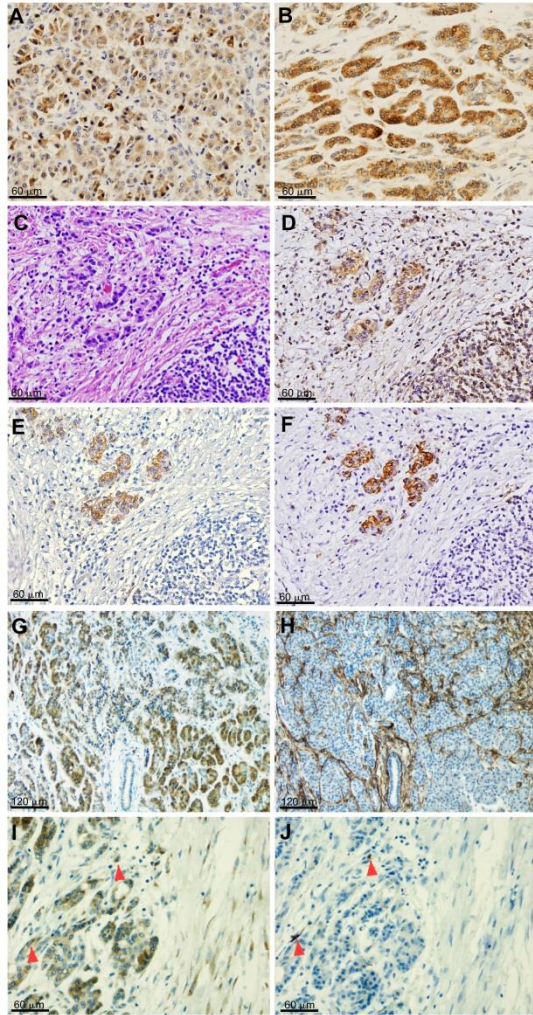
**Figure 1.3. Immmunohistochemical expression of GPR39 in human CP.** An intense GPR39 immunostaining was observed in the remaining acini in two examples of CP (**A** and **B**). Serial slices (3 μm) of the same section of pancreas with CP showing haematoxylin (**C**), GPR39 (**D**), ADRP (**E**), and GFAP (**F**) staining of the remaining acini. Scale bar= 60 μm. Serial slices (3 μm) of the same section of pancreas with CP showing GPR39 (**G**) and α-SMA (**H**) staining. Scale bar= 120 μm. Ductal cells were negative for GPR39. Serial slices of the same section of pancreas with CP in an area with fibrosis showing GPR39 (**I**) and GFAP (**J**). Scale bar= 60 μm. Red arrows show the coexpression of both proteins in two enlarged cells, the PSCs.
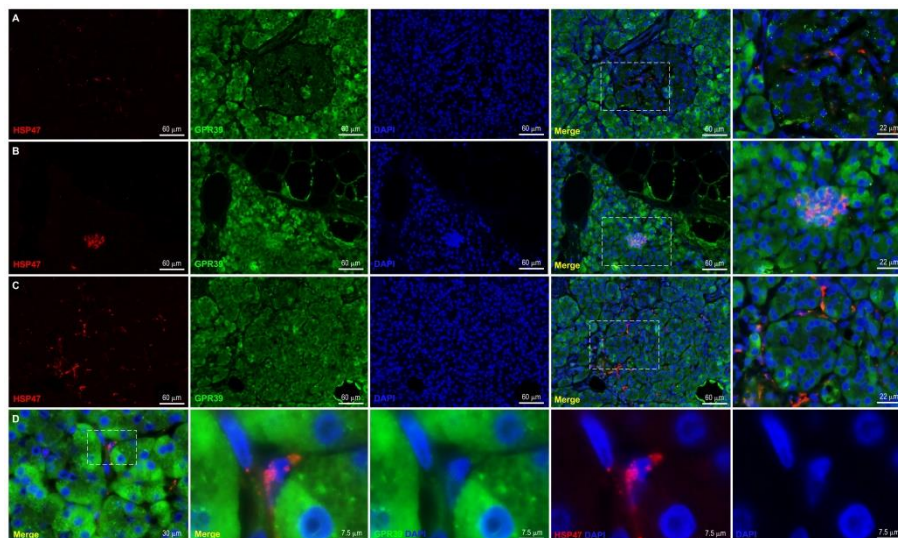
**Figure 1.4. Immunofluorescence characterization of the GPR39 positive and HSP47 positive cells in the human normal pancreas.** The figure shows the immunofluorescence detection of HSP47 (red) and GPR39 (green) in three areas of human normal pancreas. The positive cells were found in the islets (**line A**), in a niche in the acini area (**line B**) and in the periacinar area (**line C**) Scale bar= 60 µm. Pictures at the right side show magnifications of the positive cells. Scale bar= 22 µm. Magnification view of a single cell showing positivity for both proteins in the periacinar area (**line D**). Scale bar= 30 µm. Pictures at the right side show magnification of the positive cells. Scale bar= 7.5 µm. DAPI (blue) was used to counterstain nuclei.

## GPR39 expression in human pancreatic intraepithelial neoplasia (PanIN)

PanIN is a histologically well-defined precursor to invasive ductal adenocarcinoma of the pancreas[136]. **Figure 1.5** shows two low-grade[67] samples that present PanIN lesions. As it has been mentioned before, normal ducts were negative for GPR39. On the contrary, the PanIN lesions presented in pancreata with CP presented a faint positivity for GPR39

---

[136] Hruban RH, Maitra A, Goggins M. Update on pancreatic intraepithelial neoplasia. Int J Clin Exp Pathol. 2008;1:306-16.

(**Figure 1.5B**), with more intense GPR39 staining when the PanIN lesions were present in PDAC tissue (**Figure 1.5E**). In the former, only some isolated ductal cells presented strong GPR39 immunoreactivity; however, in the latter, more extended ductal areas were intensely stained for GPR39.

Ki67 is a known marker for proliferative cells [137] and it has been proposed as a useful adjunct in the diagnosis of precancerous lesions in the pancreas, providing a reliable way to identify lesions at high risk for the subsequent development of infiltrating carcinoma[138].
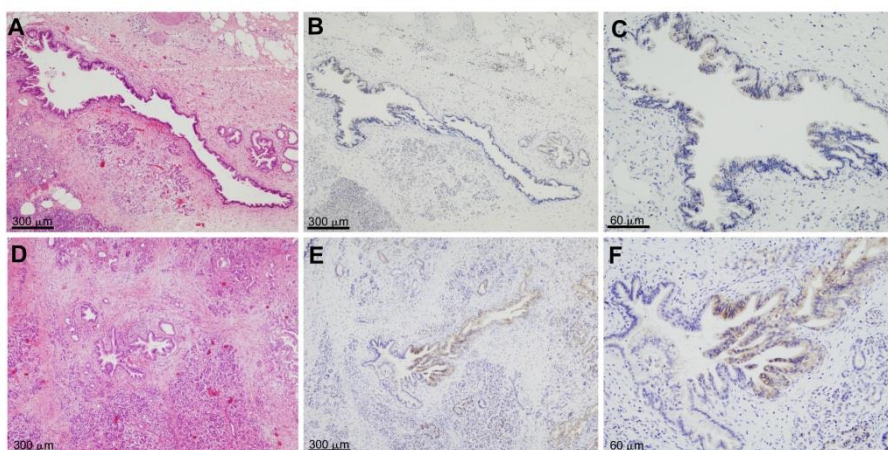


**Figure 1.5. Immmunohistochemical expression of GPR39 in pancreatic intraepithelial neoplasia (PanIN).** General view of a PanIN lesion in serial slices (3 µm) in a pancreas with CP showing HE (**A**) and GPR39 (**B**) staining. Scale bar= 300 µm. **C** shows a magnification view of the GPR39 staining, only scattered cells presented intense GPR39 immunoreactivity. Scale bar= 60 µm. General view of a PanIN lesion in serial slices (3 µm) in a pancreas with a PDAC showing HE (**D**) and GPR39 (**E**) staining Scale bar= 300 µm. **F** shows a magnification view of the GPR39 staining. In this case, intense GPR39 immunoreactivity was observed in the vast majority of the lesion. Scale bar= 60 µm.

---

[137] Schlüter C, Duchrow M, Wohlenberg C, *et al*. The cell proliferation-associated antigen of antibody Ki-67: a very large, ubiquitous nuclear protein with numerous repeated elements, representing a new kind of cell cycle-mantaining proteins. J Cell Biol. 1993;123:513-22.

[138] Klein WM, Hruban RH, Klein-Szanto AJ, *et al*. Direct correlation between proliferative activity and dysplasia in pancreatic intraepithelial neoplasia (PanIN): additional evidence for a recently proposed model of progression. Mod Pathol. 2002;15:441-7.

**Figure 1.6** shows double immunofluorescence for Ki67, and GPR39, showing that although the Ki67 positive cells expressed GPR39, the vast majority of the cells are Ki67 negative, as it has been previously described for low grade PanINs[138]. In this PanIN sample, we also observed the colocalization of GPR39 and both, the PSCs markers α-SMA and HSP47 in the fibrotic area of the tissue (**Figure 1.6**).
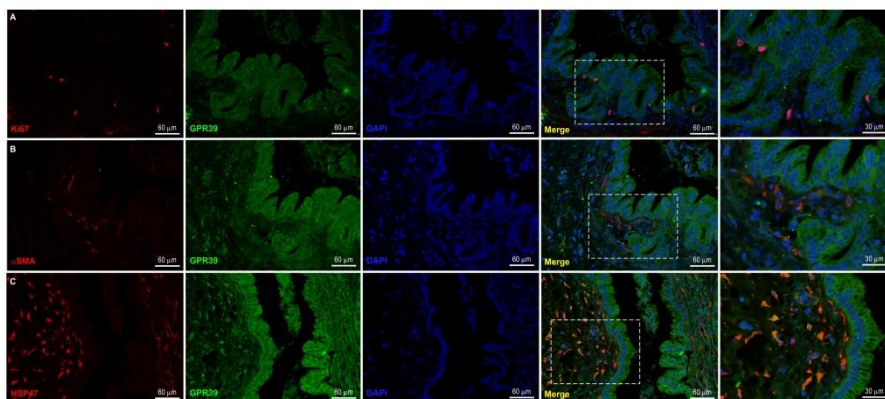


**Figure 1.6. Immunofluorescence characterization of the GPR39 positive and HSP47 positive cells in a PanIN lesion in a pancreas with CP. Line A** shows the immunofluorescence detection of Ki67 (red) and GPR39 (green). Some scattered cells in the lesion were positive for both proteins. The amount of Ki67 positive cells was in concordance with a low-grade lesion. The positive cells for α-SMA (red) were also immunoreative for GPR39 (green) (**line B**). The positive cells for HSP47 (red) were also immunoreative for GPR39 (green) (**line C**). Scale bar= 60 μm. These cells were located in the fibrotic area of the tissue. Pictures at the right side show magnifications of the positive cells. DAPI (blue) was used to counterstain nuclei. Scale bar= 30 μm.

## GPR39 expression in human pancreatic ductal adenocarcinomas

**Figure 1.7** shows the results obtained for GPR39 and obestatin in the samples of human PDAC, represented by WD, MD, PD PDAC (**Figure 1.7A-C**, **1.7D-F** and **1.7G-I**, respectively). In these samples, obestatin (**Figure 1.7C**, **1.7F**, and **1.7I**) was negative in all of the pancreatic

adenocarcinomas studied. By contrast, GPR39 positivity was present in all of the tumours with varying intensity according to the classification of the samples. Lower expression was found in WD tumours (**Figure 1.7A** and **1.7B**), with increasing expression in the MD (**Figure 1.7D** and **1.7F**), and the highest expression was observed in the PDACs (**Figure 1.7G** and **1.7H**).

The results for GPR39 expression correlated with the dedifferentiation of the tumour, with increased expression from WD (40.81 ± 6.0 a.u.), MD (51.01 ± 6.7 a.u.), to PD (58.79 ± 8.3 a.u.) (**Figure 1.8**: WD/PD, *P < 0.05).

Besides, in the cases where two degrees of differentiation were present in the samples, the same pattern of expression was observed for GPR39. **Figure 1.9A-F** shows an example of this feature. The PD tumoral area presented more intense GPR39 immunoreativity (**Figure 1.9E**) than the MD area (**Figure 1.9F**). This difference was statistically significant (**Figure 1.10**: Low Grade/High Grade, **P < 0.01).

As it has been mentioned above, Ki67 is an established and widely used marker of cell proliferation, and GPR39 is closely related to the proliferation of cancer cells. **Figure 1.11** shows H-E **(Figure 1.11A-C)**, GPR39 **(Figure 1.11D-F)** and Ki67 (**Figure 1.11G-I**) expression in serial slices (3 μm) of PDAC samples. It is remarkable the increasing Ki67 and GPR39 staining toward the tumours invasive edge. Note also that the adipocytes presented the previously described GPR39 immunoreactivity[139].

---

[139] Gurriarán-Rodríguez U, Al-Massadi O, Roca-Rivada A, *et al.* Obestatin as a regulator of adipocyte metabolism and adipogenesis. J Cell Mol Med. 2011;15:1927-40.
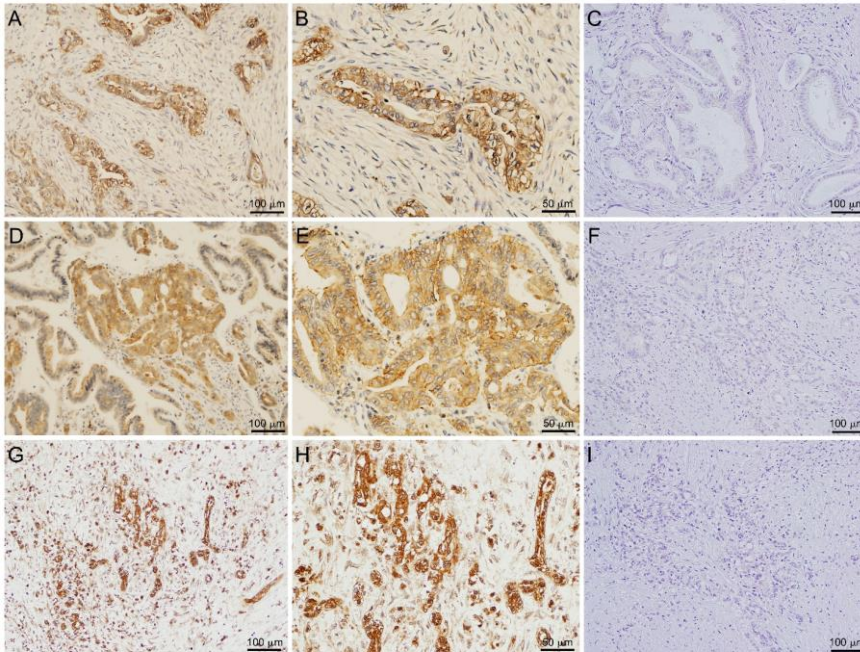
**Figure 1.7. Immmunohistochemical expression of GPR39 and obestatin in human PDAC.** Immunohistochemical expression of GPR39 and obestatin in a well-differentiated PDAC. GPR39 expression was positive in the tumour (**A**). Scale bar= 100 µm. Higher magnification view of GPR39 positivity (**B**). Scale bar= 50 µm. Obestatin expression was negative in all of the well-differentiated adenocarcinoma (**C**). Scale bar= 100 µm. Immunohistochemical expression of GPR39 and obestatin in a moderately differentiated PDAC. GPR39 expression was positive in the tumour (**D**). Scale bar= 100 µm. Higher magnification view of GPR39 positivity (**E**). Scale bar= 50 µm. Obestatin expression was negative in all of the well-differentiated adenocarcinoma (**F**). Scale bar= 100 µm. Immunohistochemical expression of GPR39 and obestatin in a poorly differentiated PDAC. GPR39 expression was positive in the tumour (**G**). Scale bar= 100 µm. Higher magnification view of GPR39 positivity (**H**). Scale bar= 50 µm. Obestatin expression was negative in all of the well-differentiated adenocarcinoma (**I**). Scale bar= 100 µm.
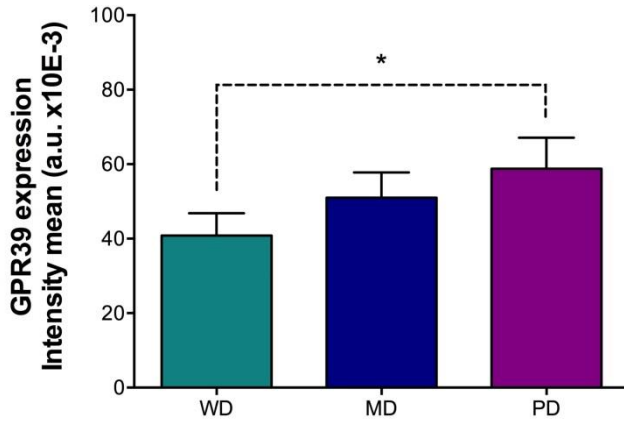
**Figure 1.8. Graphical representation of the GPR39 levels of expression in the studied pancreatic adenocarcinomas.** Data shown are mean ± SEM. The asterisk (*) denotes $P <$ 0.05 when comparing groups.
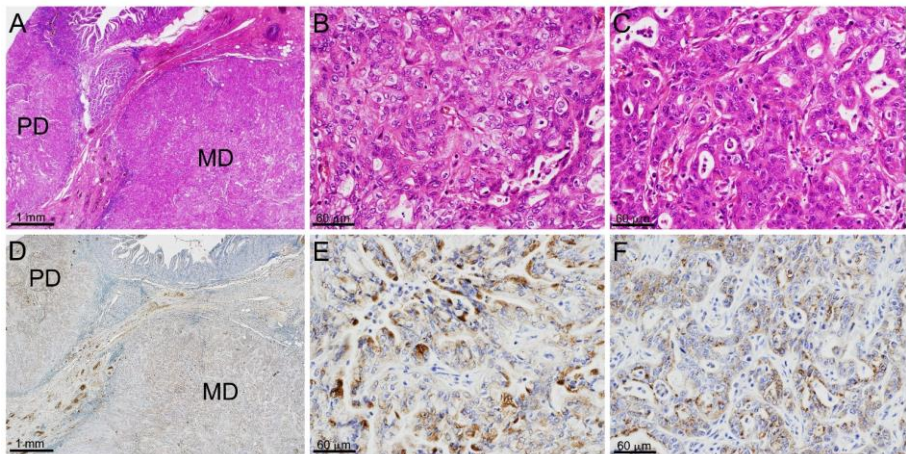


**Figure 1.9. Immmunohistochemical expression of GPR39 in a human PDAC with two grades of differentiation.** General view of the tumour with a poorly (PD) and a moderately differentiated (MD) area showing the immunostaining for HE (**A**) and GPR39 (**D**) in serial slices (3 μm) of the same section. Scale bar= 1 mm. **B** and **C** show a magnification of the HE staining of the PD area and the MD area, respectively. **E** and **F** show a magnification of the GPR39 staining of the PD area and the MD area, respectively. Scale bar= 60 μm.
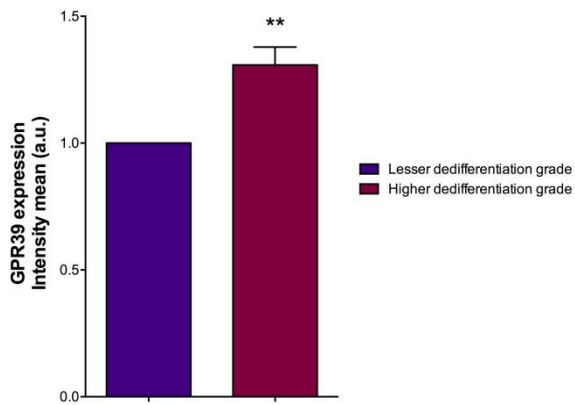
**Figure 1.10. Graphical representation of the GPR39 levels of expression in PDACs with two grades of differentiation.** The higher grade is represented as fold of the lower grade (control). The asterisks (**) denotes $P < 0.01$ when comparing groups.
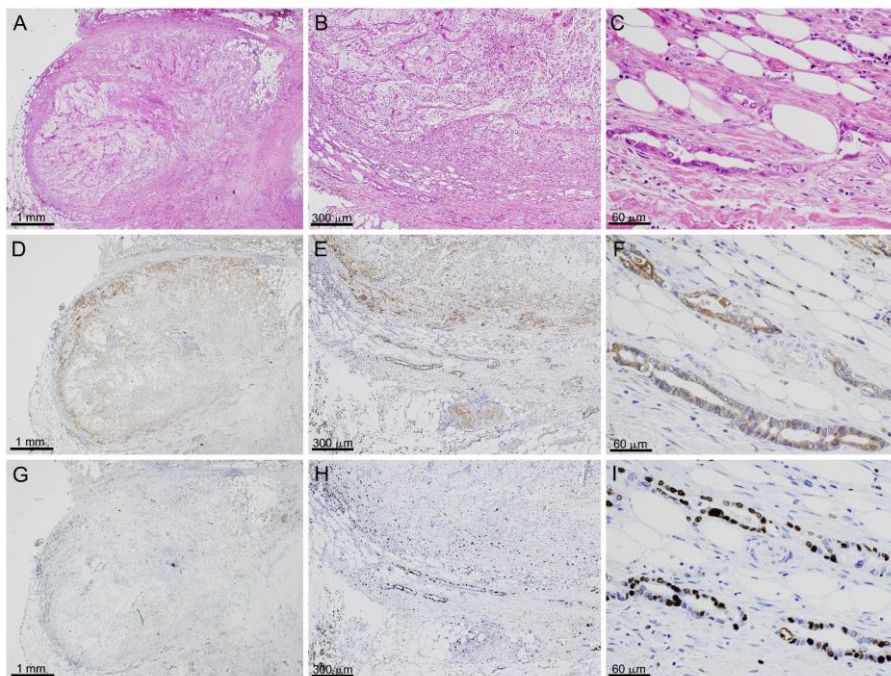


**Figure 1.11. Immmunohistochemical expression of GPR39 and Ki67 in the invasive edge of a PDAC.** General view of the tumoral area showing the immunostaining for HE (**A**), GPR39 (**D**), and Ki67 (**G**) in serial slices (3 μm) of the same section. Scale bar= 1 mm. **B** and **C** show magnifications of the HE staining. Scale bar= 300 μm and 60 μm respectively. **E** and **F** show magnifications of the GPR39 staining. Scale bar= 300 μm and 60 μm respectively. **H** and **I** show magnifications of the Ki67 staining. Scale bar= 300 μm and 60 μm respectively. Note that the most intense GPR39 staining is located in the same zone than the Ki67 positivity.

**Figure 1.12A-D** shows the presence of micrometastasis in the ganglions present in the samples. These formations also displayed positivity for GPR39 (**Figure 1.12C-D**).
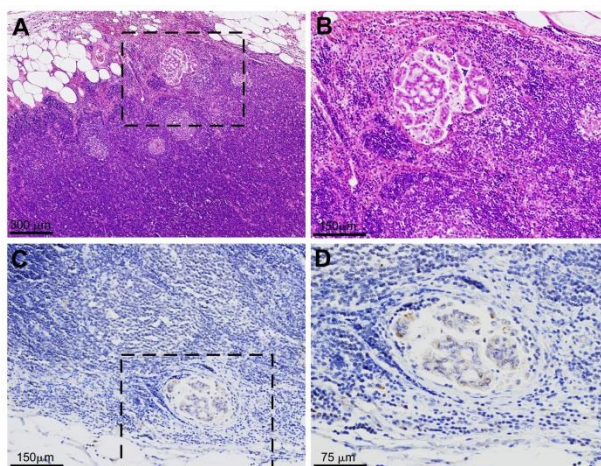


**Figure 1.12. Immmunohistochemical expression of GPR39 in the ganglion micromestastasis.** General view of the ganglion area showing the immunostaining for HE (**A**) and GPR39 (**C**). Scale bar= 300 and 150 μm respectively. **B** and **D** show magnifications of the HE and the GPR39 staining, respectively. The tumoral cells composing the micromestastasis were GPR39 positives. Scale bar= 150 and 75 μm respectively.

# CHAPTER 2: OBESTATIN/GPR39 SYSTEM AND PANCREATIC CANCER CELLS

PDAC is one of the most aggressive neoplasms due to its rapid diffusion, its lack of early specific symptoms and its late diagnosis. The study of the endogenous systems involved in the development of the disease is key for its detection and treatment. Our laboratory identified the obestatin/GPR39 system as a key system in development and progression of gastric adenocarcinoma[117], however, the relationship between the obestatin/GPR39 system and PC progression remains unknown.

The underlying obestatin/GPR39 mechanism of action was studied *in vitro* using the human PDAC cell lines PANC-1, BxPC3 and RWP-1.

## OBESTATIN/GPR39 SYSTEM EXPRESSION IS EXPRESSED IN THE HUMAN PANCREATIC DUCTAL ADENOCARCINOMA CELL LINES

As a first approach, obestatin and GPR39 expression was investigated in three human PDAC cell lines: PANC-1, RWP-1 and BxPC3. The PANC-1 cell line was established from an undifferentiated pancreatic carcinoma of ductal origin, being identical to the source provided by the depositor[140]. The disease is an epithelioid carcinoma. The RWP-1 cell line is a moderately well differentiated ductal cell adenocarcinoma[141]. This cell line grows with a typical epithelial morphology with two major morphologically distinct cell types in culture. One has a polygonal shape

---

[140] Lieber M, Mazzetta J, Nelson-Rees W, *et al.* Establishment of a continuous tumor-cell line (panc-1) from a human carcinoma of the exocrine pancreas. Int. J. Cancer. 1975;15:741-7.
[141] Dexter DL, Matook GM, Meitner PA, *et al.* Establishment and characterization of two human pancreatic cancer cell lines tumorigenic in athymic mice. Cancer Res. 1982;42:2705-14.

with abundant cytoplasm, possesses a large, somewhat indistinct nucleus with 1 to 4 nucleoli, and shows many cytoplasmic connections between the cells. The second consists of slightly elongated epithelial cells, which tend to form swirls around the smooth, well-demarcated boundaries of the polygonal cell component. The elongated cells contain much less basophilic cytoplasm than do the polygonal cells, and they have a well-defined central nucleus with two prominent nucleoli. Occasional giant cells containing numerous intracellular inclusions and vacuoles appear to form a minor component of this cell line. When inoculated in nude mice, histologically, the RWP-1 xenografts resemble the original patient's tumour. The BxPC3 cell line derived from a primary adenocarcinoma of the pancreas. BxPC3 cells produce mucin and the tumour produced in a nude mouse is moderately well to poorly differentiated adenocarcinoma like the primary adenocarcinoma.

As seen in **Figure 2.1**, the expression of the obestatin/GPR39 system was detected by immunocytochemistry in the cell lines of the study. All of the cell lines expressed the obestatin/GPR39 system at different levels of intensity. No immunostaining was found when obestatin or GPR39 antibodies were preadsorbed with homologous peptides (data not shown).

The PANC-1 cells presented an intense and localized perinuclear obestatin immunostaining, probably associated to Golgi. Intense and diffuse GPR39 immunostaining was found in the cytoplasm. In the RWP-1 cells intense and diffuse obestatin immunostaining was found in the cytoplasm. In this cell line, GPR39 cytoplasmic immunostaining was found, but in a lesser extension than obestatin.

BxPC3 presented intense and diffuse obestatin positivity located in the cytoplasm, although with a perinuclear location, probably associated to Golgi; however, faint and diffuse GPR39 immunostaining was found.
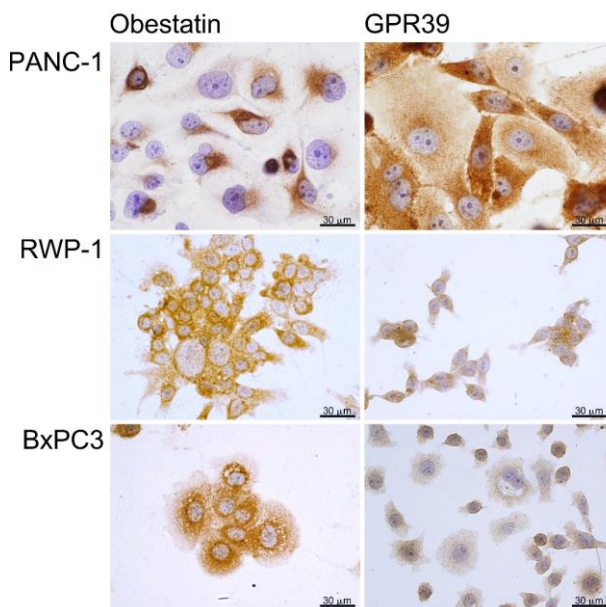
**Figure 2.1. Immunocytochemical expression of obestatin and GPR39 in human PDAC cell lines**. (See text **Figure 2.1**). Obestatin and GPR39 expression in the cell lines PANC-1, RWP-1 y BxPC3. Scale bar= 30 μm.

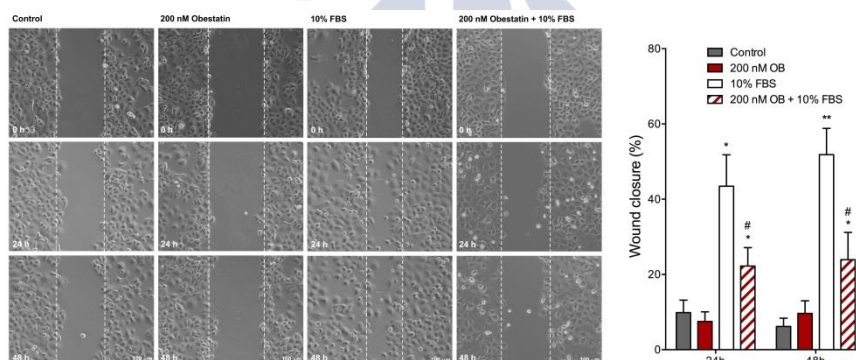## THE EFFECT OF OBESTATIN ON MIGRATION AND INVASION ON PDAC HUMAN CELLS

Our previous results in the gastric cancer cell line AGS in which the obestatin/GPR39 system was involved in the activation of the migration and invasion of this cell line[117,142], together with the observed change in PANC-1 cells morphology after 24 h obestatin treatment, prompted us to hypothesised that the PC cells presented the same behaviour regarding migration and invasion than the gastric cancer cells. In a first approach,

---

[142] Alén BO. Fundamental structural and biochemical features for the obestatin/GPR39 system mitogenic action. Thesis dissertation. Univesidad de Santiago de Compostela, Santiago de Compostela, Spain. 2016. http://hdl.handle.net/10347/14993.

PANC-1 cells migration was evaluated by the treatment with 200 nM obestatin for 24 and 48 h; using 10% FBS as positive control (**Figure 2.2**). To our surprise, obestatin treatment did not promote PANC-1 cells migration at 24 h or at 48 h (7.51 ± 2.55% and 9.65 ± 3.35%, respectively) with values similar to those of control at the same times (9.86 ± 3.30% and 6.17 ± 2.19%, respectively). However, as expected, 10% FBS significantly stimulate these cells migration both at 24 and 48 h (43.46 ± 8.36% and 51.82 ± 6.99%, respectively). The most impressive result was the observed effect of the co-treatment of 10% FBS and 200 nM obestatin, as this peptide was able to significantly inhibit the migration promoted by FBS in PANC-1 cells with a reduction in the wound closure of 48.84 ± 9.69% at 24 h and 53.82 ± 10.09% at 48 h.
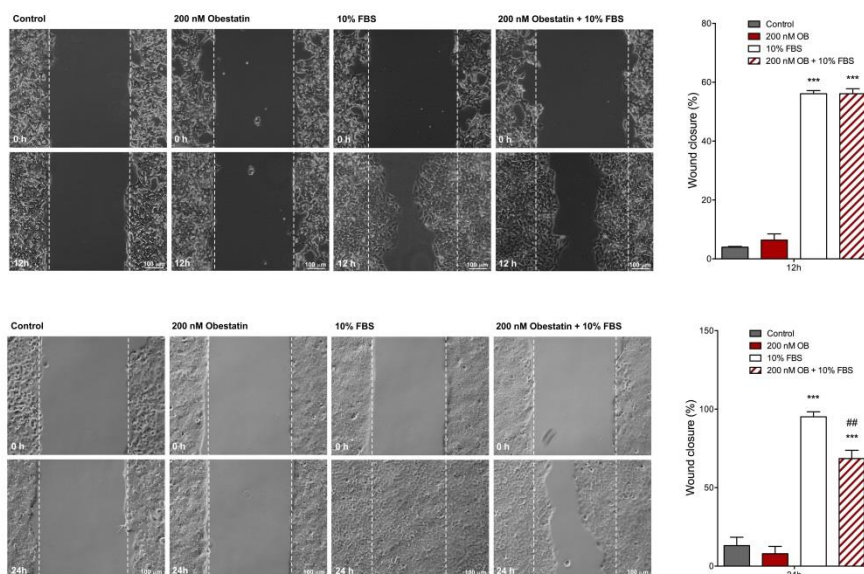


**Figure 2.2. The effect of obestatin on migration of PANC-1 cells.** The PANC-1 cells were treated or not with obestatin (200 nM), FBS (10%, v/v) or both. The wound was calculated by tracing along the border of the scratch using ImageJ64 analysis software and the following equation: %wound closure=[[wound area (0h)-wound area (xh)]/wound area (0h)] x 100. Scale bar= 100 µm. The asterisk (*, **) denotes $P<0.05$ and $P<0.01$ when comparing the treated with the untreated group, the dagger (#) denotes $P<0.05$ when comparing 200 nM obestatin+10%FBS group with 10% FBS group.
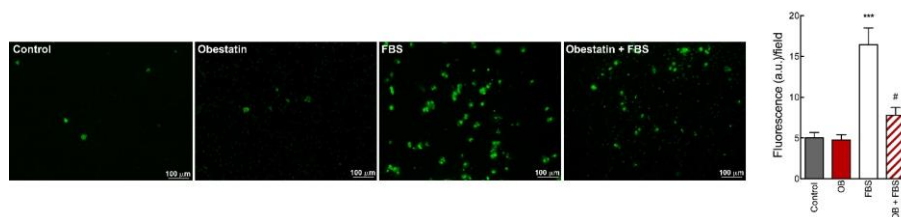
**Figure 2.3. Obestatin effect on invasion in PANC-1 cells.** PANC-1 cells were treated or not for 16h with obestatin (200 nM), FBS (10%, v/v) or both as chemoattractant. Migratory cells pass through polycarbonate membrane and cling to the bottom side. Non-migratory cells are removed from upper chamber. **Right graph.** Mean grey intensity (a.u.) quantified at the image of polycarbonate membrane bottom side. Scale bar= 100 μm. The data were expressed as mean ± SEM obtained from 6 independent experiments. The asterisk (***) denotes $P<0.001$ when comparing the treated with the untreated group, the dagger (#) denotes $P<0.05$ when comparing 200 nM obestatin+10% FBS group with 10% FBS group.

We also analysed whether obestatin was driving cell invasion using a specialized invasion chamber. As shown in **Figure 2.3**, the PANC-1 cells were able to migrate through polycarbonate membrane and cling to the bottom side. Non-migratory cells are removed from upper chamber. However, as it happened in the migration assay, obestatin (200 nM) did not affect PANC-1 cells invasion but it significantly did inhibit the effect promoted by FBS on co-treatment in a 52.58 ± 2.25% ($P<0.01$; **Figure 2.3**).

**Figure 2.4. The effect of obestatin on migration in RWP-1 and BxPC3 cells. The upper side show no migration effect of obestatin in RWP-1 cells.** The RWP-1 cells were treated or not with obestatin (200 nM), FBS (10%, v/v) or both. **The bottom side show migration inhibition of BxPC3 cells promoted by obestatin.** The RWP-1 and BxPC3 cells were treated or not with obestatin (200 nM), FBS (10%, v/v) or both. The wound was calculated by tracing along the border of the scratch using ImageJ64 analysis software and the following equation: %wound closure= [wound area (0 h)-wound area (x h)]/wound area (0 h)] x 100. Scale bar= 100 µm. The data were expressed as mean ± SEM obtained from 6 independent experiments. The asterisk (***) denotes $P<0.001$ when comparing the treated with the untreated group, the dagger (##) denotes $P<0.01$ when comparing 10% FBS group with 200 nM OB+10% FBS group.

To corroborate these findings, we studied the RWP-1 and the BxPC3 cell lines with the same approaches and the results are shown in **Figure 2.4** and **2.5**. We observed similar effects for obestatin in the BxPC3 cell line, with a significant reduction in the migration and the invasion of these cells promoted by FBS (27.95 ± 6.45% and 51.78 ± 3.28%, respectively; (**Figure 2.4** (bottom side) and **2.5**) although the time window had to be reduced (24 h) as the huge effect of FBS in the migration of this cell did not allow following the experiment for longer periods. On the

contrary, no effect was observed for the RWP-1 cell line (**Figure 2.4** upper side).
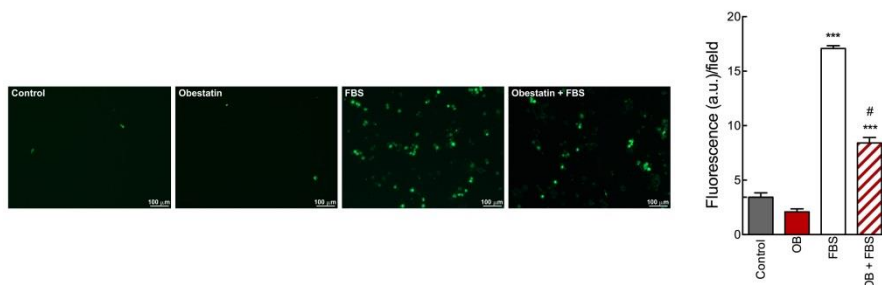


**Figure 2.5. The effect of obestatin on invasion in BxPC3 cells.** Invasion assay on BxPC3 cell following incubation for 16h with obestatin (200 nM), FBS (10%, v/v) or both. Migratory cells pass through polycarbonate membrane and cling to the bottom side. Non-migratory cells are removed from upper chamber. **Right graph.** Mean grey intensity (a.u.) quantified at the image of bottom side. Scale bar= 100 μm. The data were expressed as mean ± SEM obtained from 6 independent experiments. The asterisk (\*\*\*) denotes $P<0.001$ when comparing the treated with the untreated group, the dagger (#) denotes $P<0.05$ when comparing 10% FBS group with 200 nM obestatin+10% FBS group.

## THE EFFECT OF OBESTATIN ON THE EXPRESSION OF THE METASTATIC SUPPRESSOR, NM23H1, IN HUMAN PDAC CELLS

*Nm23-H1* was the first metastasis suppressor gene identified. Reductions in *nm23-H1* expression have been significantly associated with aggressive behaviour in melanoma, breast, colon, and gastric carcinomas. Ectopic expression of *nm23-H1* supressed metastasis without altering primary tumour growth. These findings provided the evidence that the expression of specific genes is reduced in tumour cells that have acquired the ability to form metastases and the reintroduction of such genes can suppress the metastatic phenotype[143]. The protein product of *nm23-H1*

---

[143] Marshall JC, Collins J, Marino N, *et al.* The Nm23-H1 metastasis suppressor as a translational target. Eur J Cancer. 2010;46:1278-82.

gene has activity of nucleoside diphosphate (NDP) kinase, which catalyses the phosphorylation of nucleoside diphosphates to the corresponding nucleoside triphosphates. Reductions in *nm23* expression have been significantly associated with aggressive behaviour in melanoma, breast, colon, and gastric carcinomas[144]. Moreover, expression of *nm23-H1* by a tumour could be altered during the different steps in metastases, suggesting that *nm23-H1* may act as a molecular switch between the free-floating and adherent states of cancer cells[145]. Regarding PC, early stage PC samples exhibited stronger *nm23-H1* immunoreactivity than normal controls, and early PC stages exhibited higher nm23-H1 immunostaining than advanced tumour stages[146].

Due to the observed effect of obestatin in PDAC cells regarding migration and invasion, *nm23-H1* and nm23-H1 expression were checked after obestatin treatment in the cell lines of the study. For the PANC-1 cells, **Figure 2.6** shows that obestatin treatment (200 nM, 24 h) provoked a significant reduction in the expression of the *nm23-H1* gen of 39.17 ± 12.83% (**Figure 2.6 A**) that is also associated to a significant decrease in nm23-H1 protein expression as assessed by immunoblot at 72 h (17.75 ± 8.94%; **Figure 2.6 B**).

[144] Tee YT, Chen GD, Lin LY, *et al*. Nm23-H1: a metastasis-associated gene. Taiwan J Obstet Gynecol. 2006;45:107-13.

[145] Iizuka N, Tangoku A, Hazama S, *et al*. Nm23-H1 gene as a molecular switch between the free-floating and adherent states of gastric cancer cells. Cancer Lett. 2001;174:65-71.

[146] Friess H, Guo XZ, Tempia-Caliera AA, *et al*. Differential expression of metastasis-associated genes in papilla of vater and pancreatic cancer correlates with disease stage. J Clin Oncol. 2001;19:2422-32.
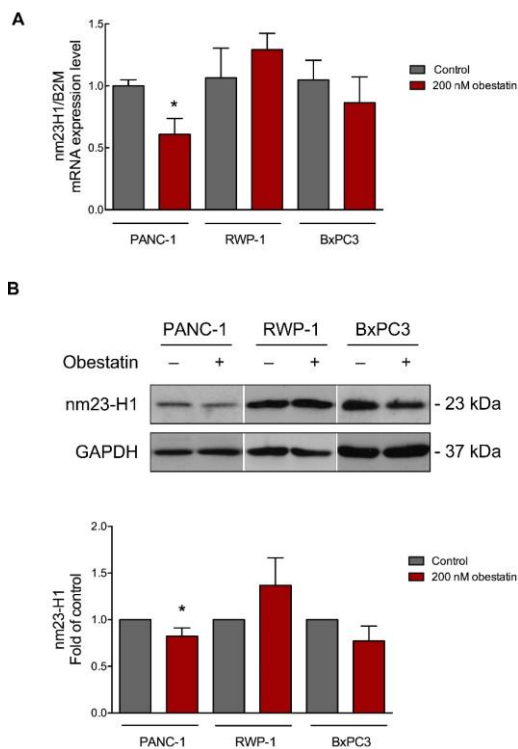
**Figure 2.6. The effect of obestatin on mRNA and protein expression of tumoral supressor nm23-H1 in PDAC cell lines.** PDAC cells were treated or not with obestatin (200 nM) and *nm23H1* mRNA levels (qPCR, left) and nm23H1 protein levels (Western Blot, right) was evaluated after 24 and 72 h respectively. **A.** qPCR values have been normalized to the B2M level and are the averages of three independent readings. **B.** The protein expression was normalized relative to GAPDH. The data were expressed as mean ± SEM obtained from 3 independent experiments. The asterisk (*) denotes *P*<0.05 when comparing the treated with the untreated control group.

Regarding the two remaining lines, no significant results were obtained, both for the synthesis of mRNA and protein expression. We can say that both have the same tendency, an increase in the case of the RWP-1 and a decrease in the case of the BxPC3 (**Figure 2.6 A, 2.6 B**). In fact, BxPC3 present a behavior similar to PANC-1 in relation to migratory and invasive processes. These results should be corroborated with additional experiments.

## THE EFFECT OF OBESTATIN ON THE EPITHELIAL-MESENCHYMAL TRANSITION AND ANGIOGENESIS IN PDAC CELLS

Epithelial-mesenchymal transition (EMT) is proposed to regulate the acquisition of migratory and invasive capability, which is a crucial mechanism in the initial steps in of the metastatic progression. The loss of the epithelial marker E-cadherin generally characterizes the EMT, as well as the up-regulation of mesenchymal markers such as N-cadherin and vimentin, and the acquisition of the fibroblast-like spindle cell shape in monolayer cultures [147, 148]. Because obestatin treatment diminished migration and invasion but increased proliferation of PANC-1 cells, we assessed obestatin's influence on the epithelial-mesenchymal plasticity (EMP) of these cells by examining the expression of E-cadherin, β-catenin, vimentin, and N-cadherin (**Figure 2.7**). Obestatin treatment (100 nM) diminished significant β-catenin (active form) (25.36 ± 21.50%), N-cadherin (32.90 ± 9.53%) and vimentin (19.41 ± 3.52%) levels after 48 h post-treatment. Although a recent article showed no immunocytochemical expression of E-cadherin in PANC-1 cells[149], in fact, Aiello *et al.* shows that, in both mouse and human PDAC, metastatic cells appear to re-acquire an epithelial phenotype with increasing lesion size[150].

We detect E-cadherin by immunoblot (**Figure 2.7**) and immunofluorescence (**Figure 2.8**). We observed an increment in E-

[147] De Wever O, Pauwels P, Craene B, *et al.* Molecular and pathological signatures of epithelial-mesenchymal transitions at the cancer invasion front. Histochem Cell Biol 2008;130:481-94.

[148] Oyanagi J, Ogawa T, Sato H, *et al.* Epithelial-mesenchymal transition stimulates human cancer cells to extend microtubule-based invasive protrusions and suppresses cell growth in collagen gel. PLoS One. 2012;7:e53209.

[149] Gradiz R, Silva HC, Carvalho L, *et al.* MIA PaCa-2 and PANC-1 - pancreas ductal adenocarcinoma cell lines with neuroendocrine differentiation and somatostatin receptors. Sci Rep. 2016;6:21648.

[150] Aiello NM, Bajor DL, Norgard RJ, *et al.* Metastatic progression is associated with dynamic changes in the local microenvironment. Nat Commun. 2016;7:12819.

cadherin after 48 h (32.44 ± 1.40%) together with the above-mentioned diminution of the mesenchymal markers.

The observed influence of obestatin on these markers was also tested in the RWP-1 and BxPC3 cell lines. Treatment with obestatin in BxPC3, causes an increase of both epithelial, E-cadherin (15.26 ± 2.41%), and mesenchymal markers, N cadherin (18.90 ± 3.17%). In contrast, in RWP-1 both, epithelial and mesenchymal markers, decrease: E-cadherin (27.27 ± 9.25%), N cadherin (37.14 ± 4.97%) and β-catenin (24.63 ± 12.33%, **Figure 2.7**).

A recent paper, established an EMT/MET metastatic tumour cell plasticity according to the histological growth pattern of liver metastases from digestive origin: colorectal, gastric and pancreatic. In this work, double immunostaining of E-cadherin/vimentin, keratin 8,18/vimentin and E-cadherin/keratin 8,18 were performed. They observed heterogeneous phenotype cells, with E-cadherin+/vimentin−, E-cadherin+/keratin 8,18+, keratin 8,18+/vimentin− cells between cells without immunoexpression of epithelial markers in the liver metastases and the corresponding primary tumours analysed [151]. However, another recent work shows that the expression of the cell-cell and cell-matrix adhesion molecules as intercellular adhesion molecule 1 (ICAM-1), E-cadherin, periostin and midkine (MK) was not significantly linked to metastatic disease in PDACs, excluding these molecules as prognostic markers in PDAC[152]. However, although it is difficult to establish whether metastases arise from tumour cells that have undergone EMT or sporadic disseminated tumour cells retaining the epithelial phenotype, some studies provide proof of principle that the metastatic cascade invokes E-cadherin rise and supports

---

[151] Ceausu AR, Ciolofan A, Cimpean AM, *et al*. The mesenchymal-epithelial and epithelial-mesenchymal cellular plasticity of liver metastases with digestive origin. Anticancer Res. 2018;38:811-6.
[152] Grupp K, Melling N, Bogoevska V, *et al*. Expression of ICAM-1, E-cadherin, periostin and midkine in metastases of pancreatic ductal adenocarcinomas. Exp Mol Pathol. 2018;104:109-13.
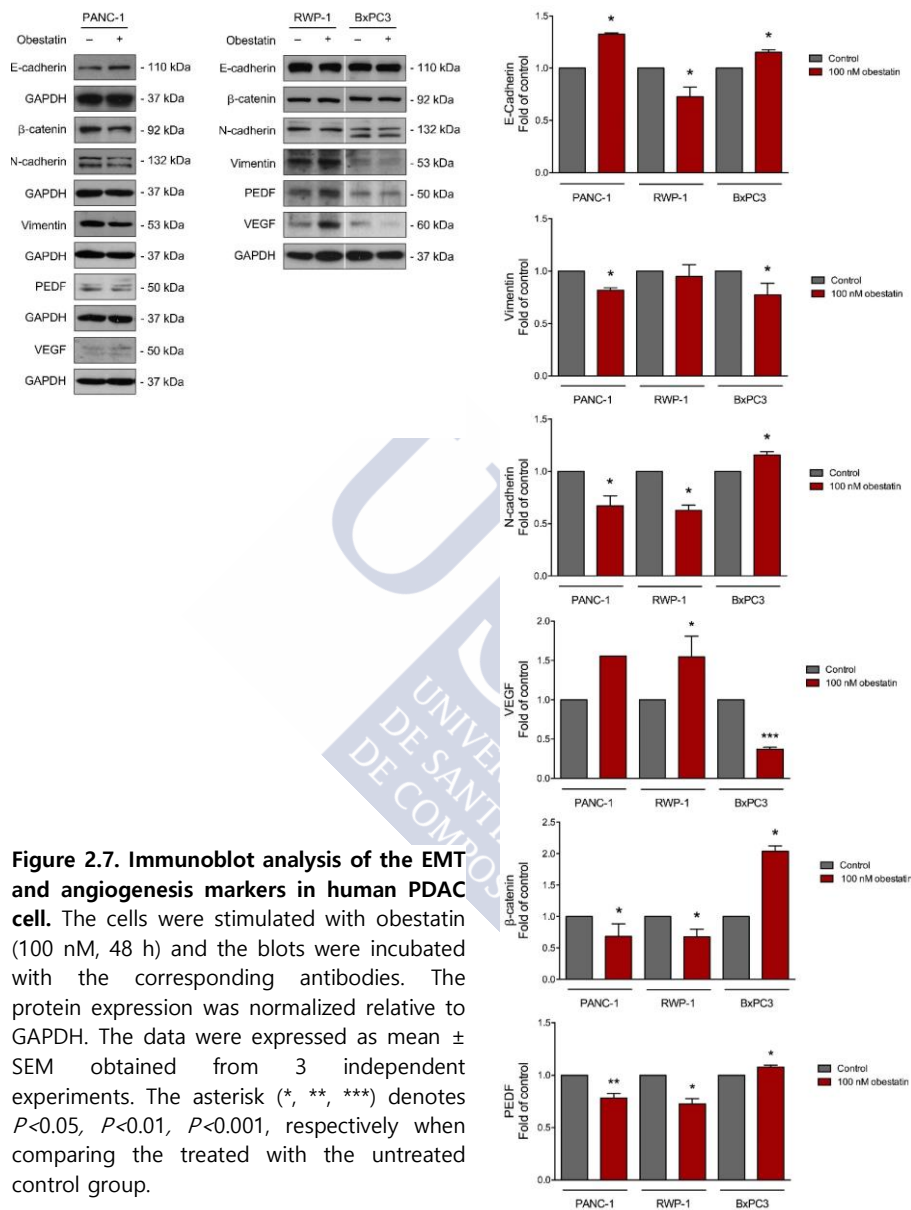
a MET-like phenomenon[150]. This cannot be addressed by examining human tumour specimens as all primary tumours present phenotypic heterogeneity, and the ontogeny of the metastases can only be indirectly inferred.

As it has been already described for gastric cancer cells[117], obestatin also upregulate the expression of angiogenic markers, VEGF and downregulate the antioangiogenic factor PEDF. The analysis of these factors in PANC-1 and RWP-1 cells (**Figure 2.7**) showed the same tendency favouring angiogenesis: the VEGF levels increase significantly at 48 h (PANC-1, 55.48%; RWP-1, 54.60 ± 26.58%) after obestatin treatment (100 nM), together with a significant decrease in the PEDF levels (PANC-1, 21.78 ± 4.29%; RWP-1, 27.41 ± 5.07%, **Figure 2.7**). On the other hand BxPC3 shows the opposite pattern where, VEGF levels decrease significantly at 48 h (62.97 ± 2.68) after obestatin treatment (100 nM), together with a significant increase in the PEDF levels (7.86 ± 1.65%, **Figure 2.7**). For many tumours, the vascular density can provide a prognostic indicator of metastatic potential, with the highly vascular primary tumours having a higher incidence of metastasis than poorly vascular tumours[153].

---

[153] Zetter BR. Angiogenesis and tumour metastasis. Annu Rev Med. 1998;49:407-24.

**Figure 2.7. Immunoblot analysis of the EMT and angiogenesis markers in human PDAC cell.** The cells were stimulated with obestatin (100 nM, 48 h) and the blots were incubated with the corresponding antibodies. The protein expression was normalized relative to GAPDH. The data were expressed as mean ± SEM obtained from 3 independent experiments. The asterisk (*, **, ***) denotes $P<0.05$, $P<0.01$, $P<0.001$, respectively when comparing the treated with the untreated control group.

The influence of obestatin in E-cadherin expression and distribution was also analysed by immunofluorescence in all PDAC cell lines (**Figure**

**2.8, Figure 2.9, Figure 2.10**). When PANC-1 and BxPC3 cells were treated with obestatin (200 nM) for 48 h, E-cadherin distribution resembled that of the control cells although with a stronger positivity for it and the cells presented an epithelial-like morphology. On the contrary, FBS treatment promoted the loss of the epithelioid morphology, with some spindle cells typical of the mesenchymal phenotype and an E-cadherin distribution completely different, forming intracytoplasmic protein aggregates in a perinuclear location. These aggregates would need further study to determine whether they are aggressomes or a specific type of protein-degradation system.

On the other hand, the cell line RWP-1 does not present differences between the controls and the cells treated with obestatin (200 nM) for 48 h, but it does present differences in co-treatment obestatin+FBS compared to FBS alone, since obestatin promotes an increase in E-cadherin favoring the epithelial phenotype, **Figure 2.9**.
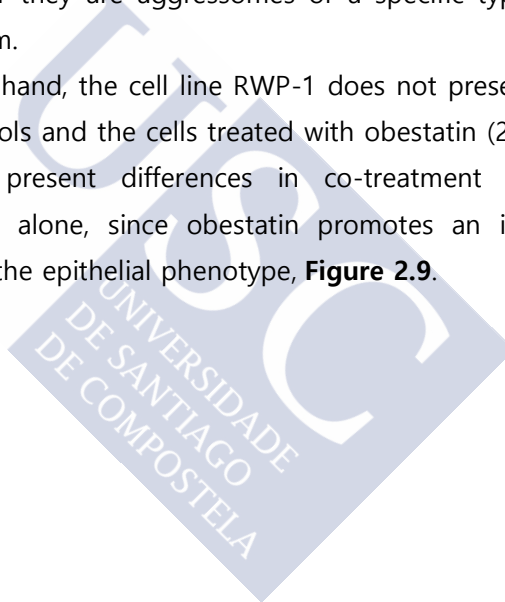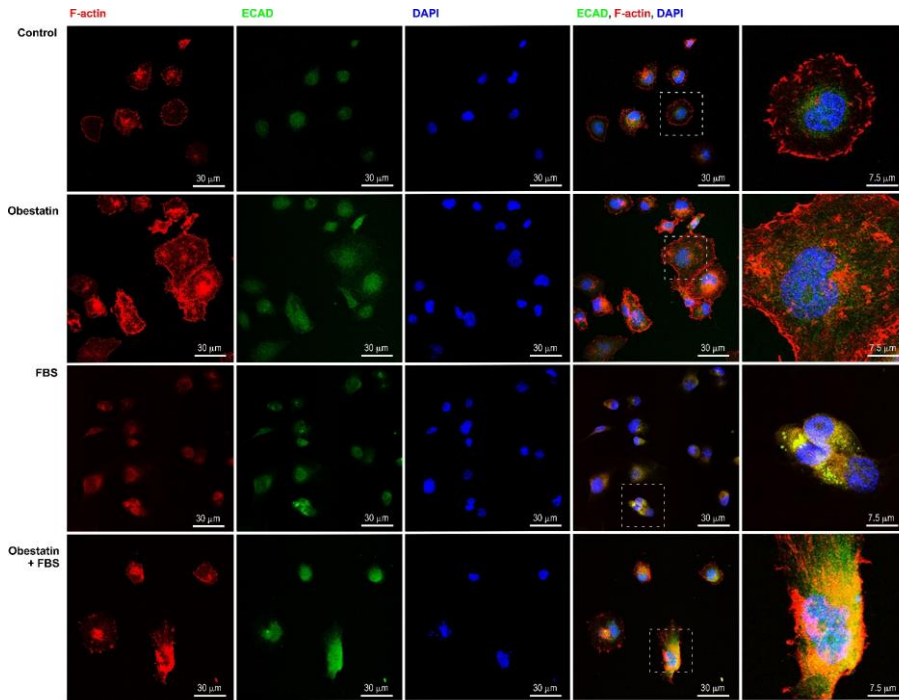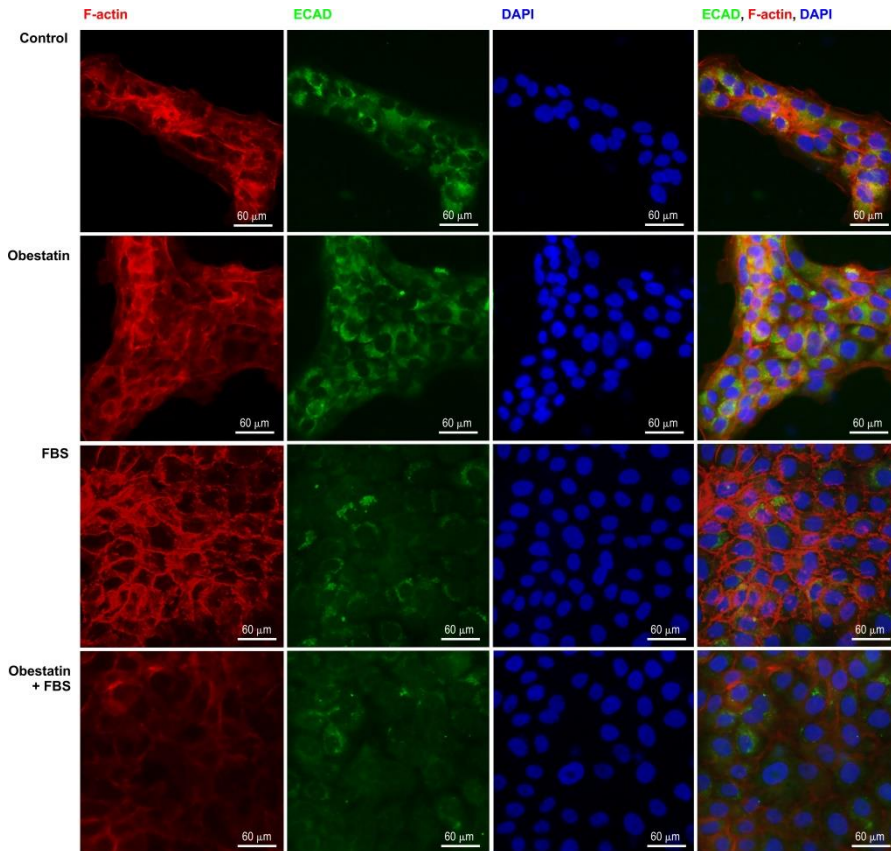
**Figure 2.8. Effect of obestatin on the E-cadherin phenotype and distribution in PANC-1 cells.** PANC-1 cells were stimulated with obestatin (200 nM), FBS (10%, v/v) or both for 48 h, then assessed for E-cadherin (green) and Phalloidin CruzFluor™ 594 Conjugate (red) to visualize F-actin and DAPI (blue) to visualize the nucleus by immunofluorescence. Scale bar= 30 µm. The images at the right represent a higher magnification view. Scale bar= 7.5 µm.
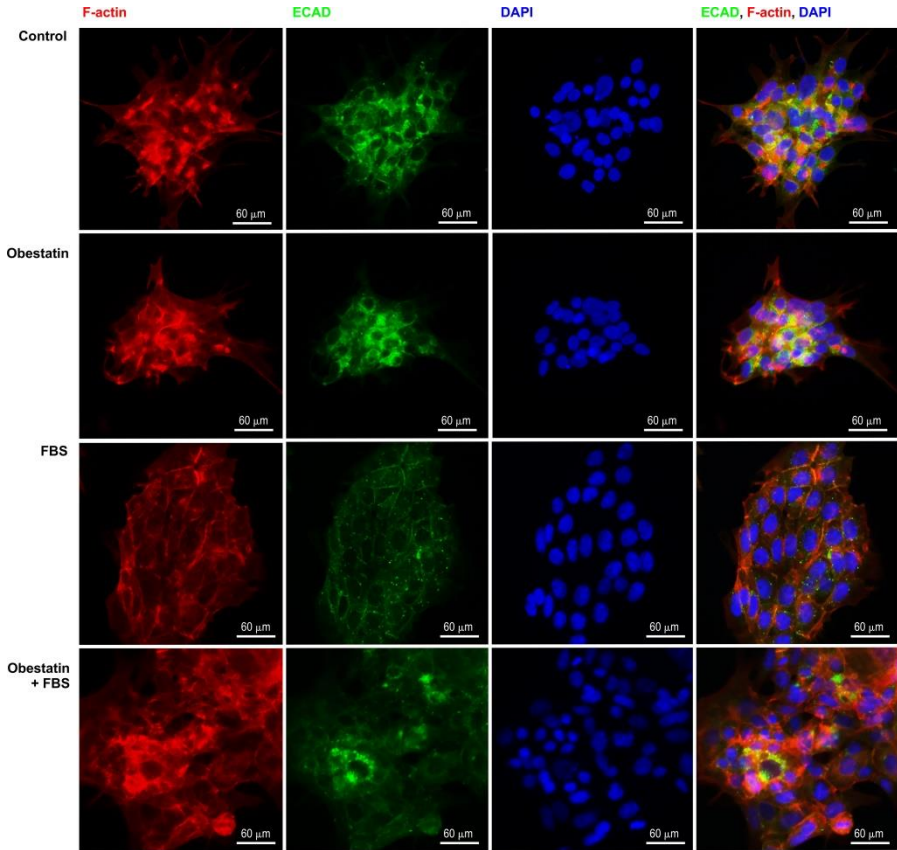
**Figure 2.9. Effect of obestatin on the E-cadherin phenotype and distribution in RWP-1 cells.** RWP-1 cells were stimulated with obestatin (200 nM), FBS (10%, v/v) or both for 48 h, then assessed for E-cadherin (green) and Phalloidin CruzFluor™ 594 Conjugate (red) to visualize F-actin and DAPI (blue) to visualize the nucleus by immunofluorescence. Scale bar= 60 μm.

**Figure 2.10. Effect of obestatin on the E-cadherin phenotype and distribution in BxPC3 cells.** BxPC3 cells were stimulated with obestatin (200 nM), FBS (10%, v/v) or both for 48 h, then assessed for E-cadherin (green) and Phalloidin CruzFluor™ 594 Conjugate (red) to visualize F-actin and DAPI (blue) to visualize the nucleus by immunofluorescence. Scale bar= 60 µm.
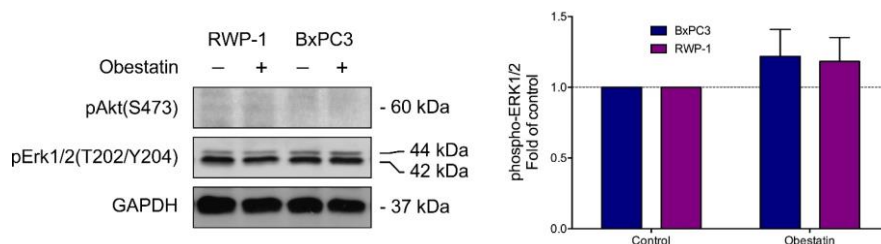
## EFFECT OF OBESTATIN ON AKT AND ERK1/2 ACTIVATION IN HUMAN PDAC CELLS

The dose response curves of Akt phosphorylation, at both the A-loop(T308) and the HM(S473), and ERK1/2 phosphorylation at T202/Y204 following stimulation of PANC-1 cells with obestatin (50, 100 and 200

nM) showed a dose-dependent pattern, being maximal at 200 nM, so this concentration was used in subsequent experiments. The kinetics of these activations showed a maximum at 5 min for all the concentrations tested **(Figure 2.11)**. With these data in mind, RWP-1 and BxPC3 cells where treated with 200 nM obestatin for 5 min. **Figure 2.12** shows that obestatin did not stimulate significantly the ERK1/2 and Akt phosphorylation in these cell lines although there is a tendency to increase the activation of ERK1/2. Surprisingly, there is no Akt phosphorylation for RWP-1 and BxPC3. These data need additional studies for confirmation.
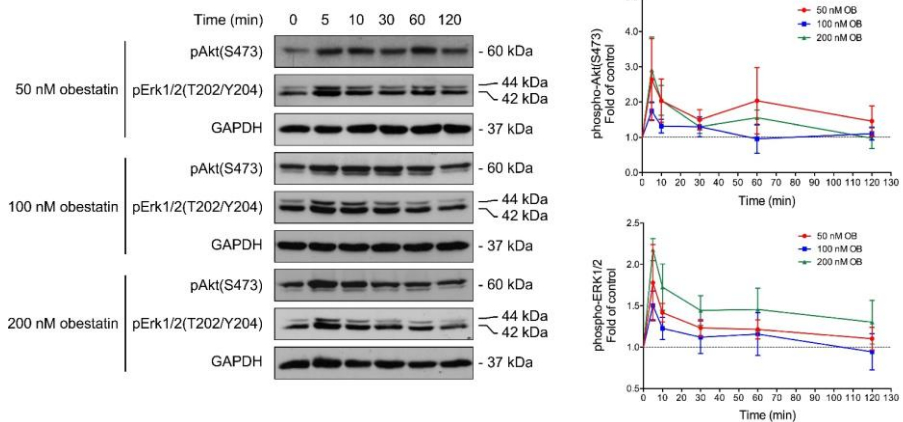


**Figure 2.11. Effect of obestatin in its main signalling targets Akt and ERK1/2 in human PC cells.** Time-course (5, 10, 30, 60, 120 min) and three doses of obestatin (50 nM, 100 nM and 200 nM) in PANC-1. pAKT and pERK1/2 were quantified by densitometry and expressed as a percentage of the maximal phosphorylation (mean ± SEM) of three independent experiments. The protein expression was normalized relative to GAPDH**.**

**Figure 2.12. Effect of obestatin on Akt and ERK1/2 activation in RWP-1 and BxPC3 cells.** RWP-1 and BxPC3 were treated with obestatin (200 nM, 5 min); pAKT and pERK1/2 were quantified by densitometry and expressed as a percentage of the maximal phosphorylation (mean ± SEM) of three independent experiments. The protein expression was normalized relative to GAPDH.

## OBESTATIN/GPR39 SIGNALLING INVOLVES EGFR AND EGFRvIII PHOSPHORYLATION IN HUMAN PDAC CELLS

Our previous studies about the obestatin/GPR39 system described the existent crosstalk between GPR39 and epidermal growth factor receptor (EGFR). This transactivation process of the EGFR by the GPR39 is produced in a "triple membrane passing signal pathway"[154] as it has been reported for other GPCRs, with the implication of β-arrestins and the activation of Src[106].

This fact together with the EGFR expression increased from PanIN to PDACS which could be related with an early event in carcinogenesis of PDAC and associated with tumour progression to invasive cancer[155]. In addition to the full-length EGFR (isoform A), three ectodomain EGFR isoforms (B, C, and D) without TK activity are generated from alternative transcripts encoding only the extracellular domain. Although little is known about isoform B, the transcripts of isoforms C and D encodes

---

[154] Wang, Z. Transactivation of epidermal growth factor receptor by G protein-coupled receptors: Recent progress, challenges and future research. Int J Mol Sci. 2016;17.pii:E95.

[155] Park SJ, Gu MJ, Lee DS, *et al.* EGFR expression in pancreatic intraepithelial neoplasia and ductal adenocarcinoma. Int J Clin Exp Pathol. 2015;8:8298-304.

protein products of 60/80 kDa and 90/110 kDa respectively. These isoforms may have a tumour-suppressive function through ligand sequestering or interaction with the full-length receptor, inhibiting its activation and are also known as sEGFRs[156].

Also several EGFR mutants exist and epidermal growth factor receptor variant III (EGFRvIII) isoform is the most common which is unable of binding any known ligand. It has been found that an aberrant signalling of EGFRvIII seems to be important in accelerating tumour progression and severe correlation with worse prognosis. EGFRvIII expression has been observed in a considerable number of patients with glioblastoma multiforme (GBM), although its presence in other tumour types, however, remains controversial[157].

To unveil the role of EGFR in obestatin/GPR39 signalling in the PDAC cells of the study, we first determined GPR39 and EGFR/EGFRvIII expression by immunoblot.

As **Figure 2.13** shows, PANC-1 and RWP-1 cells expressed considerable amounts of GPR39, although its expression is not clearly linked to the 51 kDa band. We observed extra high molecular weight bands that could reflect the presence of the GPCR-dimers or trimers. This effect has been already described for the GPR39 and the GHSR1a when samples are denatured at elevated temperatures in the prior stage to separation by electrophoresis[158].

Regarding EGFR, it was found to be overexpressed in all cell lines especially the 170 kDa isoform. However, significant differences were

---

[156] Halle C, Lando M, Svendsrud DH, *et al.* Membranous expression of ectodomain isoforms of the epidermal growth factor receptor predicts outcome after chemoradiotherapy of lymph node-negative cervical cancer. Clin Cancer Res. 201;17:5501-12.

[157] Gan HK, Cvrljevic AN, Johns TG. The epidermal growth factor receptor variant III (EGFRvIII): where wild things are altered. FEBS J. 2013;280:5350-70.

[158] Cunningham, PS. 2010. The ghrelin receptor isoforms (GHS-R1a and GHS-R1b) and GPR39: an investigation into receptor dimerization. University of Technology, Queensland, Australia. Doctoral dissertation. Queensland. https://eprints.qut.edu.au/39443/1/Peter_Cunningham_Thesis.pdf

observed in the expression of the 60 kDa isoform with increasing expression in the following order: PANC-1, RWP-1 and BxPC3. It has been postulated that this isoform can be produced by two mechanisms, one derived from EGFR mRNA alternative splicing and other derived from EGFR ectodomain (ECD) shedding by means of proteolytic cleavage of EGFR, resulting in the loss of the extracellular domains[156]. Likewise, EGFRvIII expression is observed with a tendency contrary to that of p60 EGFR, with PANC-1 cells presenting the highest expression **(Figure 2.13)**.
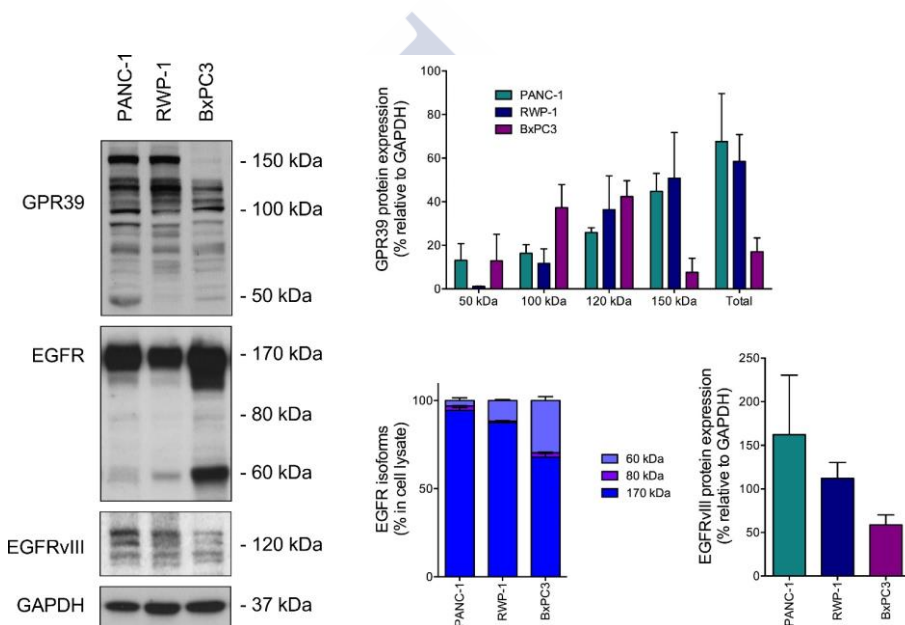


**Figure 2.13. Expression of GPR39, EGFR and EGFRvIII: study of the cross-talk process in the signalling of the obestatin/GPR39 system in the human PDAC cell lines.** Expression levels of GPR39, EGFR isoforms and EGFR vIII protein in PC cells. The protein expression was normalized relative to GAPDH. Expression levels were quantified by densitometry and expressed as (mean ± SEM) of three independent experiments.

To study the effect of obestatin on the 60 kDa isoform, BxPC3 cells were treated with obestatin (200 nM, 24 h) and both the composition of the lysate and the secretome were studied. It was found that obestatin significantly stimulated the synthesis of p170 EGFR observed in the lysate (**Figure 2.14**), but the proportion between the two isoforms, p170 and p60 EGFR is similar between controls and treated, unable to elucidate whether the increase in sEGFR comes from the *de novo* synthesis or the proteolytic cleavage of the ectodomain.

In the case of the secretome, an increase in the amount of p60 EGFR was observed. Considering that p170 EGFR is an isoform that is not secreted, the protein detected in the immunoblot can be the result of the apoptotic processes suffered by the cells. Because the increase in the soluble isoform is proportional to the increase in EGFR p170, treatment with obestatin could be increasing apoptosis in this cell line but not the secretion of the soluble isoform **(Figure 2.14).**
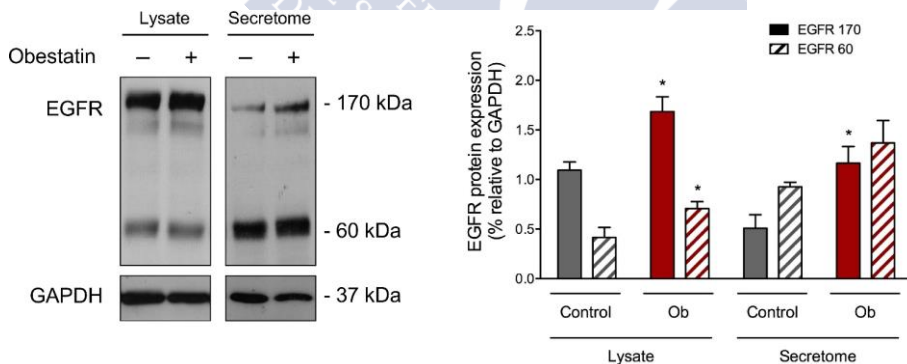


**Figure 2.14. Expression of EGFR after stimulation with obestatin in human cells BxPC3.** The BxPC3 cells were treated with obestatin (200 nM, 48 h) and the lysate and the secretome were analysed. EGFR was quantified by densitometry and expressed as a percentage of maximum phosphorylation (mean ± SEM) of three independent experiments. The protein expression was normalized relative to GAPDH.

Previously we described that the soluble form p60 EGFR is preventing the transactivation of EGFR, and Akt phosphorylation in the BxPC3 cell line. To corroborate this data, the activation, by phosphorylation, of the protein kinase S6 (Ser 240/244) was analyze. As **Figure 2.15** shows S6 activation is strongly inhibited by obestatin treatment (32.65 ± 4.12%).

One of the key proteins in the transactivation to EGFR by GRP39 driven by obestatin is Src. This protein plays a crucial role in many aspects of tumour development, including proliferation, survival, adhesion, migration, invasion and, most importantly, metastasis, in multiple tumour types[159]. In PANC-1 cells, obestatin treatment significantly stimulated Src phosphorylation (26.50 ± 0.41%; **Figure 2.16).**
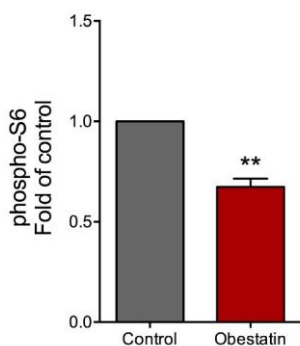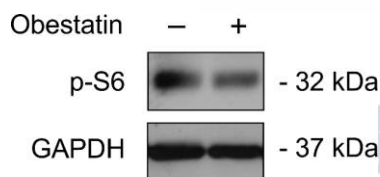


**Figure 2.15**. **Phosphorylation of S6 (Ser 240/244) after stimulation with obestatin in human cells BxPC3.** The BxPC3 cells were treated with obestatin (200 nM, 48 h) and the lysate were analysed. p-S6 was quantified by densitometry and expressed as a percentage of maximum phosphorylation (mean ± SEM) of three independent experiments. The protein expression was normalized relative to GAPDH.

---

[159] Zhang S, Yu D. Targeting Src family kinases in anti-cancer therapies: turning promise into triumph. Trends Pharmacol Sci. 2012;33:122-8.
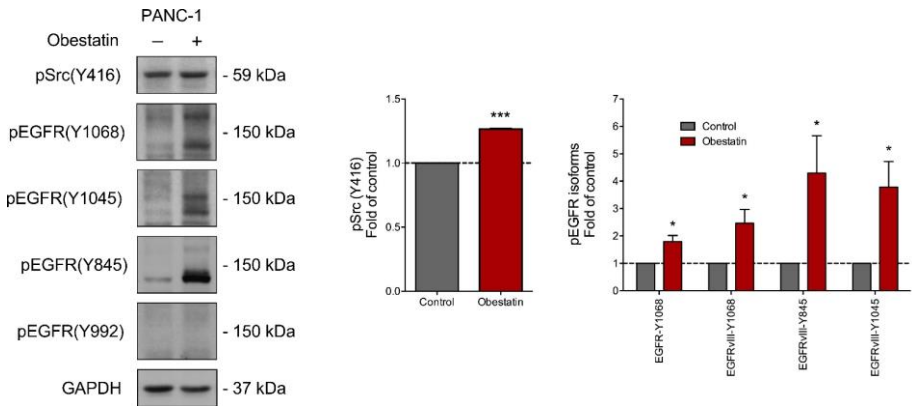
**Figure 2.16. Study of EGFR activation after stimulation with obestatin (200 nM, 10 min) in PANC-1.** Expression levels were quantified by densitometry and expressed as (mean ± SEM) of three independent experiments. The protein expression was normalized relative to GAPDH. The asterisk (*, ***) denotes $P<0.05$ and $P<0.01$ when comparing the treated with the untreated group.
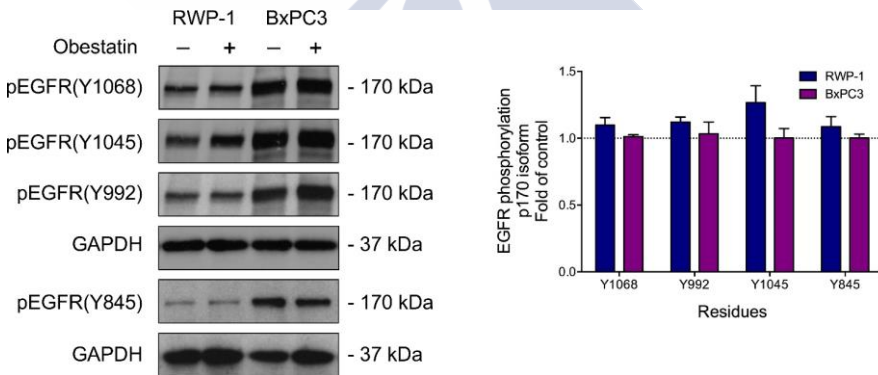


**Figure 2.17 EGFR phosphorylation p170 isoform by obestatin (200 nM, 5 min) in RWP-1 and BxPC3.** The protein expression was normalized relative to GAPDH. The data were expressed as mean ± SEM obtained from intensity scans of three independent experiments.

For the PANC-1 cells, the EGFRvIII isoform showed a clearly significant and specific stimulation of the Y845 and the Y1045 residues (4.30 ± 1.36 and 3.79 ± 0.94-fold of control, respectively), together with a shared activation with the EGFR in the Y1068 residue (1.79 ± 0.22 and 2.47 ± 0.50-fold of control, respectively), for the isoform p170 EFGR and for the EGFRvIII upon obestatin treatment (**Figure 2.16**). However, no significant modifications on EGFR phosphorylations were observed for the RWP-1 and the BxPC3 cell lines (**Figure 2.17**).

## THE EFFECT OF OBESTATIN ON THE PROLIFERATION OF PDAC HUMAN CELLS

Previous works of our research group demonstrated that the obestatin/GPR39 system operates as an autocrine/paracrine signal in the regulation of the proliferation of gastric cancer cells[117, 160]. After the corroboration of the obestatin/GPR39 system expression in the cell lines of the study, we next analysed the effect of exogenous administration of obestatin on cell proliferation by BrdU incorporation.

As **Figure 2.18** shows obestatin (100 nM and 200 nM) exerted a significant mitogenic effect in the PANC-1 cell line (∽35.88% over control) at 48 h. Nevertheless, the obestatin this effect was less pronounced in the RWP-1 cell line (∽32.55% over control) at 48h **(Figure 2.19)** and, in the case of the BxPC-3 cell line, inhibition of the proliferation was observed ( ∽55.62% over control) at 48h **(Figure 2.20)**. The observed differences in the obestatin proliferative capabilities might be due EGFR inhibition because sEGFR.

---

[160] Pazos Y, Alvarez CJ, Camiña JP, *et al.* Stimulation of extracellular signal-regulated kinases and proliferation in the human gastric cancer cells KATO-III by obestatin. Growth Factors. 2007;25:373-381.

In addition, to complete obestatin, the tumour cell lines BxPC3 and PANC-1 were tested with deamidated obestatin (DA-OB) (100 and 200nM) for 48h. The results were surprising, especially in PANC-1, because as **Figure 2.18** shows, DA-OB 200 nM exerts an effect contrary to complete OB, inhibiting proliferation (~53.84% respect the control). On the other hand, in the cell line BxPC3 the DA-OB also exerts an inhibitory effect of proliferation with DA-OB 100 nM the proliferation diminish ~ 45.65% and with DA-OB 200 nM diminish ~51.02% respect the control **(Figure 2.20)**.
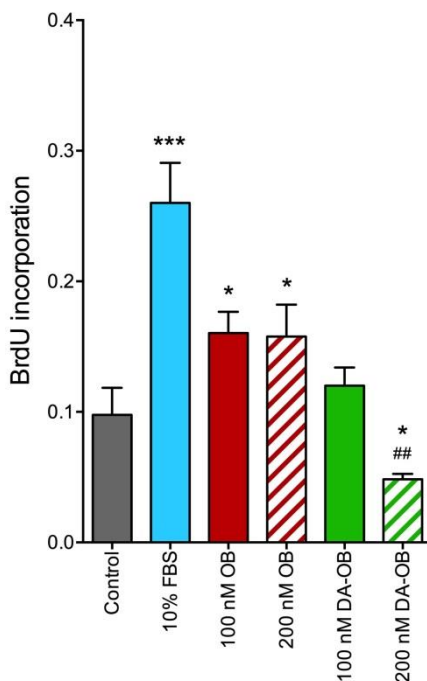


**Figure 2.18. The mitogenic effect of obestatin in the PANC-1 cell line.** The PANC-1 cells were treated with serum foetal bovin (FBS) (10%, v/v) (positive control) and obestatin (100 nM, 200 nM) and deamidated obestatin (DA-OB) (100 nM, 200 nM). PANC-1 cell proliferation was evaluated after 48 h and by means of BrdU incorporation of 8 independent experiments. The data were expressed as a percentage of the basal proliferation of the untreated cells (mean ± SEM). The asterisk (*, ***) denotes $P<0.05$ and $P<0.001$ respectively when comparing the treated with the untreated group, the dagger (##) denotes $P<0.01$ when comparing 200 nM DA-OB group with 100 nM DA-OB group.
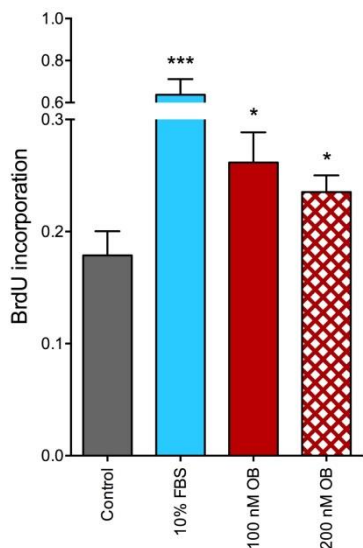
**Figure 2.19. The mitogenic effect of obestatin in the RWP-1 cell line.** The RWP-1 cells were treated with serum foetal bovin (FBS) (10%, v/v) (positive control) and obestatin (100 nM, 200 nM) and cell proliferation was evaluated after 48 h and by means of BrdU incorporation of 8 independent experiments. The data were expressed as a percentage of the basal proliferation of the untreated cells (mean ± SEM). The asterisk (*, ***) denotes $P<0.05$ and $P<0.001$ respectively when comparing the treated with the untreated group.
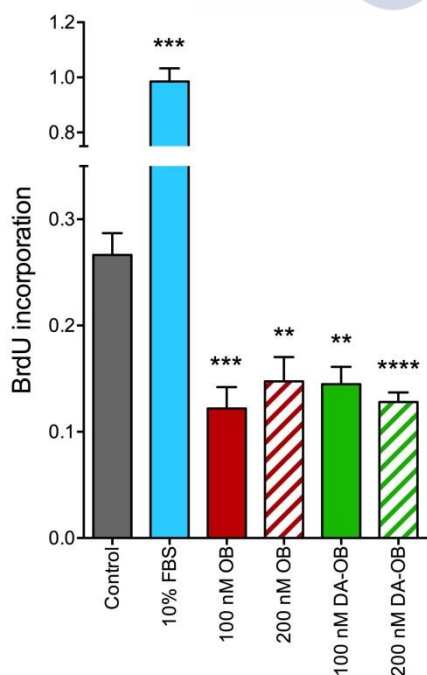


**Figure 2.20. The mitogenic effect of obestatin in the BxPC3 cell line.** The BxPC3 cells were treated with serum foetal bovin (FBS) (10%, v/v) (positive control) and obestatin (100 nM, 200 nM) and non amidated obestatin (DA-OB) BxPC3 cell proliferation was evaluated after 48 h and by means of BrdU incorporation of 8 independent experiments. The data were expressed as a percentage of the basal proliferation of the untreated cells (mean ± SEM). The asterisk (**, ***; ****) denotes $P<0.001$, $P<0.0001$ and $P<0.00001$ respectively, when comparing the treated with the untreated group.

## OBESTATIN/GPR39 SIGNALLING INVOLVES OTHER RTKS AND SRC FAMILY KINASES IN PANC-1 CELLS

GPR39/EGFR cross-talk is a key event in obestatin signalling as it has been discussed. Nevertheless, GPR39 crosstalk to RTKs is not only limited to EFGR. Previous data on gastric cancer showed that several RTKs were involved in the obestatin pathway in cancer cell lines (AGS and KATO III). Several of these activated receptors were also found to be overexpressed in gastric cancer tissues[142].

With that premise, the activation of a panel of RTKs was screened in PANC-1 cells after obestatin treatment (**Figure 2.21**). EGFR was the most activated RTK even in basal conditions; however Axl was the most activated after obestatin treatment. AXL belongs, with TYRO3 and MER, to the TAM family of RTKs and it is activated by the growth arrest-specific factor 6 (GAS6). This receptor is involved in the proliferation and invasion of many cancers, particularly in PDAC. In fact, Axl expression was predominantly observed in invasive pancreatic cells of human PDAC samples [161]. Besides, a small activation for RYK was observed after obestatin treatment. This receptor contains Wnt extracellular domains and it is implicated in Wnt signal transduction; however, whereas many other Wnt-signalling responses affect cell proliferation and differentiation, Ryk is

---

[161] Leconet W, Larbouret C, Chardès T, *et al.* Preclinical validation of AXL receptor as a target for antibody-based pancreatic cancer immunotherapy. Oncogene. 2014;33:5405-14.
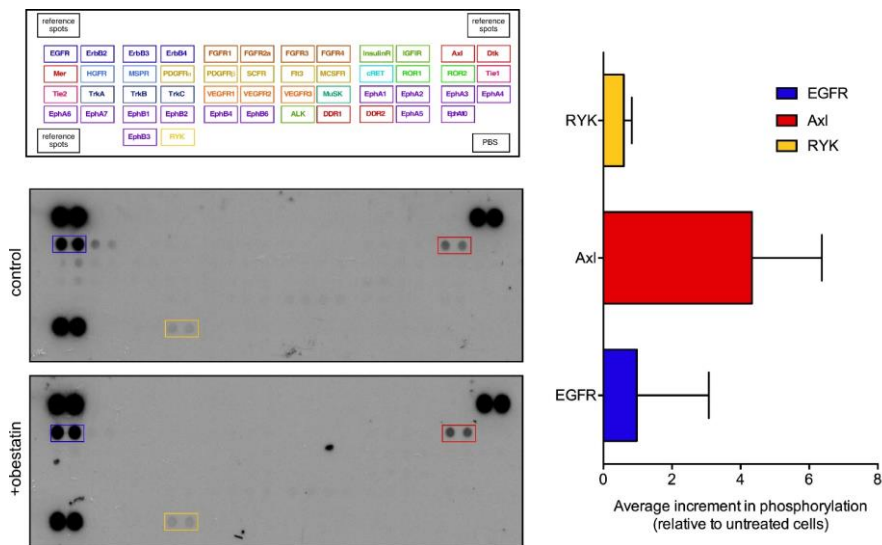
**Figure 2.21. Obestatin/GPR39 signalling involved other RTKs in PANC-1 cells.** Out of the 49 different phospho-RTKs in cell lysates three were highly expressed, EGFR, RYK and Axl, and two, RYK and Axl, were phosphorylated in obestatin-treated (100 nM 5 min). 200 µg of cell lysate were incubated on each array. Expression levels were quantified by densitometry and expressed (mean ± SEM).

mostly associated with controlling process that rely on the polarized migration of cells[162].

**Figure 2.22** shows the screening for RTKs and cytoplasmic tyrosine kinases (SFKs) in a more extended panel. In this array, we observed the activation of ACK, Hck and JAK2, as well as an inhibition in the phosphorylation of SYK. ACK/ACK1/TNK2 is a ubiquitously expressed oncogenic non–receptor tyrosine kinase, which integrates signals from ligand-activated RTKs to modulate intracellular signalling cascades. Activated ACK expression monitored by Tyr284 phosphorylation was

---

[162] Green J, Nusse R, van Amerongen R. The role of Ryk and Ror receptor tyrosine kinases in Wnt signal transduction. Cold Spring Harb Perspect Biol. 2014;6: pii: a009175.

significantly up regulated in pancreatic intraepithelial neoplasia (PanIN) and in biopsy specimens of advanced metastatic pancreatic cancer[163]. Hematopoietic cell kinase (HCK) is a member of the SRC family of SFKs, and is expressed in cells of the myeloid and B-lymphocyte cell lineages. Src is considered a rising therapeutic target for the treatment of solid tumours, and SFKs (Src, Fyn, Yes1, Lyn, Hck, and Frk) participate in pancreatic cancer cell proliferation and survival, and, therefore, in the metastatic potential of these cells[164]. The non-receptor tyrosine kinase Janus kinase 2 (JAK2) is involved in various processes such as cell growth, development, differentiation or histone modifications. Following ligand-binding to cell surface receptors, it phosphorylates specific tyrosine residues on the cytoplasmic tails of the receptor, creating docking sites for STATs proteins. The spleen tyrosine kinase, Syk, acts as a pancreatic adenocarcinoma tumour suppressor by regulating cellular growth and invasion of pancreatic cancer cells[165]. Then, the observed inhibition after obestatin treatment was in agreement with the mitogenic capabilities of this peptide.

[163] Mahajan K, Coppola D, Chen YA, *et al*. Ack1 tyrosine kinase activation correlates with pancreatic cancer progression. Am J Pathol. 2012;180:1386-93.
[164] Je DW, O YM, Ji YG, *et al*. The inhibition of SRC family kinase suppresses pancreatic cancer cell proliferation, migration, and invasion. Pancreas. 2014;43:768-76.
[165] Layton T, Stalens C, Gunderson F, *et al*. Syk tyrosine kinase acts as a pancreatic adenocarcinoma tumor suppressor by regulating cellular growth and invasion. Am J Pathol. 2009;175:2625-36.
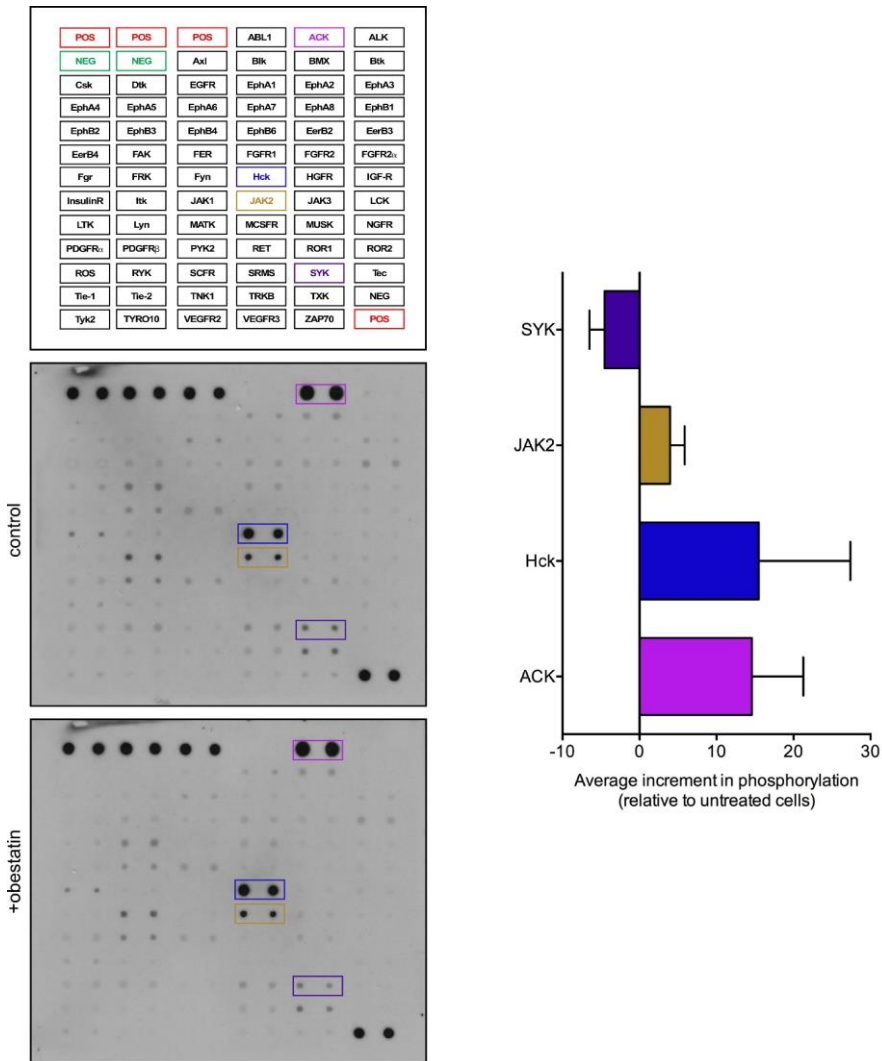
**Figure 2.22. Obestatin/GPR39 signalling involved other RTKs and SFKs in PANC-1 cells.**
Out of the 71 different phospho-RTKs in cell lysates ACK, Hck and JAK2 were phosphorylated and SYK dephosphorylated in obestatin-treated (100 nM, 10 min). 200 µg of cell lysate were incubated on each array. Expression levels were quantified by densitometry and expressed (mean ± SEM).

## OBESTATIN/GPR39 SIGNALLING INVOLVES THE ACTIVATION OF MAPK IN PANC-1 CELLS
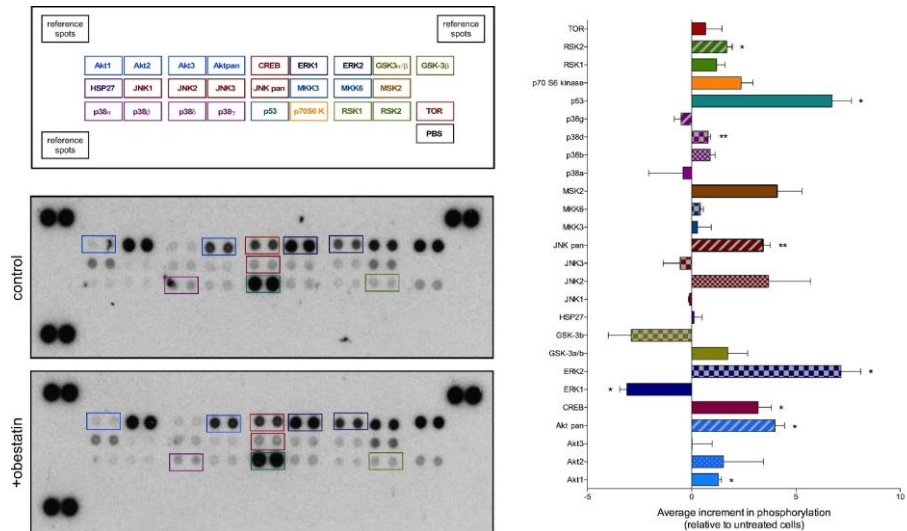


**Figure 2.23. Obestatin/GPR39 signalling involved the activation of MAPK in PANC-1 cells.** Out of the 26 different phospho-MAPKs in cell lysates eight MAPKs were highly phosphorylated and one was dephosphorylated in obestatin-treated (100 nM 5 min). 300 µg of cell lysate were incubated on each array. Expression levels were quantified by densitometry and expressed (mean ± SEM). The asterisk (*, **) denotes $P<0.05$, $P<0.01$ when comparing the treated with the untreated control group.

Obestatin stimulates cell proliferation by MEK/ERK1/2 phosphorylation in gastric cancer cells, through a Gi/o-protein dependent signalling pathway[160]. In PANC-1 cells, obestatin also stimulates ERK1/2. In the screening performed in PANC-1 cells some relevant facts were discovered. Besides the already described ERK1/2 and Akt activation some other proteins were activated, as JNK, CREB, p38δ, and p53 (**Figure 2.23**). c-Jun N-terminal kinase (JNK) is a member of the mitogen-activated protein kinase (MAPK) family, and it has a cancer-promoting effect in

133

pancreatic cancer [166] . Regarding CREB, very recently, it has been demonstrated that this protein inhibited the motility and invasiveness of PDAC cells [167] . Activated p38 MAPK α (pp38α) is a good prognostic marker in PDAC as it suppresses JNK-mediated proliferation, both in vitro and in vivo[168]; however, p38δ, presents a role in tumorigenesis linking inflammation and cancer in colitis-associated colon cancer[169]. *TP53* (also known as p53 or antigen NY-CO-13) is the tumour suppressor, which transcriptionally activates target genes in response to cellular stress such as oxidative stress or DNA damage and thus induces growth arrest or apoptosis. It also increases cyclin-dependent kinase inhibitor CDKN1A expression, thus stopping cell cycle progression. TP53 is one of the most frequently mutated genes in all cancers and is mutated in 70% of pancreatic cancers, mostly resulting in the loss of DNA binding ability and thus subsequently gene transcription activation[170]. In the case of RSK2, it is a downstream signalling protein of ERK1/2 and plays a key role in physiological homeostasis. For this reason, RSK2 is a highly conserved protein among the p90RSK family members. In its location in the signalling pathway, RSK2 is a kinase just upstream of transcription and epigenetic factors, and a few kinases involved in cell cycle regulation and protein synthesis. Moreover, activation of RSK2 by growth factors is directly involved in cell proliferation, anchorage-independent cell

---

[166] Takahashi R, Hirata Y, Sakitani K, *et al*. Therapeutic effect of c-Jun N-terminal kinase inhibition on pancreatic cancer. Cancer Sci. 2013;104:337-44.

[167] Taniuchi K, Furihata M, Naganuma S, *et al*. BCL7B, a predictor of poor prognosis of pancreatic cancers, promotes cell motility and invasion by influencing CREB signalling. Am J Cancer Res. 2018;8:387-404.

[168] Korc M. p38 MAPK in pancreatic cancer: finding a protective needle in the haystack. Clin Cancer Res. 2014;20:5866-8.

[169] Del Reino P, Alsina-Beauchamp D, Escós A, *et al*. Pro-oncogenic role of alternative p38 mitogen-activated protein kinases p38γ and p38δ, linking inflammation and cancer in colitis-associated colon cancer. Cancer Res. 2014;74:6150-60.

[170] Cicenas J, Kvederaviciute K, Meskinyte I, *et al*. KRAS, TP53, CDKN2A, SMAD4, BRCA1, and BRCA2 mutations in pancreatic cancer. Cancers (Basel). 2017;9:pii: E42.

transformation and cancer development [171]. In summary, the protein modifications observed in the screening performed in PANC-1 cells after obestatin treatment, supported the findings of this work; however, further investigations are needed to corroborate these data.

## OBESTATIN PROMOTES AUTOPHAGY IN PANC-1 CELLS
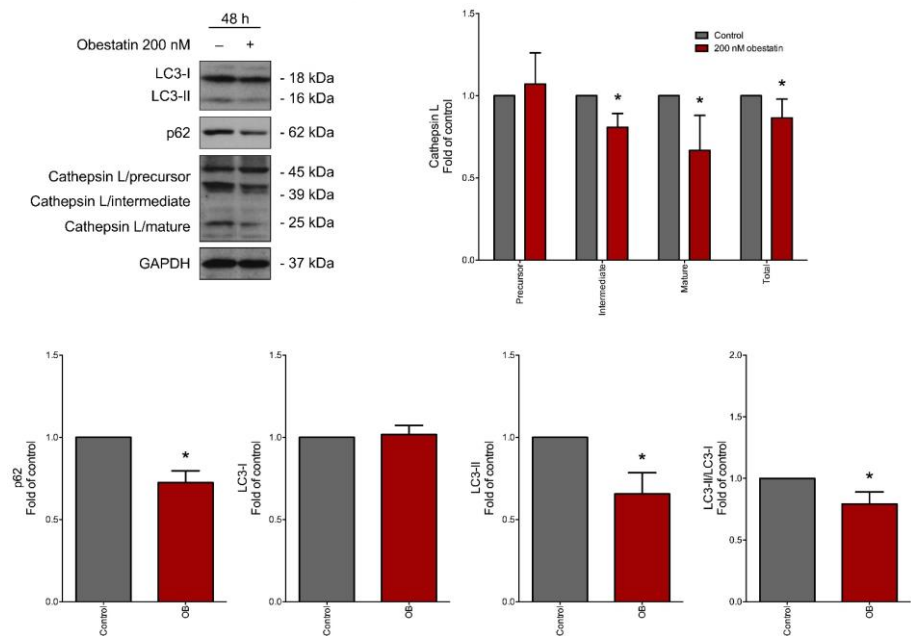


**Figure 2.24. Obestatin promoted autophagy in PANC-1 cells.** Immunoblot analysis of the autophagy in PANC-1 cells stimulated with obestatin (200 nM, 48 h). The blots were incubated with the corresponding antibodies to LC3 I/II, p62 and Cathepsin L. The protein expression was normalized relative to GAPDH. The data were expressed as mean ± SEM obtained from intensity scans of six independent experiments. The asterisk (*) denotes $P<0.05$, when comparing the treated with the untreated control group.

[171] Yoo SM, Cho SJ, Cho YY. Molecular targeting of ERKs/RSK2 signalling axis in cancer prevention. J Cancer Prev. 2015;20:165-71.

Despite conflicting evidence, the majority of data points to an essential role for autophagy in PDAC growth and survival, in particular constitutively activated autophagy, can provide crucial fuel to PDAC tumour cells in their nutrient-deprived environment. Autophagy, which is required for cell homeostasis, can both suppress and promote tumorigenesis and tumour survival in a context-dependent manner[172]. **Figure 2.24** shows the effects of obestatin treatment in the autophagy markers cathepsin L, p62 and LC3. Although the results support a role for obestatin on the increase of the autophagic process in PANC-1 cells, significantly diminishing cathepsin L and p62 (0.87 ± 0.06 and 0.73 ± 0.07, expressed as fold of control, respectively), there is a discrepancy in the expected value for LC3-II/LC3-I (0.79 ± 0.10, expressed as fold of control) as obestatin diminishes this ratio.
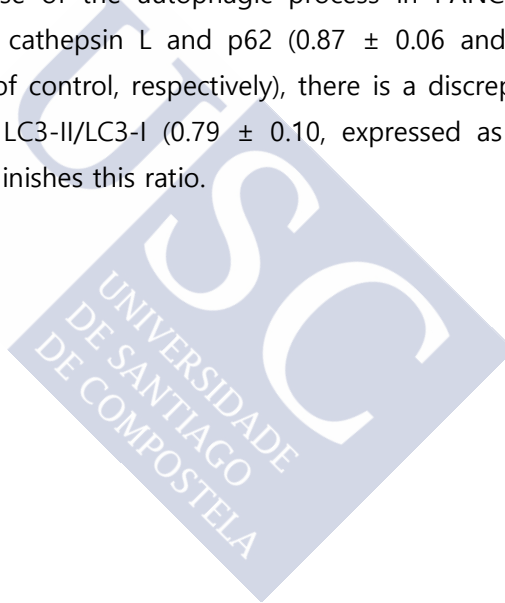
---

[172] New M, Van Acker T, Long JS, *et al.* Molecular Pathways Controlling Autophagy in Pancreatic Cancer. Front Oncol. 2017;7:28.

# CHAPTER 3: THE ROLE OF THE OBESTATIN/GPR39 SYSTEM IN THE HUMAN PANCREATIC STELLATE CELLS, RLT-PSCs.

It has been known that the pancreas is capable of at least partial regeneration of both, the endocrine and exocrine unit from a variety of injuries[173,174] but due the lack of appropriate in vitro models and the unavailability of histological samples, the molecular mechanism remained largely unknown [175]. Several years ago, the PSCs were described as potential regenerative cells after partial pancreatectomy in rats, and even early regeneration after acute necrotising pancreatitis in humans[25,37,38]. Also, some studies propose that, their homologs, the hepatic stellate cells (HSCs) contribute to liver regeneration, suggesting that these cells represent a source of liver progenitor cells[176]. This, together with the protective and regenerative effect described for obestatin in induced acute pancreatitis in rats[104, 177] and, mainly, the discovered of the GPR39^{+}/HSP47^{+} cells in human pancreas (Chapter 1), prompted us to study the regulatory function of the obestatin/GPR39 system in these pancreatic cells.

---

[173] Lehv M, Fitzgerald PJ. Pancreatic acinar cell regeneration. IV. Regeneration after resection. Am J Pathol. 1977;53:513-35.

[174] Pearson KW, Scott D, Torrance B. Effects of partial surgical pancreatectomy in rats. I. Pancreatic regeneration. Gastroenterology. 1997;72:469-73.

[175] Masamune A, Shimosegawa T. Pancreatic stellate cells-multi-functional cells in the pancreas. Pancreatology. 2013;13:102-5.

[176] Kordes C, Sawitza I, Götze S, *et al*. Hepatic stellate cells contribute to progenitor cells and liver regeneration. J Clin Invest. 2014;124:5503-15.

[177] Ceranowicz P, Warzecha Z, Dembinski A, *et al*. Pretreatment with obestatin inhibits the development of cerulein-induced pancreatitis. J Physiol Pharmacol. 2009;60:95-101.

## OBESTATIN/GPR39 SYSTEM AND STELLATE CELLS MARKERS ARE EXPRESSED IN ACTIVATED PANCREATIC STELLATE CELLS (aRLT-PSC).

As a model for this study, we selected the immortalized human pancreatic stellate cell line, RLT-PSC. This cell line has the ability to transform or transdifferentiate into an activated/quiescent state (aRLT-PSC/qRLT-PSC) and both forms retained characteristics of the original physiological state[128]. As seen in **Figure 3.1A**, the expression of obestatin/GPR39 was detected by immunochemistry. Intense and diffuse obestatin immunoreactivity was found in the cytoplasm (**Figure 3.1A.a**), whereas GPR39 was detected in the perinuclear region (**Figure 3.1.c**). No immunostaining was found in the cytoplasm when obestatin or GPR39 antibodies were preadsorbed with the homologous peptides (**Figure 3.1A.b** and **Figure 3.1A.d**, respectively).

In order to verify that RLT-PSCs preserved pancreatic stellate cell markers, the expression of different characteristic markers for activated stellate cells were analysed by immunohistochemistry. In that sense, **Figure 3.1B** shows the immunoreactivity found for: vimentin (**a**), S100 (**b**), GFAP (**c**), desmin (**d**), collagen I (**e**) and α smooth muscle actin (α-SMA) (**f**), even after prolonged culture of the cells.
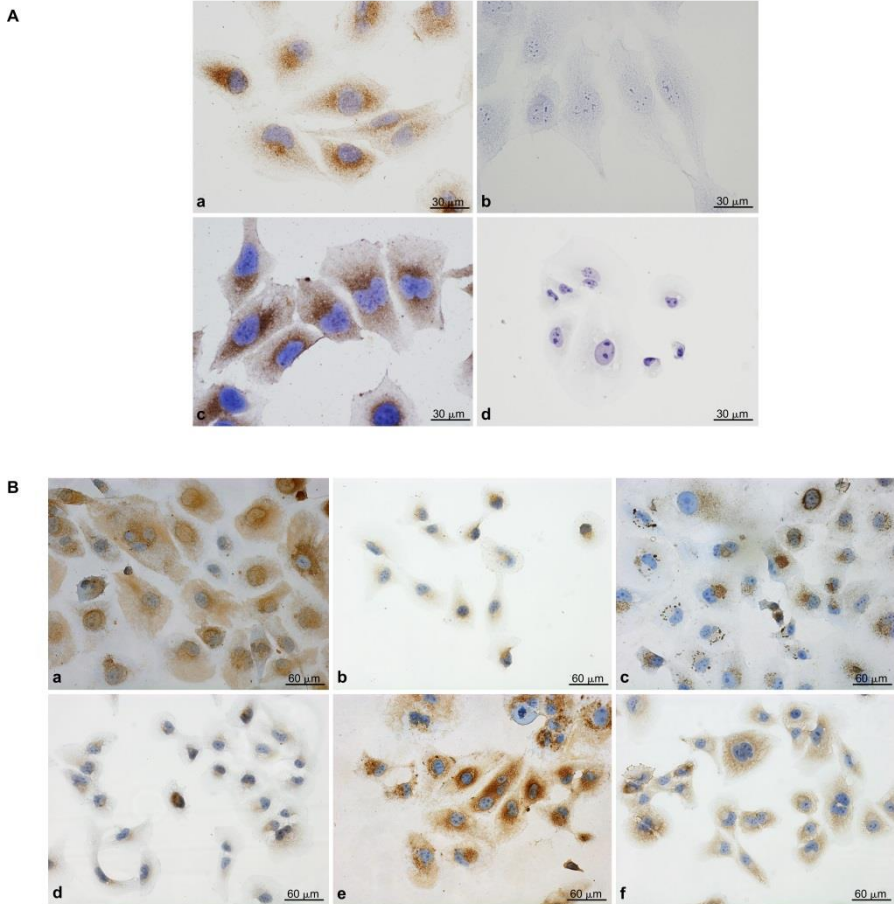
**Figure 3.1. Immunocytochemical expression of GPR39, obestatin, vimentin, S100, GFAP, desmin, collagen, α-SMA in activated RLT-PSC. A)** GPR39 and obestatin are expressed in activated RLT-PSC. a) GPR39 immunohistochemistry. b) The preadsorption control [performed applying the primary antibody plus obestatin (10 nmol/mL per control peptide)] showed no immunoreactivity. c) Obestatin expression. d) The preadsorption control [performed applying the primary antibody plus GPR39 control peptide (10 nmol/mL per control peptide)] showed no immunoreactivity. Scale bar= 30 µm. **B)** Immunocytochemistry revealed expression of the stellate cells activation markers, vimentin (a), S100 (b), GFAP (c), desmin (d), collagen I (e) and α-SMA (f) in the immortalized PSC. Scale bar= 60 µm.

The quiescence of the activated RLT-PSC cells can be induced by seeding on collagen I coating, nutrients deprivation and 2.5 mM NAC treatment. After 24 h of culturing in these conditions, the cells regained the ability to store retinol (vitamin A alcohol) in cytoplasmic vesicles, a hallmark of non-activated native PSC, as evidenced by measurement of the fluorescence of retinol (excitation 335 nm; emission 458 nm) (**Figure 3.2A.d**) and oil red staining (**Figure 3.2B.c-d**). Conversely, the activated counterpart did not present the lipid droplets (**Figure 3.2A.c** and **Figure 3.2B.a**). The quantification of these lipid vesicles by means of Oil red staining showed an increase by approximately 20% in lipids uptake (**Figure 3.2B**).

As it was mentioned before, PSCs are characterized for being a type of pluripotent cell that comprise several different cell subpopulations on the basis of different cell surface markers. PSCs CD271^{+} subpopulations of activated PSCs, which exist near human premalignant lesions and PC and are correlated with good prognosis[40]. Indeed, RLT-PSCs were obtained from CP patients and, subsequently immortalised. CD271 expression was confirmed by immunohistochemistry (**Figure 3.3.a**) in this cell line. **Figure 3.3.b** shows CD271 negative control in the absence of the primary antibody.
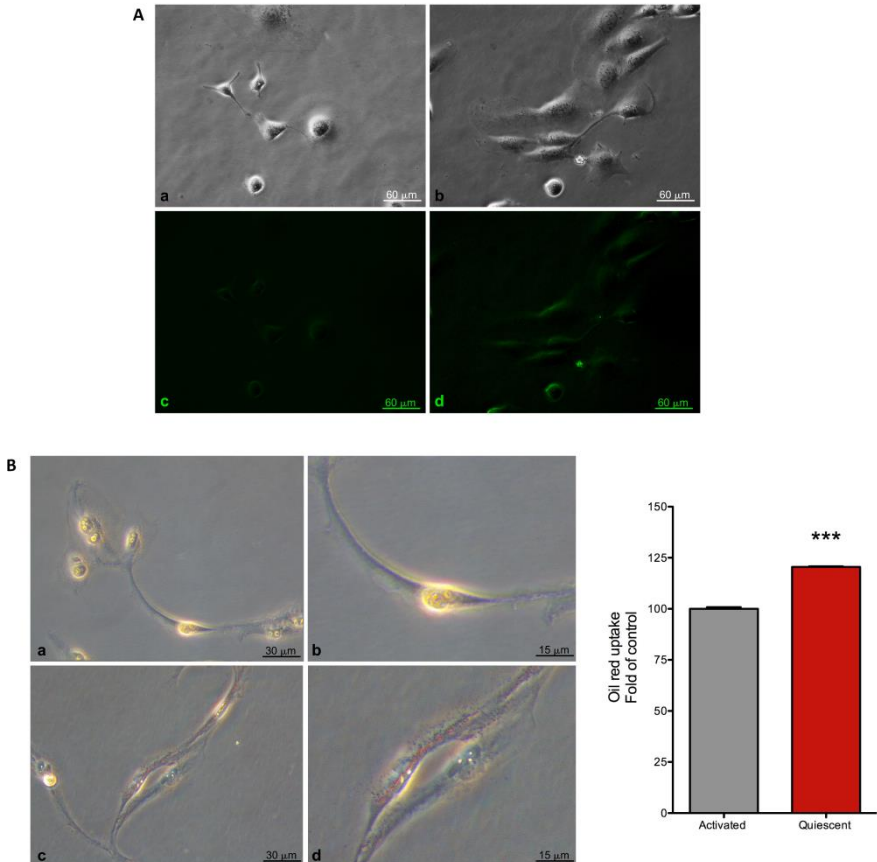
**Figure 3.2. Differences between aRLT-PSC and qPSC-RLT on morphology and vitamin A storage. A)** aRLT-PSC and qRLT-PSC phase contrast and autofluorescence images a) Observation of aRLT-PSC cultured in FBS 10% (v/v) at the inverted microscope showing cell culture. b) Observation of qRLT-PSC at the inverted microscope showing cell culture. c) aRLT-PSC no regained the ability to store vitamin A in cytoplasmic vesicles as shown using fluorescence microscopy, d) vitamin A was detectable in this vesicles by its auto fluorescence at an excitation wavelength of 320-380 nm in qRLT-PSC cultured for 24 h on presence of collagen I, 2.5 mM NAC and absence of FBS. Scale bar= 60 µm. **B)** Lipid droplets detected by Oil Red O staining. a) Absence of lipid droplets on aRLT-PSC. c) Presence of lipid droplets on qRLT-PSC. Scale bar= 30 µm. b) and d) represents a higher magnification view of RLT-PSC (scale bar= 15 µm). The graph shows up take Oil Red O quantification. Data shown are mean ± SEM (n=8).
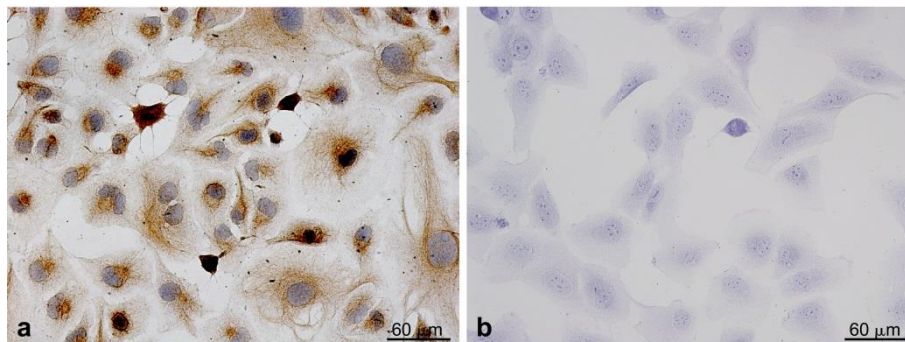
**Figure 3.3. Immunocytochemical expression of CD271 in aRLT-PSC.** a) CD271 is expressed in aRLT-PSC cell line. b) Negative control in the absence of primary antibody shows no staining. Scale bar= 60 μm.

## OBESTATIN INDUCES PROLIFERATION IN AN AUTOCRINE/PARACRINE MANNER IN aRLT-PSC CELLS.

One of the main characteristics of the obestatin/GPR39 system is the regulation of mitogenesis. In fact, obestatin treatment (100 nM, 48h) showed to increase by 30% the BrdU incorporation in RLT-PSC cells (**Figure 3.4**). Obestatin neutralization by anti-obestatin antibody (Ab) diminished BrdU incorporation by ⁓49% compared to obestatin treatment even below control levels. The antibody control treatment also decreased significantly BrdU incorporation by ⁓25% respect to untreated cells. This treatment might neutralize endogenous obestatin secreted by the cells.

The autocrine/paracrine role of obestatin was tested by a combination of serum-free conditioned medium from aRLT-PSCs obtained at 24 and 48 h (CM24 and CM48 respectively) with neutralizing obestatin antibody. The treatment of aRLT-PSC cells with CM24 and CM48 caused a significant increase in proliferation (⁓79% and ⁓49%, respectively). **Figure 3.4** shows a non-significant trend to decrease in the treatment with CM24

or CM48 + anti-obestatin antibody. This lack of effect might be due to factors secreted by the cells.
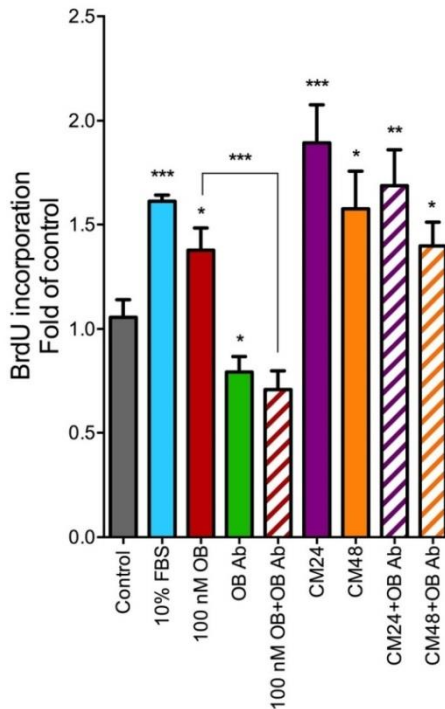


**Figure 3.4. Mitogenic effect of obestatin in the aRLT-PSC cells**. aRLT-PSC were treated with FBS (10%, v/v), obestatin ((OB (100 nM)), obestatin-antibody (OB-Ab (10 µg/mL)), obestain (100 nM) plus OB-Ab, conditioned medium (CM) 24 and 48 h, CM24+OB-Ab and CM48+OB-Ab, and cell proliferation was evaluated after 48 h by means of BrdU incorporation of 8 independent experiments. The asterisk (*, **, ***) denotes $P<0.05$, $P<0.01$ and $P<0.001$ when comparing the treated with the untreated group. The data were expressed as a percentage of the basal proliferation of the untreated cells.

**OBESTATIN PROMOTES CELL MOBILITY AND INVASION VIA EMT, ADHESION AND CYTOSKELETON REMODELLING IN ARLT PSC CELLS.**

It is well established that aPSCs migrate to sites of tissue damage, undergo regulated contraction, proliferate, phagocytose, and generate products that modulate the ECM by facilitating repair or promoting fibrosis[35]. The ability of obestatin to drive cell invasion was tested by using a specialized invasion chamber.

As shown in **Figure 3.5**, obestatin (100 nM, 16 h) significantly promoted the invasion of aRLT-PSC cells (4.29 fold of control).

Additionally, a migration assay was performed on aRLT-PSC cells under obestatin stimulation (100 nM). Confluent cell monolayers were physically wounded with a scratch and allowed to migrate for 24 h. As shown in **Figure 3.5**, obestatin-treated cells exhibited an increase of 47.75 ± 18.91% in the migration capability when compared with the control.

Besides migration, cell adhesion processes to the ECM are a key event for growth, survival and communication of these cells. As **Figure 3.6** shows, obestatin (100 nM, 30 min) increased RLT-PSCs adhesion to the collagen I matrix (25.80 ± 4.35%).
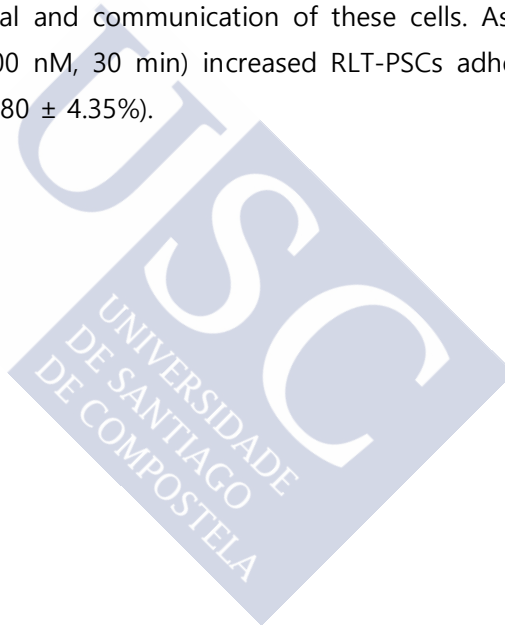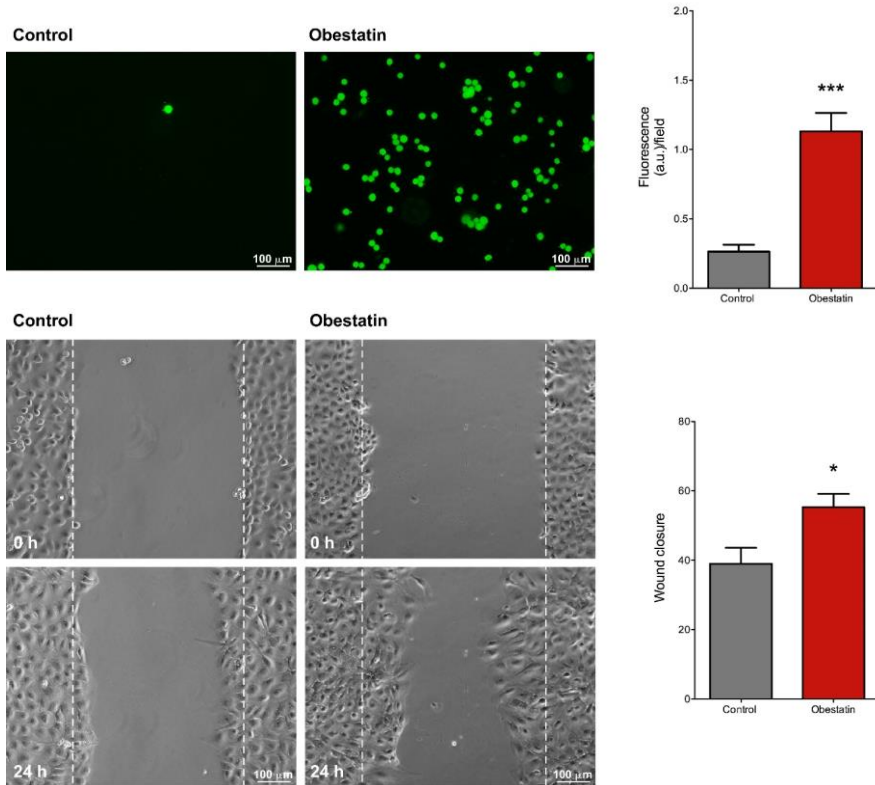
**Figure 3.5. Obestatin effect on invasion and migration on aRLT-PSC**. **Upper panel**: Invasion assay on aRLT-PSC following incubation or not with obestatin (100 nM) for 16h. Migratory cells pass through polycarbonate membrane and cling to the bottom side. Non-migratory cells are removed from upper chamber. The graph indicates mean grey intensity (a.u.) quantified at the image of bottom side. Scale bar= 100 μm. **Bottom panel:** Migration assay promoted by obestatin, cells were treated or not with obestatin (100 nM) for 24 h. The wound was calculated by tracing along the border of the scratch using ImageJ64 analysis software and the following equation: %wound closure= [wound area (0 h)-wound area (x h)]/wound area (0 h)] x 100. Scale bar= 100 μm. The data were expressed as mean obtained from 6 independent experiments. The asterisk (*, ***) denotes $P<0.05$ and $P<0.001$ when comparing the treated with the untreated group. Data shown are mean ± SEM.
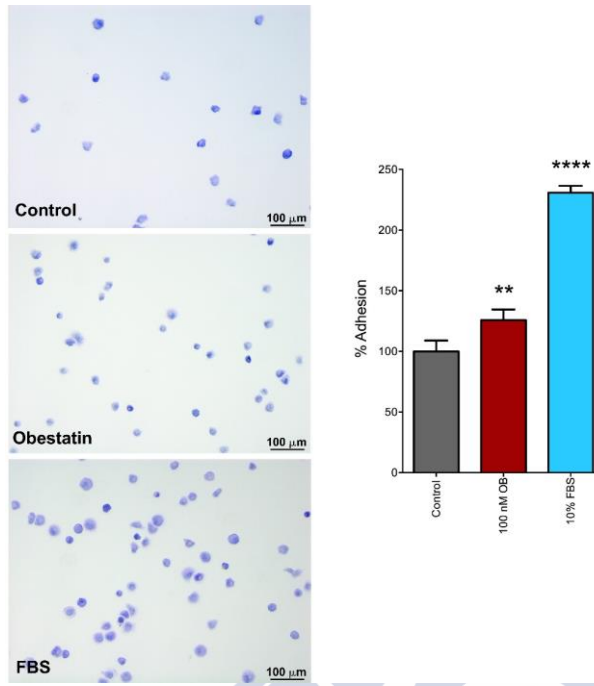
**Figure 3.6 Obestatin effect on adhesión on activated RLT-PSC.** aRLT-PSC were stimulated or not with obestatin (100 nM) and FBS 10% (v/v), as positive control, for 30 min. On a collagen I coating, the attached cells were fixed with paraformaldehyde 3.7% and stained with trypan blue. Non-attached cells are removed with PBS wash. Scale bar= 100 µm. The data were expressed as mean ± SEM obtained from 6 independent experiments. The asterisk (**, ****) denotes $P<0.01$ and $P<0.0001$ when comparing the treated with the untreated group.
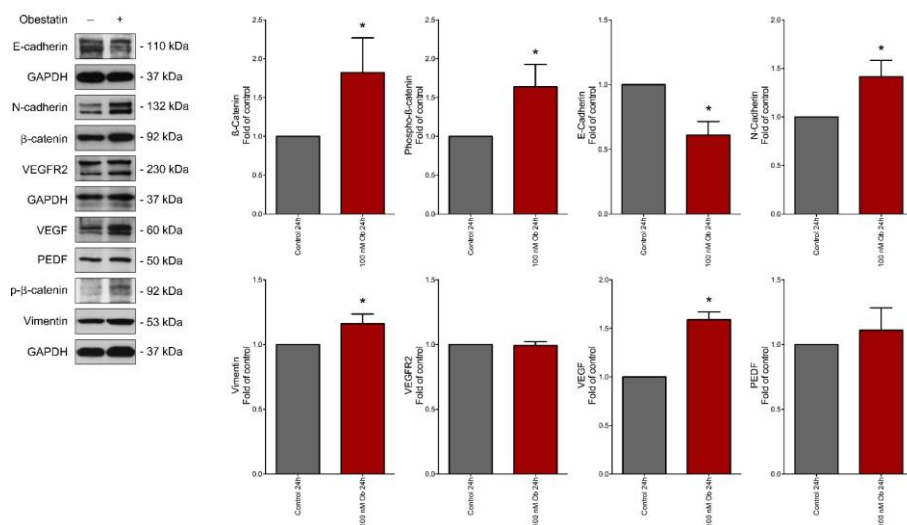
**Figure 3.7. Immunoblot analysis of the EMT and angiogenesis in aRLT-PSC cells.** The aRLT-PSC cells were stimulated with obestatin (100 nM) for 24 h and the blots were incubated with the corresponding antibodies to β-catenin, phospho-β-catenin, E-cadherin, N-cadherin, vimentin, VEGFR2, VEGF and PDF. The protein expression was normalized relative to GAPDH. The data were expressed as mean ± SEM obtained from intensity scans of six independent experiments. The asterisk (*) denotes P<0.05 when comparing the treated with the untreated control group.

The EMT is an essential trans-differentiation process, which plays a critical role in embryonic development, wound healing, tissue regeneration, organ fibrosis, and cancer progression. It is the fundamental mechanism by which epithelial cells lose many of their characteristics while acquiring features typical of mesenchymal cells, such as migratory capacity and invasiveness[178].

Since obestatin increased migration and invasion, we assessed obestatin's influence on EMT by examining the expression of β-catenin, phospho-β-catenin, E-cadherin, N-cadherin and vimentin. As **Figure 3.7**

---

[178] Forte E, Chimenti I, Rosa P, *et al.* EMT/MET at the crossroad of stemness, regeneration and oncogenesis: the ying-yang equilibrium recapitulated in cell spheroids. Cancers (Basel). 2017;9:98pii: E98.

shows, treatment with obestatin (100 nM, 24 h) caused a diminution of the epithelial marker E cadherin (38.08 ± 10.62%), and an increase of mesenchymal markers such as β-catenin (active form; 82.21 ± 44.69%), p-β-catenin (63.90 ± 29.00%), N-cadherin (41.46 ± 17.00%) and vimentin (16.10 ± 7.51%), favouring the EMT process in the aRLT-PSC cells. Another key process is the angiogenesis: the formation of new blood capillaries from pre-existing vasculature is crucial during physiological and pathologic conditions[179]. The angiogenic marker VEGF increased after obestatin treatment (100 nM, 24 h) by 58.90 ± 8.05% (**Figure 3.7**), whereas VEGFR and PEDF did not undergo significant changes.

The changes observed on vimentin and E-caherin in these cells, prompted us to study the distribution of these proteins by immunofluorescence. Vimentin reorganization is an important regulator of the intracellular changes in cytoplasmic mechanics, which is related to diverse physiological activities such as cell contraction, migration, proliferation, and organelle positioning. In fact, obestatin (100 nM, 24 and 48 h) caused a dramatic rearrangement of vimentin forming intricate structures surrounding the nucleus (**Figure 3.8**). These structures, commonly known as vimentin cages, alter the position of the nucleus in migrating cells[180].

---

[179] Saghiri M.A, Asatourian A, Sorenson CM, *et al.* Role of angiogenesis in endodontics: contributions of stem cells and proangiogenic and antiangiogenic factors to dental pulp regeneration. J Endod. 2015;41:797-803.

[180] Lowery J, Kuczmarski ER, Herrmann H, *et al.* Intermediate filaments play a pivotal role in regulating cell architecture and function. J Biol Chem. 2015;290:17145-53.
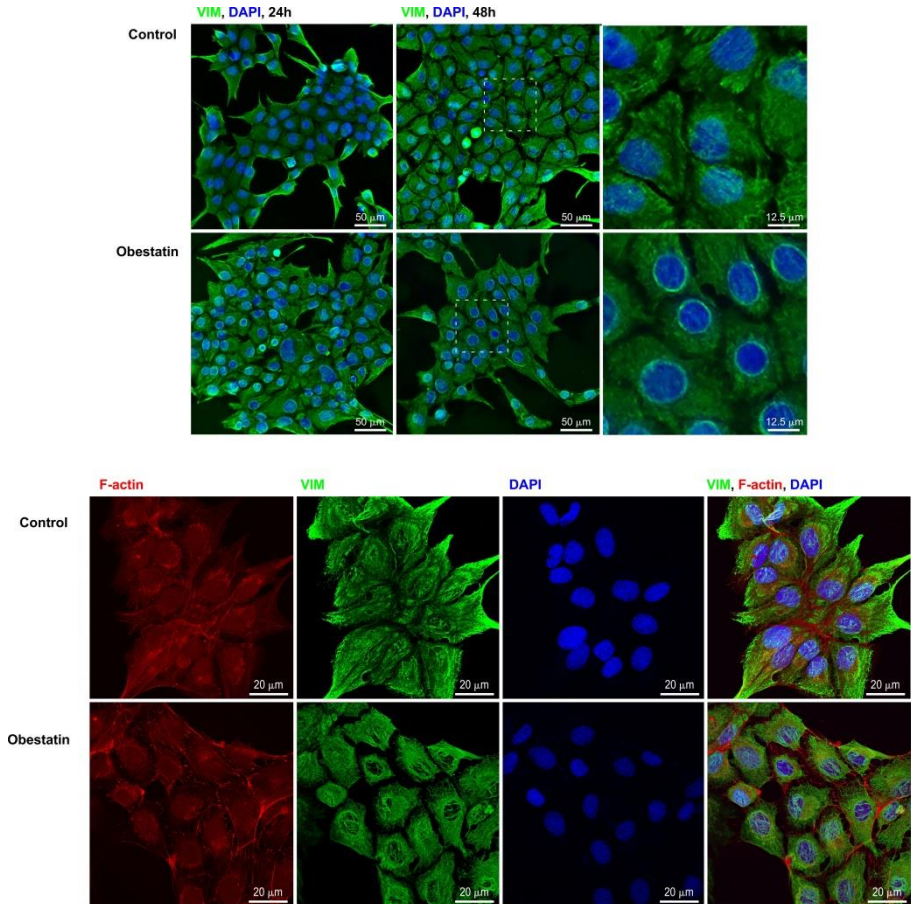
**Figure 3.8. Effect of obestatin on the vimentin phenotype and distribution in aRLT-PSCs.** The upper panel shows aRLT-PSCs stimulated with obestatin (100 nM) for 24 and 48 h, and then assessed for vimentin (green) and DAPI (blue) to visualize the nucleus by immunofluorescence. Scale bar= 50 μm. The images at the right represent a higher magnification view. Scale bar= 12.5 μm. The bottom panel shows aRLT-PSCs stimulated with obestatin (100 nM) for 48 h, and then assessed for vimentin (green) and Phalloidin CruzFluor™ 594 Conjugate (red) to visualize F-actin and DAPI (blue) to visualize the nucleus by immunofluorescence. Scale bar= 20 μm. Images are representative for at least three independent experiments.
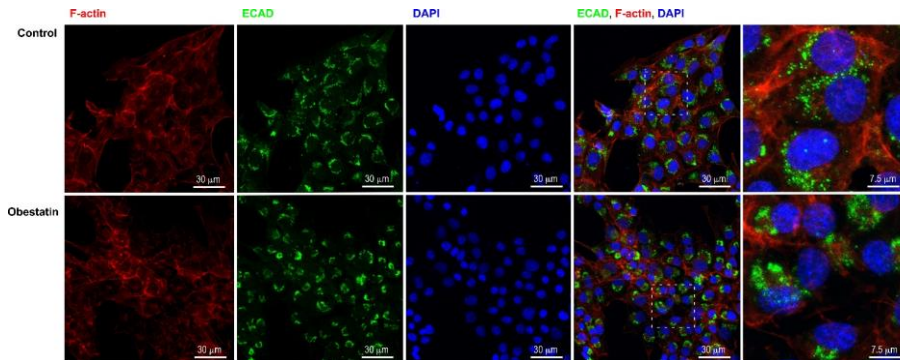
**Figure 3.9**. **Effect of obestatin on the E-cadherin phenotype and distribution in aRLT-PSCs.** aRLT-PSCs were stimulated with obestatin (100 nM) for 48 h, and then assessed for E-cadherin (green) and Phalloidin CruzFluor™ 594 Conjugate (red) to visualize F-actin and DAPI (blue) to visualize the nucleus by immunofluorescence. Scale bar= 30 µm. The images at the right represent a higher magnification view. Scale bar= 7.5 µm. Images are representative for at least three independent experiments.

E-cadherin is critical for the maintenance of tissue architecture and is a major component of the adherens junctions. Obestatin caused a redistribution of E-cadherin in perinuclear zones. This might be the result of endoplasmic reticulum-associated degradation (ERAD), a mechanism by which misfolded proteins are translocated to the cytosol and degraded by the ubiquitin–proteasome machinery (**Figure 3.9**). When these proteins are not coupled to rapid proteolysis, they have a serious risk of cytoplasmic aggregation, developing structures called aggresomes. These are located around the microtubule-organizing center (MTOC) by active minus end-directed transport of misfolded protein on microtubules[181]. In order to address this point, E-cadherin reorganization was studied for aggresome formation by the ProteoStat® Aggresome kit. Thus, the cells were treated or not with the following compounds: obestatin (100 nM, 48 h), the potent proteasome inhibitor MG-132 (7 µM, 16 h), the vehicle

---

[181] Kopito RR, Sitia R. Aggresomes and Russell bodies. Symptoms of cellular indigestion? EMBO Rep. 2000;1:225-31.

control DMSO (0.05% v/v, 18 h) and their combinations with obestatin. However, E-cadherin clusters did not colocalize with the aggresome structures induced by MG-132. Additional assays are needed to exactly determine which is E-cadherin fate. Surprisingly, obestatin treatment caused the formation of aggresome structures. **Figure 3.10** shows the aggresomes detected by ProteoStat® Aggresome dye (red). These aggregates were quantified and represented by means of a number of aggregates present by cell, as show the **Figure 3.11**. Obestatin (100 nM) significantly stimulated the formation of aggresomes (~15.88 fold of control). As expected, MG-132 induced aggresome formation by ~7.14 fold of control, and MG-132+obestatin treatment caused an even more intense effect (~10.23 fold of control). Vehicle alone, DMSO, did not stimulate aggresome formation. Obestatin treatment, in the presence of vehicle, induced aggresome formation with similar values to those of obestatin treatment alone (~16.20 fold of control). Further research is needed to determine the composition of such structures caused by obestatin.
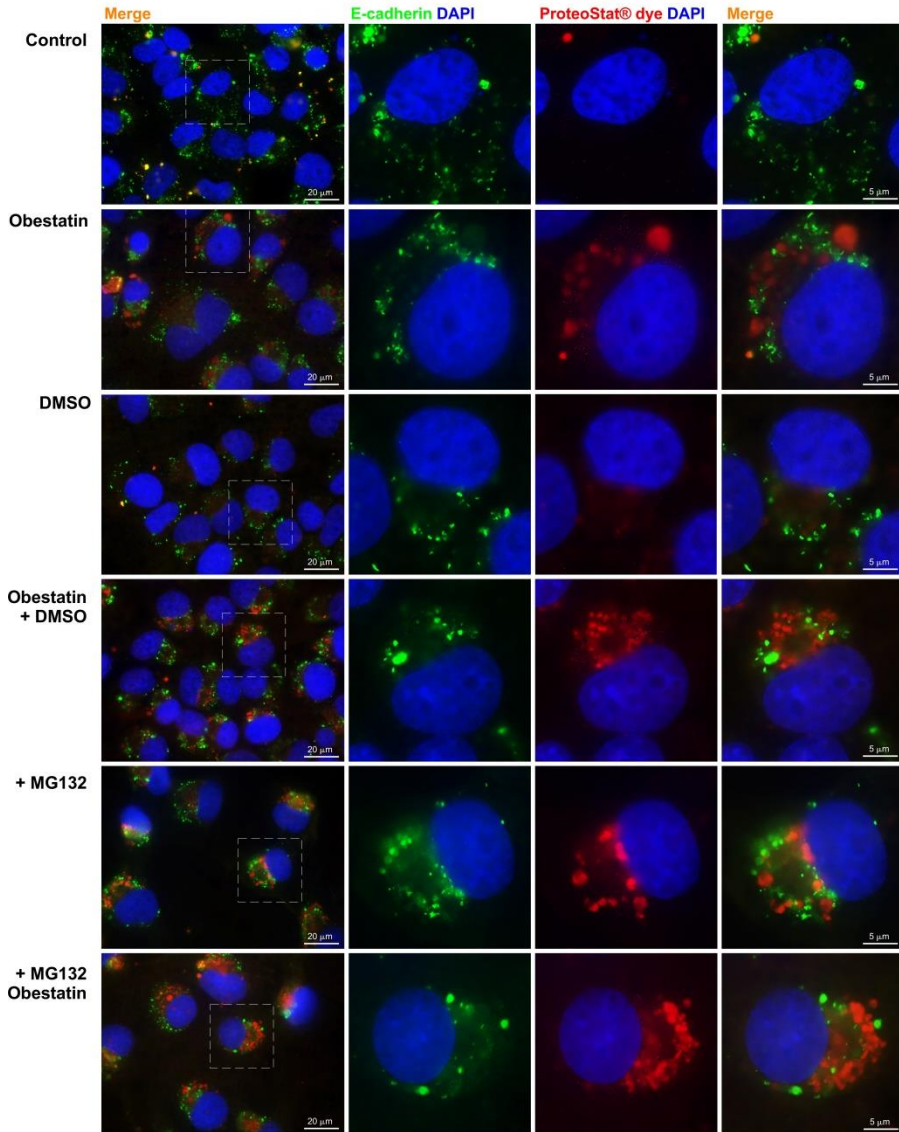
**Figure 3.10. Effect of obestatin on the aggresome formation and E-cadherin distribution in aRLT-PSCs.** aRLT-PSCs were stimulated or not with obestatin (100 nM, 48 h), DMSO (0.05% v/v, 18 h), MG132 (7 µM, 18 h) and their respective combinations with obestatin. Then was assessed aggresome detection with ProteoStat® dye (red) to visualize aggresomes, E-cadherin (green), and DAPI (blue) to visualize the nucleus by immunofluorescence. Scale bar= 20 µm. The images at the right represent a higher magnification view. Scale bar= 5 µm. Images are representative for at least three independent experiments.
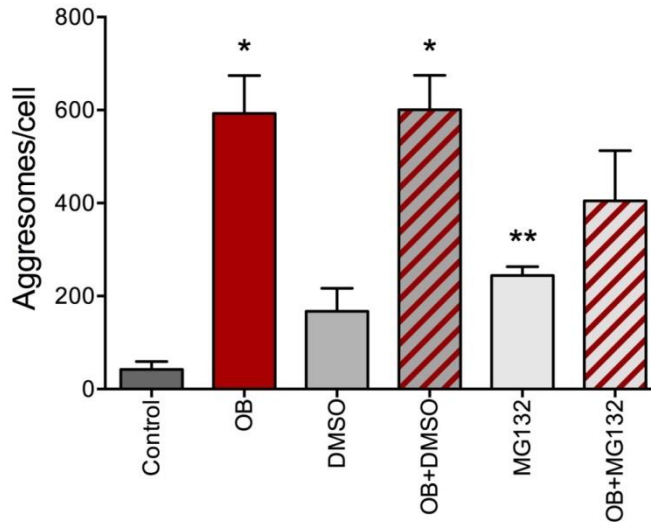
**Figure 3.11 Quantitative analysis of number of aggresomes/cell.** Aggregates formed in each treatment were calculated using the ImageJ64 analysis software

## OBESTATIN IS INVOLVED IN THE REGULATION OF THE AUTOPHAGIC PROCESS IN aRLT-PSCs.

Processing of misfolded proteins is important to maintain cell normal functioning and homeostasis. Aggresomes can potentially be cleared by the autophagy pathway, called aggrephagy but the biochemical mechanism that regulates this process is still an unknown[182]. The ubiquitin proteasome system and the autophagy are functionally coupled. Autophagy contributes to the processing of aggregated proteins resistant to proteasomal degradation. MG-132 caused the formation of aggresome-like aggregates and the bibliography shows a relationship between MG-132 and enhanced induction of autophagy signalling, which

---

[182]Hyttinen JM, Amadio M, Viiri J, *et al*. Clearance of misfolded and aggregated proteins by aggrephagy and implications for aggregation diseases. Ageing Res Rev. 2014;18:16-28.

was accompanied by increased turnover of the autophagy process and protein clearance[183].

Recently Camiña´s group have pointed out the role of the obestatin/GPR39 system in autophagic processes in myotube C2C12 cells[184], so our goal is to determine the effect of obestatin on the autophagic process in cell line aRLT-PSC. This fact, together with the capability of obestatin to form aggresomes led us to study this intracellular degradation pathway in the aRLT-PSCs. To address this purpose we investigated the level of three proteins key on autophagic processes in aRLT-PSC cells treated with obestatin (100 nM, 48 h): the microtubule-associated protein 1 light chain 3 (LC3), cytosolic form (LC3-I) and its conjugated form, LC3-phosphatidylethanolamine (LC3-II), p62 and cathepsin L.

The LC3-I marker is in the cytoplasm, and the LC3-II is a reliable marker associated with the autophagosomal membrane, was slightly elevated (**Figure 3.12**), as revealed by an increase in the LC3-II/LC3-I (6.10 ± 1.78%) ratio. LC3II accumulation indicates a progression in autophagic process. LC3I does not present significant changes of expression respect to the control. However, p62, which binds directly to LC3 towards autophagic degradation of ubiquitinated proteins, presented a significant accumulation (11.86 ± 6.84%; **Figure 3.12**) indicating that the autophagic flux is blocked. Also obestatin stimulation was associated with a reduction, at 24 h, in the expression of the mature lysosomal enzyme cathepsin L (33.22 ± 9.473%) further supporting an at least partial

[183] Bang Y, Kang BY, Choi HJ. Preconditioning stimulus of proteasome inhibitor enhances aggresome formation and autophagy in differentiated SH-SY5Y cells. Neurosci Lett. 2014;566:263-8.

[184] Cid-Díaz T, Santos-Zas I, González-Sánchez J, *et al*. Obestatin controls the ubiquitin-proteasome and autophagy-lysosome systems in glucocorticoid induced muscle cell atrophy. Journal of Cachexia, Sarcopenia and Muscle 2017;8:974-90.

inactivation of autophagy; at 48 h we also detected a slight but significant reduction of cathepsin L (13.21 ± 4.28%).
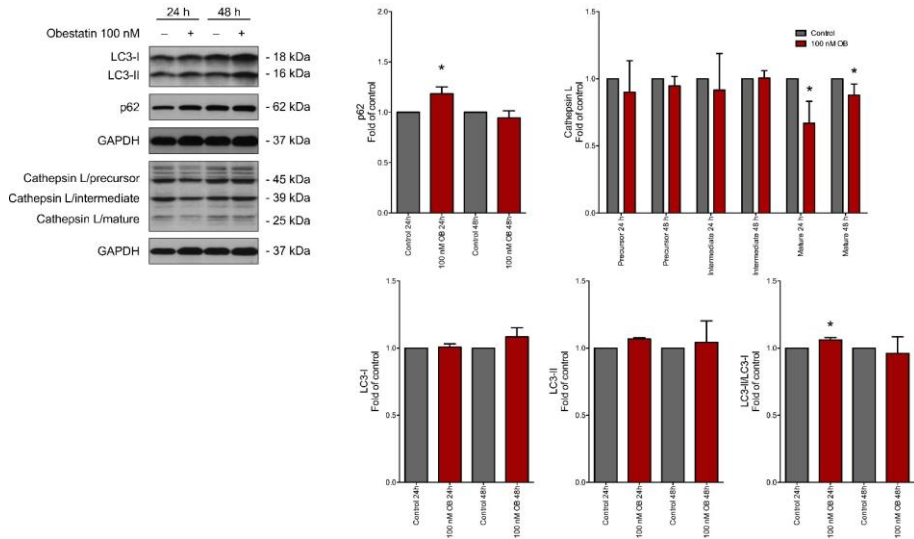


**Figure 3.12. Effects of obestatin on the autophagy regulation in aRLT-PSCs.** Immunoblot analysis of autophagy-related proteins LC3-I, LC3-II, p62 and cathepsin L in aRLT-PSCs under obestatin treatment (100 nM) or not at 24 and 48 h. The graph represents the relative ratios of signal intensities for LC3II/LC3-I, p62 and cathepsin L normalized relative to GAPDH. The data were expressed as mean ± SEM obtained from intensity scans of three independent experiments. The asterisk (*) denotes $P<0.05$ when comparing the treated with the untreated control group

## DIFFERENTIAL MAPK PHOSPHORYLATION PATTERN ACTIVATED BY OBESTATIN IN aRLT-PSC CELLS.
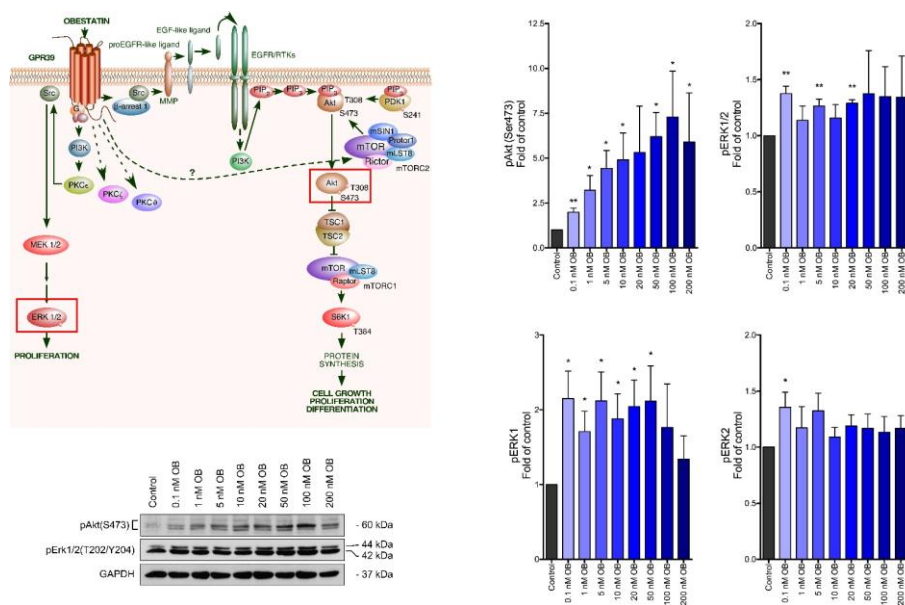


**Figure 3.13. Immunoblot analysis of dose responsive effect of obestatin on phosphorylation on key proteins on in activated RLT-PSCs**. Proposed model of signalling pathway for Akt and ERK1/2 activation in response to obestatin (upper pannel); Alvarez CJ *et al.* Endocr-Relat Cancer. 2009;16:599-611. With permissions from Bioscientifica Limited. The RLT-PSCs were stimulated with obestatin (0.1, 1, 5, 10, 20, 50, 100, and 200 nM) for 10 min and the blots were incubated with the corresponding antibodies for pAkt (S473) and pERK1/2 (T202/Y204). The protein expression was normalized relative to GAPDH. The data were expressed as the fold of control obtained from intensity scans of six independent experiments. The asterisk (*, **) denotes $P<0.05$ and $P<0.01$ when comparing the treated with the untreated control group.

The dose-response curve of Akt(S473) phosphorylation, following stimulation of aRLT-PSC cells with obestatin showed a dose-dependent pattern for Akt, being maximal at 100 nM (~7.29 fold of control), so this concentration was used in subsequent experiments. However, ERK1/2,

ERK1 and ERK2 showed activation at lower doses (0.1-20nM and 0.1-50nM, respectively; **Figure 3.13**).

Mitogen-activated protein kinases/extracellular signal regulated kinase (MAPK/ERK) pathway is reported to be associated with the cell proliferation, differentiation, migration, senescence and apoptosis[185].
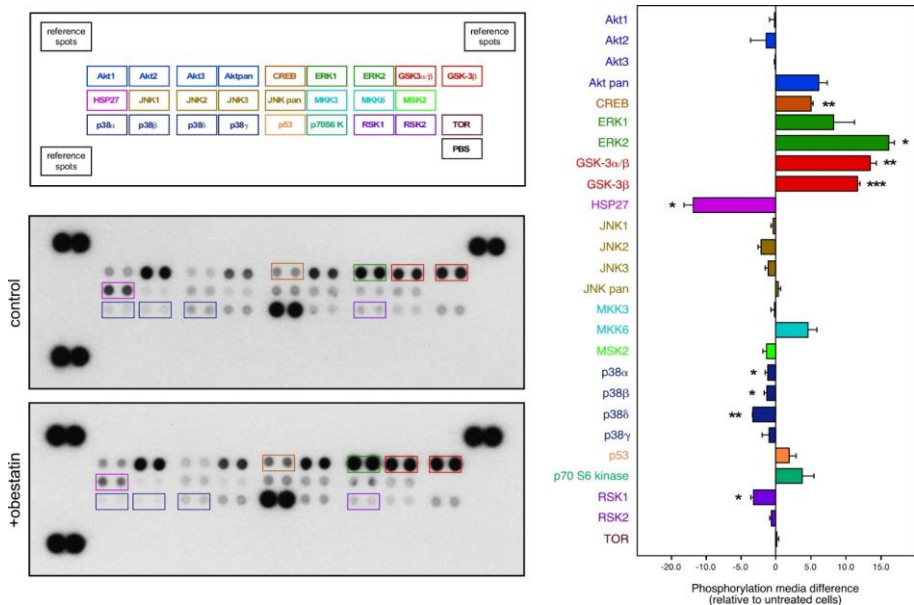


**Figure 3.14. Differential expression of phosphorylated MAPK in obestatin treated compared to untreated aRLT-PSCs.** Upper template showing the location of MAPK antibodies spotted onto the Human Phospho-MAPK Array Kit (Proteome ProfilerTM; R&D Systems). Lower template shows the detection of obestatin-modulated intracellular kinases (100 nM, 5 min). Out of the 26 MAPKs and other serine/threonine kinases analysed in the Phosphorylation of Human Phospho-MAPK Array Kit, 9 were differentially phosphorylated/dephosphorylated (P <0.05, P <0.01, P <0.001) in obestatin-treated compared to untreated RLT-PSCs. 200 μg of tissue lysate was run on each array.

To investigate the intracellular signalling pathways activated downstream of GPR39 in aRLT-PSC cells in response to obestatin (100

---

[185] Sun Y, Liu WZ, Liu T, *et al*. Signalling pathway of MAPK/ERK in cell proliferation, differentiation, migration, senescence and apoptosis. J Recept Signal Transduct Res. 2015;35:600-4.

nM, 5 min), the degree of the differential activation of MAPK proteins was analysed by a phospho-kinase array (**Figure 3.14**). CREB (~39.5%), ERK2 (~33.60%), glycogen synthase kinase-3 (GSK-3) α/β (~34.3%) and GSK-3β (~26.8%) exhibited increased phosphorylation following obestatin treatment (**Figure 3.14**). Additionally, the proteins HSP27 (~56.55%), p38α (~61.95%), p38β (~58.92%), p38δ (~56.86%) and RSK1 (~37.77%) were partially inhibited in response to obestatin. These data supported roles for obestatin/GPR39 system in multiple processes including cell growth, proliferation and survival.

To examine by western blot the activation/inhibition observed on the previous MAPK array, the aRLT-PSCs were stimulated with obestatin (100 nM) for the indicated times (5-120 min). **Figure 3.15** shows that Akt phosphorylation (measure as phosphorylation at S473 and T308) reached maximal levels at 30 and 10 min after obestatin stimulation, respectively (3.40 ± 0.49-fold and 2.47 ± 0.22-fold, respectively), keeping the sustained activity over control by 60 min (2.59 ± 0.40-fold phosphorylation at S473 and 1.82 ± 0.14-fold phosphorylation at T308). Akt (S473) maintained the activation sustained in time by at least 120 min (2.15 ± 0.57-fold); however, Akt (T308) recovered basal levels by 120 min (1.16 ± 0.35-fold).
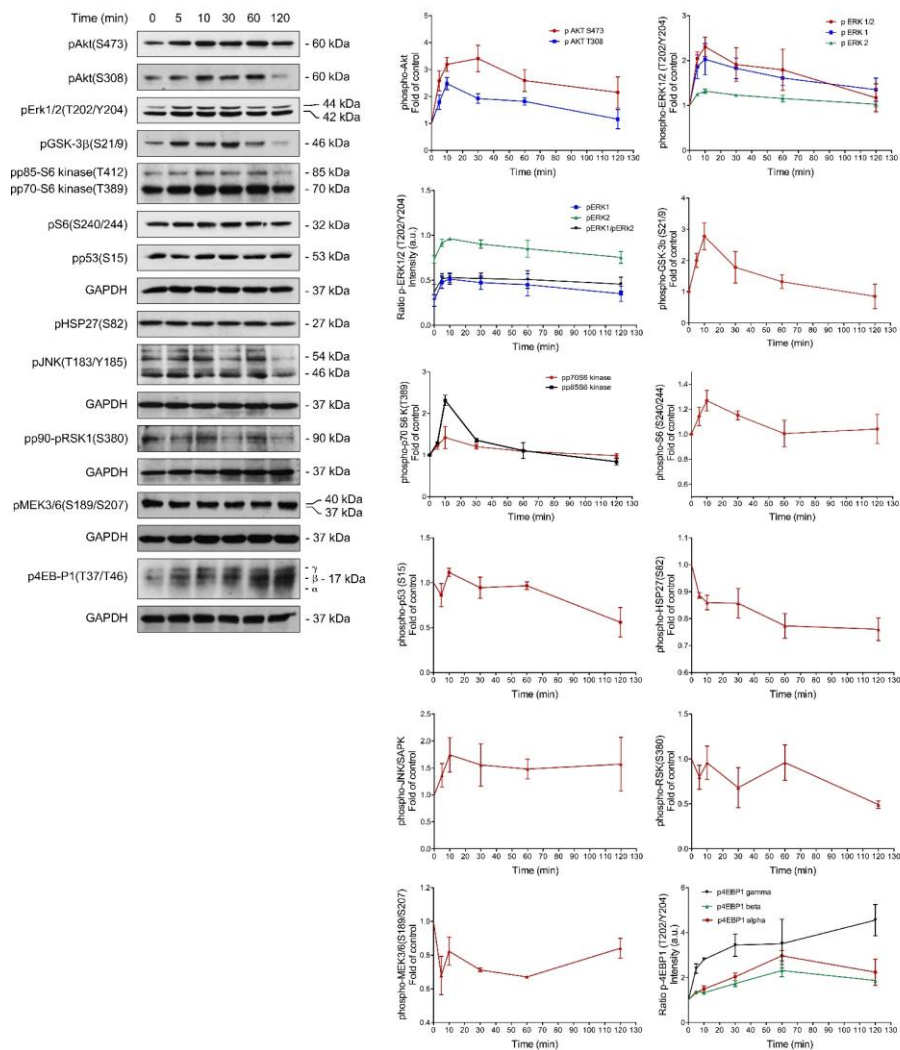
**Figure 3.15 Obestatin-activated intracellular signalling nodes in aRLT-PSCs.** WB analysis of pAkt (S308/S473), pERK 1/2 (T202/Y204), pp85-S6 kinase (T412), pp70-S6 kinase (T389), pS6 (S240/244), pGSK-3β (S219), pp53 (S15), p4EBP1(T202/Y204), pJNK(T183/Y185), pHSP27(S82), pp90-pRSK(S308), pMEK3/6(S189/S207) in aRLT-PSCs under treatment of obestatin (100 nM) at 5, 10, 30, 60, 120 min. The protein expression was normalized relative to GAPDH. The data were expressed as fold of control, obtained from intensity scans of three independent experiments.

Also ERK1/2, ERK1 and ERK2 phosphorylation reached maximal levels within 10 min of obestatin stimulation with a phosphorylation level of 2.31 ± 0.22-fold for ERK1/2, 2.03 ± 0.35-fold for ERK1 and 1.32 ± 0.046-fold for ERK2, keeping activated for 60 min to decrease to basal levels at 120 min. This pattern is reproduced in other proteins of the obestatin/GPR39 system-signalling pathway: pGSK-3β (S21/9), pp85-S6 kinase (T412), pp70-S6 kinase (T389), pS6 (S240/244), and pJNK/SAPK (T183/Y185) reaching its maximum phosphorylation at 10 min (2.78 ± 0.43-fold, 2.31 ± 0.12-fold, 1.42 ± 0.26-fold, 1.27 ± 0.081-fold, and 1.74±0.32, respectively). Phospho eukaryotic translation initiation factor 4E binding protein 1 (p4E-BP1) T202/Y204 suffered a different pattern of phosphorylation, 4E-BP1 γ form presented an upward phosphoryaltion during, at least, 120 min reaching phosphorylation levels of 4.56 ± 0.69-fold. α and β forms present an ascendant activation with a maximum at 60 min (2.32 ± 0.66-fold and 1.99±0.36-fold respectively) and decreasing levels at 120 min (1.75 ± 0.59-fold and 1.86 ± 0.014-fold respectively). Immunoblot analysis revealed a significant decrease in the phosphorylation levels of p-HSP27(S82), in a time-dependent manner, reaching a minimum at 60 min (0.77 ± 0.045-fold). Also pMEK3/6(S189/S207), pp53(S15), and pp90-pRSK(S308) presented a decrease in their phosphorylation by 0.67 ± 0.0006-fold, 0.56 ± 0.16-fold, and 0.46 ± 0.086-fold.

## OBESTATIN ACTIVATES CANONICAL WNT SIGNALLING PATHWAY
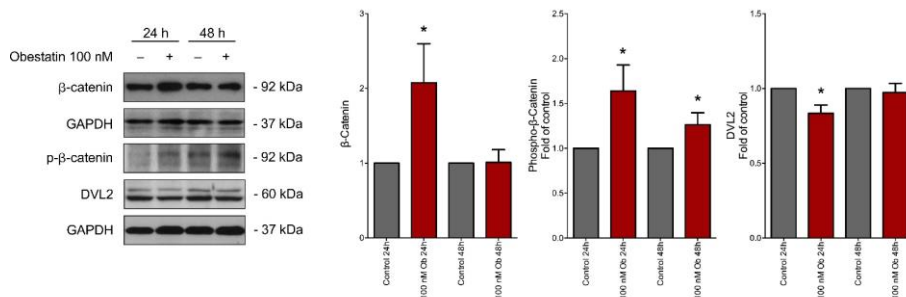


**Figure 3.16. The obestatin/GPR39 system controls canonical Wnt pathways on aRLT-PSC**. The aRLT-PSCs were stimulated with obestatin (100 nM) for 24 and 48 h, the blots were incubated with the corresponding antibodies: β-catenin, p-β-catenin and DVL2. The protein expression was normalized relative to GAPDH. The data were expressed as fold of control obtained from intensity scans of six independent experiments. The asterisk (*) denotes $P<0.05$ when comparing the treated with the untreated control group.

In recent years, it has been published that β-catenin is required for the establishment and maintenance of the acinar cell mass, extending from embryonic specification through juvenile and adult self-renewal and regeneration [186] . Due to the involvement of PSCs in pancreatic regeneration, we investigated the canonical Wnt signalling pathway in the RLT-PSC cells.

As shown in **Figure 3.16**, obestatin treatment (100 nM, 24 h) promotes a significant increase in the synthesis of β-catenin (2.25 ± 0.52-fold) and p-β-catenin (1.64 ± 0.50-fold and 1.26 ± 0.13-fold, at 24 h and at 48 h, respectively) in aRLT-PSC. On the contrary, DVL2 expression was decreased in response to obestatin treatment (0.83 ± 0.054-fold at 24 h).

---

[186] Keefe MD, Wang H, De La O JP, *et al.* β-catenin is selectively required for the expansion and regeneration of mature pancreatic acinar cells in mice. Dis Model Mech. 2012;5:503-14.

**OBESTATIN INFLUENCES THE POLARITY OF THE ARLT-PSC CELLS DIVISION**
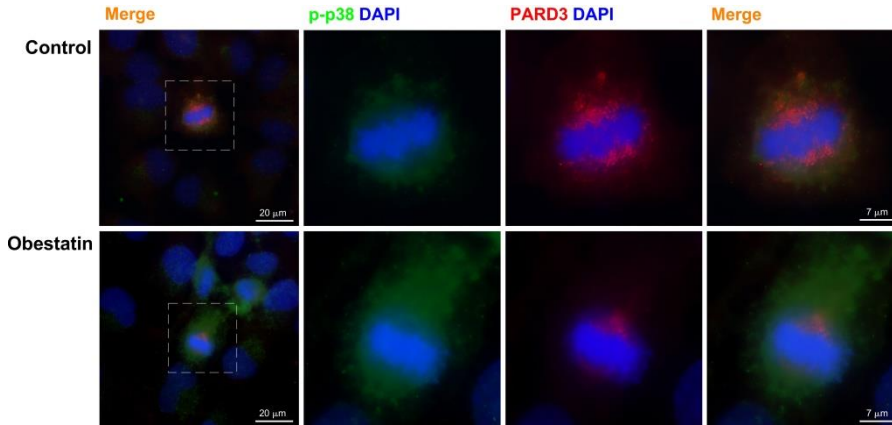


**Figure 3.17. Obestatin regulates the basal-apical division.** aRLT-PSCs were stimulated with obestatin (100 nM) for 6 h, and then assessed for p-p38 α/β/γ (green), PARD3 (red) and DAPI (blue) to visualize the nucleus by immunofluorescence. Scale bar= 20 μm. The images at the right represent a higher magnification view. Scale bar= 7 μm. Images are representative for at least three independent experiments.

As we reference above, the canonical Wnt signalling pathway (Wnt/b-catenin pathway) is required for stem cell expansion during regeneration in several systems[187,188]. Stem cells present two types of division, symmetrically to generate two stem cells, or asymmetrically to generate a stem cell, which retains self-renewal ability and differentiation potential, and one daughter cell that enters the path of differentiation[189]. P-p38α/β and Pard-3 participate in the asymmetric distribution of

---

[187]Reya T, Duncan AW, Ailles L, *et al.* A role for Wnt signalling in self-renewal of haematopoietic stem cells. Nature. 2003;423:409-14.
[188]Kalani MY, Cheshier SH, Cord BJ, *et al.* Wnt-mediated self-renewal of neural stem/progenitor cells. Proc Natl Acad Sci USA. 2008;105:16970-75.
[189]Potten CS, Loeffler M. Stem cells: Attributes, cycles, spirals, pitfalls and uncertainties. Lessons for and from the crypt. Development. 1990;110:1001-20.

intracellular proteins in satellite cells[190]. As **Figure 3.17** shows Pard-3 also presents a clearly asymmetric distribution in aRLT-PSC after obestatin treatment. In this first approximation, we use p-p38α/β/γ so we are not able to observe if the distribution of p-p38α/β is asymmetric or not. Additional experiments will be necessary to confirm this hypothesis.

[190] Troy A, Cadwallader AB, Fedorov Y, *et al*. Coordination of satellite cell activation and self-renewal by par-complex-dependent asymmetric activation of p38a/b MAPK. Cell Stem Cell. 2012;11:541-53.

# DISCUSSION

**CHAPTER 1**

In this study, we determined the expression of the obestatin/GRP39 system in human pancreas, both healthy and diseased. Firstly, we determined the location of GPR39 in human healthy pancreas, specifically defining the cellular location, and, second, we described the expression observed in several diseased conditions: CP, premalignant lesions and PC.

In healthy human pancreas, positive expression of obestatin was observed in some scattered cells in the periphery of the islets of Langerhans. Grönberg *et al* have already described this immunoreactivity for obestatin in an extensive analysis of the obestatin and ghrelin expression in human adult tissues. They also demonstrated by immunofluorescence that obestatin was synthesized by the ghrelin-producing cells in both stomach and pancreas[131]. No obestatin expression was observed in the diseased tissues studied so far.

Regarding GPR39 expression, it was detected mainly in the exocrine pancreas. The most intense positivity was observed in the acinar cells. In fact, Kapica *et al* reported that obestatin exogenous administration increased the protein content of the pancreatic juice, and therefore, the enzymatic content of it, namely, trypsin, amylase and lipase. The effect is dose-dependent and requires intact vagal supply, although a direct effect is also possible but with opposite consequences[100,191]. Indeed, the need of an intact vagal structure for a correct exocrine function was already demonstrated in humans over forty years ago[192]. These results are not conflicting with the expression found for GPR39 in our work as obestatin

---

[191] Kapica M, Puzio I, Kato I, *et al.* Exogenous obestatin affects pancreatic enzyme secretion in rat through two opposite mechanisms, direct inhibition and vagally-mediated stimulation. J Anim Feed Sci. 2018;27:155-62.

[192] McKelvey ST, Toner D, Connell AM, *et al.* Coeliac and hepatic nerve function following selective vagotomy. Br J Surg. 1973;60:219-21.

might increase the synthesis of these enzymes via the GPR39, but intact vagal connections are needed for a correct functioning and discharge of the exocrine pancreas. This relationship between the obestatin/GPR39 system and the pancreatic zymogens was not unexpected. Recently, we described the GPR39 expression in the chief cells of the oxyntic mucosa of the human stomach[117], and observed that exogenous administration of obestatin increased pepsinogen[90] and gastric lipase[91] release in an *in vitro* system of human stomach explants. The direct action of obestatin on pepsinogen and gastric lipase release is not inconsistent with a vagal control of the zymogenic secretion. Some residual and direct action on secretion must be needed to compensate vagus nerve blockade.

GPR39 expression was also found in the islets of Langerhans, with an uneven expression throughout the islets structure. The most intense expression was located in the glucagon positive cells, the α cells, and in some other scattered cells.

Glucagon and insulin are two molecules with opposite and collaborative functions to fine-tuning the glucose needs of the human body. Physiologically, glucagon stimulates insulin release to prepare the body for nutrients ingest, to stabilize glucose levels as soon as possible after a meal. At the preprandial state, ghrelin levels raise, the vagal nerve transmits the need of eating, but what is the meaning of the increase in obestatin circulating levels before a meal[193]? It might be that obestatin was the signal for the α-cells in the pancreas to produce glucagon, which in turns accomplished the glucogenolysis in the liver maintaining the balance in glucose levels until it is necessary further glucose uptake. Regarding this fact, and setting aside the differences between humans

---

[193] Beasley JM, Ange BA, Anderson CA, *et al.* Characteristics associated with fasting appetite hormones (obestatin, ghrelin, and leptin). Obesity (Silver Spring). 2009;17:349-54.

and the experimental model used[194,195], some work has been done in rat and mouse isolated pancreatic islets about obestatin effect on glucagon, insulin, SS and PP[96]. In the work of Qader *et al*, obestatin stimulated glucagon release and inhibited insulin, PP and SS secretion at physiologically relevant concentrations. Of especial interest is the observation that obestatin effects are similar to that of concomitant treatments with ghrelin and desacyl-ghrelin at physiological plasma concentrations. Also, and as it happens for the exocrine functioning of the pancreas, the need of an intact vagal structure for a correct glucagon and insulin release has been already demonstrated in humans[196].

Some scattered cells, both in the endocrine and the exocrine pancreas, presented immunoreativity for GPR39 and HSP47. HSP47 is considered a reliable marker for the PSCs[25]. PSCs present a dual effect: on one side, they synthesized ECM components[197,198]; and in the other side, they have a key function on the regeneration of the injured pancreas[25,37]. Several studies from Bukowczan group have demonstrated the regenerative properties of obestatin in the rat pancreas, although they do not demonstrate the mechanism by which obestatin or the obestatin/GPR39 system exerted this effect. They point out to the anti-inflammatory properties of this peptide[105].

One of the most intriguing facts of our results is the null GPR39 expression in the pancreatic ducts of healthy samples and the progressive

[194] Dolenšek J, Rupnik MS, Stožer A. Structural similarities and differences between the human and the mouse pancreas. Islets. 2015;7:e1024405.

[195] Skelin Klemen M, Dolenšek J, Slak Rupnik M, *et al*.The triggering pathway to insulin secretion: Functional similarities and differences between the human and the mouse β cells and their translational relevance. Islets. 2017;9:109-39.

[196] Russell RC, Thomson JP, Bloom SR. The effect of truncal and selective vagotomy on the release of pancreatic glucagon, insulin and enteroglucagon. Br J Surg. 1974;61:821-4.

[197] Apte MV, Pirola RC, Wilson JS: Battle-scarred pancreas: role of alcohol and pancreatic stellate cells in pancreatic fibrosis. J Gastroenterol Hepatol. 2006;3:S97-S101.

[198] McCarroll JA, Phillips PA, Santucci N, *et al*. Vitamin A inhibits pancreatic stellate cell activation: implications for treatment of pancreatic fibrosis. Gut. 2006;55:79-89.

increment of this expression in diseased tissues. CP itself did not presented positive ducts for GPR39 as GPR39 positivity was limited to the remaining non-fibrotic healthy-like tissue and to the increased number of PSCs; however the onset of a duct lesion, as a low grade PanIN, showed GPR39 in the ducts cells, with increasing intensity when the PanIN was surrounded by PC tissue. Within the PC tissue, GPR39 was aberrantly expressed in the cancer cells and the PSCs with an increasing intensity significantly correlated with the dedifferentiation of the tumour, even when two grades were present in the same pancreatic tissue, GPR39 immunoreactivity was equally correlated. Besides, GPR39 expression was augmented in the proliferation border of the tumour indicating a role for GPR39 in cancer cells growth. It was also found a positive GPR39 expression in the ganglion micrometastasis, supporting a role for this receptor in the metastatic process. These facts prompted us to postulate the use of this receptor as a marker of tumour progression and its applicability for antagonising the basic mechanisms associated to the development of PC. However, additional research is needed to clarify the way of action of the obestatin/GPR39 system and to define its potential as a therapeutic target in PC.

**CHAPTER 2**

In Chapter 1, we demonstrated the expression of GPR39 in PC and in related premalignant lesions. However, the aberrant GPR39 expression was found in the PDAC samples, with an increasing expression as the tumour dedifferentiates.

The main aim of this chapter was the study of obestatin effects on three human pancreatic cancer cell lines bearing the GPR39 receptor. The selected cell lines were three human pancreatic ductal adenocarcinoma

cell lines: PANC-1, RWP-1, BxPC3. The first one was established from an undifferentiated pancreatic carcinoma of ductal origin[199]. Regarding the second one, it derives form a moderately well differentiated ductal cell adenocarcinoma[141]. The latter cell line originated from a primary adenocarcinoma of the pancreas [200], which corresponds to a moderately well to poorly differentiated adenocarcinoma.

The results with these cell lines were unexpected. Our previous experience regarding gastric cancer showed the obestatin/GPR39 system as an endogenous system that controls and regulates processes as proliferation, migration, invasion, angiogenesis, skeleton reorganization and EMT. However, when analysing the pancreatic cancer cells, some intriguing results were observed. First of all, proliferation: obestatin does not activate BxPC3 proliferation. Previous work of our research group demonstrated that in a selected group of seven cancer cell lines from different tissues, which expressed GPR39, obestatin treatment activates proliferation in all of them[142]. In fact, the most intense proliferative effect was observed in the PANC-1 cell line, where EGFR was also found overexpressed together with a considerable expression of the mutant EGFRvIII. Then, what happens with BxPC3 cell line? The answer must be in the obestatin-signalling pathway of this system. The route to proliferation is mainly driven by the activation of Akt after EGFR transactivation. However, obestatin is not able to activate Akt in this cell line. The explanation to this must underlie in the amount of soluble EGFR that prevents Akt and the subsequent S6 phosphorylation, thus inhibiting proliferation. The antiproliferative effect is also observed in PANC-1 cells when stimulating with non-amidated obestatin, maybe through similar

---

[199] Lieber M, *et al.* Establishment of a continuous tumor-cell line (PANC-1) from a human carcinoma of the exocrine pancreas. Int. J. Cancer. 1975;15:741-7.
[200] Tan MH, Nowak NJ, Loor R, *et al.* Characterization of a new primary human pancreatic tumor line. Cancer Invest. 1986;4:15-23.

mechanisms. Some additional experiments are needed to clarify these points.

The other interesting data is the inhibition of the migration and the invasion observed in PANC-1 and BxPC3 cells. When analysing EMT, via E-cadherin and several mesenchymal markers as N-cadherin or vimentin, a change in behaviour is observed. While obestatin stimulated EMT in the adenocarcinoma gastric cancer cell line, the AGS cells, we observe the opposite effect in the pancreatic cancer cells, in other words, obestatin stimulates MET. This fact is also supported by the data of the metastatic suppressor nm23-H1, which diminishes after obestatin treatment. Moreover, in these conditions, E-cadherin expression increases in PANC-1 and BxPC3 cells, in the same way that occurs in incipient metastasis. Also, the cellular distribution resembles that of an epithelial cell. However, RWP-1 presents other behaviour, maybe due to the complex mixture of different cell populations.

A more detailed incursion in the signalling pathway of the obestatin/GPR39 system in PANC-1 cells shows that the cross-talk process, GPR39-EGFR, might involve some other RTK receptors as Axl or RYK; however, specific experiments should be performed to elucidate their contribution. Regarding EGFR, only phosphorylation in the residue Y1068 is observed after obestatin treatment. However, in the mutant EGFRvIII, phosphorylations on Y1068, Y1045 and mainly in Y845 are triggered by obestatin. Y845 is the target site of Src in the communication of both proteins. Y845 phosphorylation exerts an important role in cancer as well as in normal cells, regulating cell proliferation, cell cycle control, mitochondrial regulation of cell metabolism, and other cellular functions[201]. Moreover, not only Src is

---

[201] Sato K. Cellular Functions Regulated by Phosphorylation of EGFR on Tyr845 Int J Mol Sci. 2013;14:10761-90.

activated by obestatin but other SFKs as ACK, Hck and JAK2, as well as an inhibition in the phosphorylation of SYK (see the Results section for a detailed analysis). Obestatin also activates ERK1/2 and Akt in PANC-1 cells, the two main targets described in its route in gastric cancer cells. However, not only these conventional MAPKs are activated by this peptide. In fact, a protein array analysis showed the activation of other proteins as JNK, CREB, p38δ, and p53, although these results need subsequent validation.

As it was stated in the Results section, autophagy is a mechanism by which the cell eliminates superfluous or damaged proteins and organelles, thus regulating the homeostasis of the cell. In cancer, autophagy can have a dual effect: it can prevent the initiation of cancer in a chronic damage tissue, but also, can enhance the aggressiveness of cancer once it is initiated[202]. In this situation, the analysis of key molecules of the autophagic process in PANC-1 cells shows contradictory results. Although obestatin might increase autophagy, rise of cathepsin L and p62, a reduction is observed in the LC3 ratio. Recent studies have also demonstrated that p53, located outside the autophagy pathway, may greatly influence autophagy's role in PDAC growth. Specifically, the functional state of p53 (whether it is mutated or not) may determine whether autophagy promotes or inhibits PDAC growth. Although there is still controversy and further research in this field is necessary to clarify if mutations in p53 influence PDAC development, it seems that non-functional p53 diminishes the inhibitory effect that defective autophagy has on PDAC progression. It might be that the high activation of p53 promoted by obestatin could influence the exact role of these proteins in the autophagy process in PANC-1 cells.

---

[202] Chen HY, White E. Role of autophagy in cancer prevention. Cancer Prev Res. 2011;4:973-83.

In summary, the obestatin/GPR39 system is involved not only in the progression of pancreatic cancer, but also in the metastatic capability of this cancer. Some additional research is needed to validate this system as a therapeutic target in pancreatic cancer.

**CHAPTER 3**

The PSCs present a dual behaviour in the damaged pancreas: i) they are synthesizers of ECM; and, ii) they possess a role in the regeneration of the pancreatic tissue[25,37]. In Chapter 1, we demonstrated the expression of GPR39 in the human pancreatic stellate cells. In an in vitro model of these cells, the RLT-PSC cells, the obestatin/GPR39 system regulates processes as proliferation, migration and invasion, adhesion, as well as markers of EMT and proangiogenenic factors, and the activation of pathways involved in regeneration as the asymmetric division of PSCs. These data reveal the possible role of the obestatin/GPR39 system in the recovery of the damaged pancreas by activating the pancreatic stellate cells.

The PSCs are characterized by being a type of pluripotent cell, which comprises several different cell subpopulations on the basis of different cell surface markers [203,204].

Obestatin induces PSCs proliferation, migration, invasion, adhesion, EMT and the expression of the proangiogenic VEGF. Migration, invasion, EMT and adhesion are essential steps for the stellate cells to fulfil the regenerative process[205]. These effects are mediated by a kinase panel, in which ERK1/2 and Akt are the key signalling nodes. These facts agree

---

[203] Ikenaga N, Ohuchida K, Mizumoto K, *et al.* CD10+ pancreatic stellate cells enhance the progression of pancreatic cancer. Gastroenterology. 2010;139:1041-51.

[204] Birtolo C, Pham H, Morvaridi S, *et al.* Cadherin-11 is a cell surface marker up-regulated in activated pancreatic stellate cells and is involved in pancreatic cancer cell migration. Am. J. Pathol. 2017;187:146-55.

[205] Thiery JP, Acloque H, Huang RYJ, *et al.* Epithelial-mesenchymal transitions in development and disease. Cell. 2009;25,139:871-90.

with the previously described signalling for the obestatin/GPR39 system. Indeed, GPR39 activation by obestatin triggers two pathways in parallel: in one pathway ERK1/2 is activated by sequential activation of Gi, PI3K, and novel PKCε. This metabolic pathway is characterized mainly by its proliferative role. In parallel Akt is phosphorylated mediated by β-arrestin 1 signalling pathway and cross-activation of EGFR, S6K1 is the final protein of the signalling pathway triggering effects of cell growth, proliferation and differentiation[113].

One of the intriguing data obtained from this study is the obestatin effect on the constitutive formation of aggresomes in the stellate cells. Taking into account that these structures are transient microtubule-dependent inclusion bodies and are ultimately removed by autophagy, it would be expected to find a consequent increase in the autophagic flux. However, the analysis of the conventional autophagic marker LC3II together with the data of p62 and cathepsin L, did not show a clear effect in this process. Recent reports indicate that LC3II contributes to one type of autophagosome induced under stress, which is different from LC3I positive autophagosomes. Thus, autophagic flux can be activated independently of LC3II and, in this way, of the macroautophagy[206]. In line with previous reports, aggresome can understand as a way of clearance to achieve adequate cellular homeostasis, with the recruitment of vacuoles and lysosomes to their vicinity in order to facilitate the degradation following proteosoma inhibition[207,208]. Of great interest will be the identification of the proteins involved in aggresome formation after obestatin treatment.

[206] Yue Z, Jin S, Yang C, *et al.* Beclin 1, an autophagy gene essential for early embryonic development, is a haploinsufficient tumor suppressor. Proc Natl Acad Sci US. 2003;100:15077-82

[207] Koukourakis MI, *et al.* Autophagosome proteins LC3A, LC3B and LC3C have distinct subcellular distribution kinetics and expression in cancer cell lines. PLoS One. 2015;10:e0137675.

[208] Zaarur N, *et al.* Proteasome failure promotes positioning of lysosomes around the aggresome via local block of microtubule-dependent transport. Mol. Cell. Biol. 2014;34:1336-48.

The other interesting result is the observed vimentin structures after obestatin treatment. Obestatin seem to confine the vimentin networks to the central parts of the cells by internal crosslinking and anchoring to basal focal adhesion underlying the nucleus and thus moving the nucleus from the borders to the centre of the cell. This might lead to a mechanical stable vimentin cage-like structure encapsulating and immobilizing the nucleus, also colocalizing with actin patches. As it was mentioned in the Results section, this could have an involvement in stabilizing the inner structure of the cell for migration processes, but also could have an implication on the correct positioning of the nucleus for further divisions[209,210].

Wnt proteins include a major family of signalling molecules that play a critical role in several biological processes, including cell proliferation, migration, polarity establishment and stem cell self-renewal. In the canonical, or β-catenin-dependent, Wnt pathway, the dishevelled segment polarity protein 2 (Dvl2) is recruited by the receptor Frizzled and prevents the constitutive destruction of cytosolic β-catenin[211]. Binding of β-catenin with the transcription factors turn on the transcription of Wnt target genes. Indeed, Dvl interacts with some nuclear factors, such as Hipk1[212] and XNET[213]. These reports suggest the transcriptional function of Dvl in the nucleus. Therefore, it is likely that there are two pools of Dvl: one translocate to the nucleus to mediate the canonical signalling, and the other remains in the cytoplasm or moves to the plasma membrane to

[209] Wiche, G. and Winter, L. Plectin isoforms as organizers of intermediate filament cytoarchitecture. Bioarchitecture 2011;1:14-20.

[210] Wiche G, Osmanagic-Myers S, Castañon MJ. Networking and anchoring through plectin: a key to IF functionality and mechanotransduction. Curr. Opin. Cell Biol. 2015;32:21-29.

[211] Gao C, Chen YG. Dishevelled: The hub of Wnt signalling. Cell Signal. 2010;22:717-27.

[212] Louie SH, Yang XY, Conrad WH, *et al.* Modulation of the beta-catenin signalling pathway by the dishevelled-associated protein Hipk1. PLoS One. 2009;4:e4310.

[213] Miyakoshi A, Ueno N, Kinoshita N. Rho guanine nucleotide exchange factor xNET1 implicated in gastrulation movements during Xenopus development. Differentiation. 2004;72:48-55.

mediate both canonical and non-canonical signalling, upon Wnt stimulation. It is unclear how the nuclear localization of Dvl is regulated[211].

Wnt signalling pathway also involves GSK-3 activity. It is inhibited through phosphorylation of Ser21 in GSK-3α and Ser9 in GSK-3β. GSK-3α/β is phosphorylated by obestatin treatment in both Ser in aRLT-PSC cells and, thus, blocks its activity[214], which allows β-catenin to accumulate and to co-activate transcription in the nucleus. In addition, Wnt can also signal via Dvl to activate Rho/JNK planar cell polarity (PCP) as downstream effectors that control rearrangements in the cytoskeleton and gene expression. This pathway regulates cell polarity in morphogenetic processes in vertebrates[215,216]. Also, hepatic counterparts of aPSCs, the activated hepatic stellate cells (aHSCs), showed evidences for non-canonical signalling in these cells involving phosphorylation of Dvl2 and JNK[217]. As mentioned before, exposure of aRLT-PSCs to obestatin led to an induction of the active phosphorylated pJNK/SAPK (T183/Y185) and a downregulation of Dvl2, confirming the possibility of this non-canonical pathway activity.

In summary, the results obtained in this study indicate that obestatin/GPR39 system is an endogenous system, which regulates key processes related to the regenerative capacity of the pancreatic stellate cells.

---

[214] Schwarz-Romond T, Merrifield C, Nichols BJ, *et al*. The Wnt signalling effector Dishevelled forms dynamic protein assemblies rather than stable associations with cytoplasmic vesicles. J. Cell Sci. 2005;118:5269-77.

[215] Logan CY, Nusse R. The Wnt signalling pathway in development and disease. Annu Rev Cell Dev Biol. 2004;20:781-810.

[216] Angers S, Moon RT. Proximal events in Wnt signal transduction. Nat Rev Mol Cell Biol. 2009;10:468-77.

[217] Corbett L, Mann J, Mann DA. Non-canonical Wnt predominates in activated rat hepatic stellate cells, influencing HSC survival and paracrine stimulation of kupffer cells. PLoS ONE 2015;10:e0142794.

# CONCLUSIONS

**Chapter 1**

The expression of the obestatin/GPR39 system found in human pancreas indicates a possible regulatory role of the exocrine pancreas, as well as a possible mechanism in exocrine and endocrine pancreatic regeneration. The GPR39 expression in α-cells indicates a possible implication in the balance of blood glucose levels. Likewise, expressions found in pathological conditions (PC and PDAC) as well as in premalignant lesions (PanIN) would imply this system in the pathogenesis and/or clinical outcome of human pancreatic adenocarcinomas. These facts prompted us to postulate the use of this receptor as a marker of tumour progression and its applicability for antagonising the basic mechanisms associated to the development of PC.

**Chapter 2**

The obestatin/GPR39 system is involved in the proliferative, migratory, invasive, adhesion, metastatic and angiogenic processes, favouring the invasive phenotype in the tumour lines PANC-1, BxPC3 and RWP-1. Likewise, the obestatin/GPR39 system participates in the settlement of the tumour in the PANC-1 and BxPC3 cell line.

**Chapter 3**

The obestatin/GPR39 system is expressed in aRLT-PSC cells and regulates the proliferation, migration, invasion, and adhesion of these cells, as well as markers of EMT, angiogenesis, activation of pathways involved in regeneration and asymmetric division of aRLT-PSC. These data reveal that obestatin/GPR39 system is an endogenous system, which regulates key processes related to the regenerative capacity activating regenerative capacity of PSCs.

# RESUMEN

El páncreas humano es una glándula de forma cónica situada en el abdomen que se divide en 4 regiones; cabeza, cuello, cuerpo y cola. El páncreas tiene 2 funciones principales. La función exocrina, desempeñada por las células acinares que se encargan de la producción y secreción de enzimas digestivos (amilasa, lipasa, tripsina) y la función endocrina, desempeñada por los islotes de Langerhans, que se encarga de la producción de hormonas (insulina, glucagón, somatostatina, polipéptido pancreático y ghrelina) claves en el metabolismo energético.

El tejido pancreático humano rara vez se reseca, por lo que hay pocas oportunidades para que los patólogos observen su histología normal. Debido a este difícil acceso, en los últimos años son numerosos los ensayos realizados en rata y ratón. Aunque actualmente sabemos que algunos de los resultados obtenidos no pueden ser inmediatamente extrapolables a humanos, ya que entre el páncreas de ambas especies radican una serie de diferencias tanto a nivel estructural como celular. El órgano de rata presenta una estructura informe sin una división clara entre cabeza, cuello, cuerpo y cola. Además, el páncreas endocrino de ratón tiene una disposición y porcentaje de células endocrinas que no se corresponde con la humana.

Desde hace casi un siglo se conoce la importante regeneración que sufre el páncreas de rata/ratón. Debido a la dificultad para realizar estudios en páncreas humano, a día de hoy, todavía se desconocen los mecanismos moleculares que están implicados en dicha regeneración.

Actualmente, tanto en animales como en humanos, las investigaciones se centran principalmente en las fuentes de células encargadas de reparar el páncreas. Una de las fuentes celulares destacadas en la regeneración pancreática humana son las células estrelladas pancreáticas. Este tipo celular presenta características de célula pluripotente encontrándose localizada entre los acinos y ductos del

páncreas exocrino, así como entre las células de los islotes. En un páncreas normal, este tipo celular se presenta en estado quiescente y se activa ante estímulos externos de daño.

Las principales patologías del páncreas en la actualidad son la pancreatitis crónica (en España se estima una incidencia de 4,66 casos por $10^5$ habitantes/año) y el adenocarcinoma pancreático de origen ductal que afecta en Europa a $5,6/10^5$ habitantes/año. Las patologías pancreáticas vienen precedidas de lesiones premalignas como son neoplasia intraepitelial pancreática (PanIN), las neoplasias mucinosas papilares intraductales (IMPN) y los cistoadenomas mucinosos (MCN). Actualmente los principales factores ambientales de riesgo son el tabaquismo y abuso del alcohol, aunque estas enfermedades también presentan un componente genético.

El sistema obestatina/GPR39 tiene dos protagonistas principales, por una parte, la hormona obestatina, un péptido pequeño de 23 aminoácidos proveniente del mismo prepropéptido que la ghrelina. Por otra parte, su receptor, GPR39, es un receptor con 7 dominios transmembrana perteneciente a la familia de los GPCRs. Son numerosas las funciones que se le atribuyen tanto a GPR39 como a la obestatina. El sistema funciona como regulador de la proliferación, regeneración, diferenciación, migración e invasión en diversos sistemas. Ofrece protección frente a daños isquémicos y participa en la regulación de procesos apoptóticos e inflamatorios. Modula el metabolismo de la glucosa y metabolismo lipídico, entre otros. También, en sistemas patológicos como los adenocarcinomas gástricos humanos, se presenta un patrón de expresión aberrante para GPR39 que se correlaciona con la dediferenciación del tumor, lo que resalta la utilidad de GPR39 como un marcador pronóstico de estos tumores.

Con esta vista general, el principal objetivo de tesis fue definir el potencial del sistema obestatina/GPR39 como una diana terapéutica en pancreatitis crónica y cáncer de páncreas. Este objetivo se dividió en los dos siguientes puntos:

1. Estudio de la expresión del sistema de obestatina/GPR39 en los sistemas pancreáticos del estudio.

2. Estudio de la funcionalidad del sistema de obestatina/GPR39 en los sistemas pancreáticos del estudio.

Para el estudio del sistema obestatina/GPR39 y su posible función en el páncreas fue necesario describir y determinar la expresión del mismo en páncreas normal y patológico. Determinamos la expresión del sistema de obestatina/GRP39 en el páncreas humano, tanto normal como enfermo. En primer lugar, determinamos la ubicación del sistema en el páncreas normal, definiendo específicamente la ubicación celular y, en segundo lugar, describimos la expresión observada en pancreatitis crónica, lesiones premalignas y cáncer de páncreas.

En el páncreas humano normal, se observó una expresión positiva de obestatina en algunas células dispersas en la periferia de los islotes de Langerhans. Grönberg et al. ya habian descrito esta inmunorreactividad para la obestatina en tejidos humanos adultos. No se observó expresión de obestatina en los tejidos enfermos estudiados hasta el momento.

Respecto a la expresión de GPR39, la positividad más intensa se observó en las células acinares. De hecho, Kapica *et al.* ya habían descrito que la administración exógena de obestatina incrementaba el contenido de proteína del jugo pancreático y, por lo tanto, su contenido enzimático, a saber, tripsina, amilasa y lipasa. El efecto es dosis-dependiente y requiere suministro vagal intacto, aunque también es posible un efecto directo, pero con consecuencias opuestas. De hecho, la necesidad de una estructura vagal intacta para una función exocrina correcta ya se

demostró en los seres humanos hace más de cuarenta años. Estos resultados no están en conflicto con la expresión encontrada para GPR39 en nuestro trabajo, ya que la obestatina podría aumentar la síntesis de estas enzimas a través del GPR39, pero se necesitan conexiones vagales intactas para un correcto funcionamiento y descarga del páncreas exocrino. Esta relación entre el sistema obestatina/GPR39 y los zimógenos pancreáticos no fue inesperada. Recientemente, describimos la expresión de GPR39 en las células principales de la mucosa oxíntica del estómago humano y observamos que la administración exógena de obestatina incrementaba la liberación de pepsinógeno y lipasa gástrica en un sistema in vitro de explantes de estómago humano. La acción directa de la obestatina sobre el pepsinógeno y la liberación de la lipasa gástrica no es inconsistente con un control vagal de la secreción zimogénica. Se necesita alguna acción residual y directa sobre la secreción para compensar el bloqueo del nervio vago.

La expresión de GPR39 también se encontró en los islotes de Langerhans, con una expresión desigual en toda la estructura de los islotes. La expresión más intensa se localizó en las células positivas al glucagón, las células alfa, y en algunas otras células dispersas.

Glucagón e insulina son dos moléculas con funciones opuestas y colaborativas para equilibrar de forma exacta las necesidades de glucosa del cuerpo humano. Fisiológicamente, el glucagón estimula la liberación de insulina para preparar al cuerpo para la ingesta de nutrientes, para estabilizar los niveles de glucosa tan pronto como sea posible después de una comida. En el estado preprandial, los niveles de ghrelina aumentan, el nervio vago transmite la necesidad de comer, pero ¿cuál es el significado del aumento en los niveles circulantes de obestatina antes de una comida? Podría ser que la obestatina fuese la señal para que las células alfa en el páncreas produzcan glucagón, lo que a su vez lleva a

cabo la glucogenolisis en el hígado manteniendo el equilibrio de los niveles de glucosa hasta que sea necesario el almacenamiento posterior de glucosa. Con respecto a este hecho, y dejando de lado las diferencias entre los seres humanos y el modelo experimental utilizado, se ha realizado algún trabajo en islotes pancreáticos aislados de ratas y ratones sobre el efecto de la obestatina sobre la secreción de glucagón, insulina, somatostatina (SS) y polipéptido pancreático (PP). En el trabajo de Qader *et al*, la obestatina estimula la liberación de glucagón e inhibe la secreción de insulina, PP y SS en concentraciones fisiológicamente relevantes. Además, los efectos de la obestatina son similares a los de los tratamientos concomitantes con ghrelina y desacilghrelina en concentraciones plasmáticas fisiológicas. Además, y como sucede con el funcionamiento exocrino del páncreas, la necesidad de una estructura vagal intacta para una secreción correcta de glucagón e insulina ya se ha demostrado en los seres humanos.

A lo largo del estudio del sistema en tejidos pancreáticos, hallamos algunas células dispersas, tanto en el páncreas endocrino como en el exocrino, que presentaron inmunoreactividad para GPR39 y HSP47. HSP47 se considera un marcador fiable para las células estrelladas pancreáticas (PSCs). Como mencionamos anteriormente, las PSCs son sintetizadoras de la ECM y además tienen una función clave en la regeneración del páncreas dañado. Varios estudios del grupo de Bukowczan han demostrado las propiedades regenerativas de la obestatina en el páncreas de rata, aunque no demuestran el mecanismo por el cual la obestatina o el sistema de obestatina/GPR39 ejercen este efecto, señalando propiedades antiinflamatorias para la obestatina.

Uno de los hechos más intrigantes de nuestros resultados es la expresión nula de GPR39 en los conductos pancreáticos de muestras sanas y el incremento progresivo de esta expresión en los ductos de

tejidos enfermos. La pancreatitis crónica en sí misma no presentó conductos positivos para GPR39, ya que la positividad para GPR39 se limitó al tejido normal no fibrótico remanente y al mayor número de PSCs; sin embargo, la aparición de una lesión en el conducto, como es un PanIN de bajo grado, mostró la expresión de GPR39 en las células de los conductos, con una intensidad creciente cuando el PanIN estaba rodeado por tejido tumoral. Con respecto al cáncer de páncreas, el GPR39 se expresó de forma aberrante en las células cancerosas con una intensidad creciente que se correlaciona significativamente con la desdiferenciación del tumor, incluso en tejidos que presentan dos grados de diferenciación, la inmunorreactividad de GPR39 se correlaciona igualmente. Además, la expresión de GPR39 se incrementó en el borde de proliferación del tumor, lo que indica un papel para GPR39 en el crecimiento de células cancerosas. También se encontró una expresión positiva de GPR39 en la micrometástasis de los ganglios, lo que apoya el papel de este receptor en el proceso metastásico. Estos hechos nos llevaron a postular el uso de GPR39 como un marcador de la progresión del tumor y su aplicabilidad para antagonizar los mecanismos básicos asociados al desarrollo del PC. Sin embargo, se necesitan investigaciones adicionales para aclarar el modo de acción del sistema de obestatina/GPR39 y definir su potencial como diana terapéutica.

Tras demostrar el alto nivel de expresión del GPR39 en el tumor pancreático, y la correlación con la dediferenciación del tumor, estudiamos el efecto de la obestatina en tres líneas tumorales de adenocarcinoma pancreático de origen ductal: PANC-1, RWP-1, BxPC3. Los resultados con estas líneas celulares fueron inesperados. Nuestros datos previos con respecto al cáncer gástrico demostraron que el sistema de obestatina/GPR39 es un sistema endógeno que controla y regula procesos como la proliferación, migración, invasión, angiogénesis, la

reorganización del citoesqueleto y la EMT. Sin embargo, en células tumorales pancreáticas observamos resultados sorprendentes. En primer lugar, la obestatina no promueve la proliferación en la línea BxPC3. Los trabajos previos de nuestro grupo demostraron el efecto proliferativo de la obestatina en siete líneas tumorales de diferentes tejidos. De hecho, la línea tumoral con mayor proliferación fue PANC-1 en la que EGFR y el mutante EGFRvIII se hayan sobreexpresados. Entonces, ¿qué puede estar ocurriendo con BxPC3? La respuesta podría estar en la ruta de señalización de la obestatina. La vía proliferativa se desencadena mediante la activación de Akt a través de la transactivación de EGFR, pero, en esta línea celular, la obestatina es incapaz de activar Akt lo cual puede ser debido a la cantidad de EGFR soluble que impide dicha activación y consecuente fosforilación de S6, inhibiendo así la proliferación. El efecto antiproliferativo también se observa en las células PANC-1 cuando se estimula con obestatina no amidada, quizás a través de mecanismos similares, aunque se necesitan experimentos adicionales para aclarar este punto.

El otro dato interesante es la inhibición de la migración y la invasión observada en las células PANC-1 y BxPC3. Al analizar la EMT, mediante E-cadherina y varios marcadores mesenquimales como N-cadherina o vimentina, se observa un comportamiento contrario con respecto al estudiado anteriormente en las líneas tumorales gástricas. Es decir, la obestatina está promoviendo la MET. Este hecho lo respaldan los datos del supresor metastático nm23-H1, que disminuye tras el tratamiento con obestatina. Además, en estas condiciones, la expresión de E-cadherina aumenta en PANC-1 y BxPC3, de la misma manera que ocurre en la metástasis incipiente y la redistribucion celular se asemeja a la de una célula epitelial. Sin embargo, RWP-1 presenta otro comportamiento, tal vez debido a la compleja mezcla de diferentes subpoblaciones celulares.

Una incursión más detallada en la vía de señalización del sistema de obestatina/GPR39 en células PANC-1 muestra que el proceso de intercomunicación, GPR39-EGFR, podría involucrar a otros receptores RTK como Axl o RYK; sin embargo, se deben realizar experimentos específicos para dilucidar su contribución. Con respecto al EGFR, solo se observa fosforilación en el residuo Y1068 después del tratamiento con obestatina. Sin embargo, en el mutante EGFRvIII, la obestatina provoca las fosforilaciones en Y1068, Y1045 y principalmente en Y845. La fosforilación de Y845 ejerce un papel importante tanto en el cáncer como en las células normales, al regular la proliferación celular, el control del ciclo celular, la regulación mitocondrial del metabolismo celular y otras funciones celulares. La obestatina también activa ERK1/2 y Akt en las células PANC-1, las dos vías de señalización del sistema descritas en cáncer gástrico. No solo estas MAPK convencionales son activadas por este péptido, sino que otras proteínas como JNK, CREB, p38δ y p53 se ven activadas por obestatina.

La autofagia es un mecanismo por el cual la célula elimina restos proteicos y orgánulos con el fin de regular la homeostasis celular. En el cáncer, la autofagia puede tener un doble efecto: puede prevenir el inicio del cáncer en un tejido de daño crónico, pero también puede aumentar la agresividad del cáncer una vez que se inicia. En esta situación, el análisis de moléculas clave del proceso autofágico en células PANC-1 muestra resultados contradictorios. Aunque la obestatina podría aumentar la autofagia, ya que aumenta la catepsina L y p62, se observa una reducción en la proporción de LC3. Estudios recientes también han demostrado que p53, ubicada fuera de la vía de autofagia, puede influir enormemente en el papel de la autofagia en el crecimiento del PDAC. Específicamente, el hecho de que p53 esté mutado o no puede determinar que la autofagia promueva o inhiba el crecimiento del PDAC.

Todavía hay controversia y es necesario realizar más investigaciones en este campo para aclarar si las mutaciones en p53 influyen en el desarrollo de PDAC. En resumen, el sistema de obestatina/GPR39 está involucrado no solo en la progresión del cáncer pancreático, sino también en la capacidad metastásica de este tumor. Se necesita investigación adicional para validar este sistema como un objetivo terapéutico en el cáncer de páncreas.

Actualmente sabemos que el páncreas posee capacidad regenerativa, tanto para la parte exocrina como endocrina, pero debido a la falta de modelos in vitro apropiados y la difícil disponibilidad de muestras histológicas, el mecanismo molecular sigue siendo un gran desconocido. Además, en los últimos años se ha descrito la capacidad regenerativa de las PSCs. Este tipo celular participa en la regeneración pancreática tras una pancreatectomía parcial en ratas, e incluso en la regeneración temprana después de pancreatitis necrotizante aguda en humanos.

Paralelamente algunos estudios proponen que, sus homólogas, las células estrelladas hepáticas (HSCs) contribuyen a la regeneración del hígado, lo que sugiere que estas células representan una fuente de células progenitoras del hígado. Todo ello, junto con el efecto protector y regenerador descrito para la obestatina en la pancreatitis aguda inducida en ratas y, principalmente, el descubrimiento de las células GPR39$^+$/HSP47$^+$ en el páncreas humano, nos llevaron a estudiar la función reguladora del sistema obestatina/GPR39 en estas células pancreáticas.

Las PSCs se caracterizan por ser un tipo de célula pluripotente y por presentar un comportamiento dual en el páncreas dañado: por una parte, son sintetizadores de ECM y al mismo tiempo tienen un papel en la regeneración del tejido pancreático.

Tras demostrar la expresión de GPR39 en las células estrelladas pancreáticas en tejido humano, utilizamos un modelo in vitro de este tipo celular, las células RLT-PSC, y demostramos que el sistema obestatina/GPR39 regula procesos como la proliferación, migración e invasión, adhesión, así como marcadores de EMT y factores proangiogenénicos, y la activación de vías involucradas en la regeneración, como la división asimétrica. Estos datos revelan el posible papel del sistema de obestatina/GPR39 en la recuperación del páncreas dañado mediante la activación de las células estrelladas pancreáticas. Los cuatro primeros procesos son esenciales para llevar a cabo el proceso regenerativo. De hecho, la obestatina activa la ruta de señalización del sistema obestatina/GPR39 que desencadena la activación de la vía de ERK1/2 y la vía de Akt. Esta segunda vía transactiva a EGFR, y, finalmente, S6K1 lo que desencadena efectos de crecimiento celular, proliferación y diferenciación.

También observamos que el tratamiento con obestatina favorecía la formación de cajas de vimentina rodeando el núcleo. Esta reestructuración parece estar implicada en el anclaje del núcleo al eje central de la célula y, por lo tanto, mueve el núcleo desde los bordes de la célula hasta el centro de la misma. Este hecho podría formar parte la estabilización de la estructura interna de la célula para los procesos de migración, pero también podría tener una implicación en el posicionamiento correcto del núcleo para las divisiones celulares.

Las proteínas Wnt incluyen moléculas de señalización que desempeñan una serie de funciones críticas como son la proliferación celular, la migración, el establecimiento de la polaridad y la auto-renovación de las células madre. La ruta de señalización de Wnt también implica la actividad de GSK-3. Esta se inhibe por la fosforilación de Ser21 en GSK-3α y Ser9 en GSK-3β. El tratamiento con obestatina inhibe GSK-

3α/β y, por lo tanto, bloquea su actividad, lo que permite que la β-catenina se acumule y co-active la transcripción en el núcleo. Además, Wnt también puede indicar a través de Dvl la activación de Rho/JNK, implicados en la polaridad celular planar que controlan los reordenamientos en el citoesqueleto y la expresión génica. Además, sus homólogas, las células estrelladas hepáticas activadas mostraron evidencias de señalización no canónica que involucran la fosforilación de Dvl2 y JNK. Como se mencionó anteriormente, la exposición de aRLT-PSC a obestatina condujo a una inducción del pJNK/SAPK y una regulación a la baja de Dvl2, confirmando la posibilidad de esta actividad de la vía no canónica. Estos resultados indican que el sistema de obestatina/GPR39 es un sistema endógeno, que regula procesos clave relacionados con la capacidad regenerativa de las células estrelladas pancreáticas.

En conjunto, los resultados de esta tesis nos llevan a postular el uso de este receptor como un marcador de las condiciones precancerosas y la progresión tumoral en el PC, y su aplicabilidad para antagonizar los mecanismos básicos asociados al desarrollo del PC. Además, nuestros datos revelan el posible papel del sistema de obestatina/GPR39 en la recuperación del páncreas dañado, así como un aumento en el conocimiento del sistema del PC, clave para el desarrollo de moléculas moduladoras.

# ACKNOWLEDGEMENTS

La tesis doctoral es una etapa larga y en la que se necesita el trabajo y dedicación de un buen número de personas a las que me gustaría agradecer la confianza, apoyo y ayuda recibida a lo largo de estos años.

En primer lugar quiero agradecer a mis tres directores. Al Dr. Enrique Domínguez su amabilidad, preocupación y haberme facilitado estos últimos años. También quiero agradecer a la Dra. Rosalía Gallego, por su disposición y ser un ejemplo de enseñanza. A la Dra. Yolanda Pazos por, hacer que sea posible y valga la pena, gracias por el apoyo y la confianza puesta en mi para desarrollar este proyecto.

No me gustaría dejar aquí mis agradecimientos sin mencionar al Dr. Jesús Camiña, gracias por estar siempre disponible, por tus consejos, apoyo y asesoramiento.

Me gustaría agradecer al Dr. Matthias Löhr, al Dr. Ralf Jesenofsky y al Dr. Francisco Real por acceder a colaborar con este proyecto.

No me puedo olvidar del equipo de Anatomía Patológica, Dr. Tomás García-Caballero, Dr. Javier Caneiro y María Otero, no puedo hacer menos que agradeceros vuestro meticuloso trabajo, disponibilidad y palabras de ánimo.

A mis compañeros, a los que llegaron conmigo hasta el final y a los que ya volaron: Carlos, Mónica, Bego, Tania, Saúl, Jess y Gus. Muy difícil resumir aquí lo que cada uno de vosotros ya sabéis. A Carlos por haberme echado una mano. A Mónica, por tu alegría contagiosa. A Tania, por tu disponibilidad. Bego, gracias por enseñarme y haber sido un apoyo. A Saúl, porque me has mostrado mucho más allá de las vicisitudes del laboratorio. Jess, gracias una y mil veces por haberme dado la herramienta más valiosa que puede tener una mujer. Y a Gus, por enseñarme a ser más que una estudiante predoctoral, eres un ejemplo a seguir. Gracias a todos vosotros, por vuestro cariño y por los grandes momentos que hemos pasado juntos.

A mis amigas, Michelle, Sarita, Minia, Suiza y Sheila, gracias por no haberos olvidado nunca, os llevaré siempre conmigo.

A mis padres, Magdalena y Moncho, y a mis hermanos, Ramón y Pedro, gracias por haberme dado las herramientas para completar esta etapa, gracias por haberme enseñado a no rendirme.

# BIBLIOGRAPHY

1. Klimstra DS, Hruban RH & Pitman MB. (2012). Pancreas. In Mills, Stacey E. (Ed.), *Histology for Pathologists*. (4th ed., pp. 778-816). PA: Philadelphia. Lippincott Williams & Wilkins.

2. Moore KL. (1980). *Clinically oriented anatomy*. Baltimore. MD: Williams & Wilkins.

3. Akao S, Bockman DE, Lechene de la Porte P, *et al.* Three-dimensional pattern of ductuloacinar associations in normal and pathological human pancreas. Gastroenterology. 1986;90:661-8.

4. Kodama T. A light and electron microscopic study on the pancreatic ductal system. Acta Pathol Jpn. 1983;33:297-321.

5. Wittingen J, Frey CF. Islet concentration in the head, body, tail and uncinate process of the pancreas. Ann Surg. 1974;179:412-14.

6. Grube D, Bohn R. The microanatomy of human islets of Langerhans, with special reference to somatostatin (D-) cells. Arch Histol Jpn. 1983;46:327-53.

7. Stefan Y, Grasso S, Perrelet A, *et al.* The pancreatic polypeptide-rich lobe of the human pancreas: Definitive identification of its derivation from the ventral pancreatic primordium. Diabetologia. 1982;23:141-2.

8. Stefan Y, Orci L, Malaisse-Lagaeet F, *et al.* Quantitation of endocrine cell content in the pancreas of nondiabetic and diabetic humans. Diabetes. 1982;31:694-700.

9. Slack JMW. Developmental biology of the pancreas. Development. 1995;121:1569-80.

10. Baetens D, Malaisse-Lagae F, Perrelet A, *et al.* Endocrine pancreas: three-dimensional reconstruction shows two types of islets of langerhans. Science. 1979;206:1323-5.

11. Lehv M, Fitzgerald PJ. Pancreatic acinar cell regeneration. IV. Regeneration after resection. Am J Pathol. 1968;53:513-35.

12. Pearson KW, Scott D, Torrance B. Effects of partial surgical pancreatectomy in rats. I. Pancreatic regeneration. Gastroenterology. 1997;72:469-73.

13. Zhou Q, Melton DA, *et al.* Pancreas regeneration. Nature. 2018;557:351-8.

14. The English acronym will be used.

15. Bonner-Weir S, Baxter LA, Schuppin GT, *et al.* A second pathway for regeneration of adult exocrine and endocrine pancreas. A possible recapitulation of embryonic development. Diabetes. 1993;42:1715-20.

16. Xu X, D'Hoker J, Stangé G, *et al.* Beta cells can be generated from endogenous progenitors in injured adult mouse pancreas. Cell. 2008;132:197-207.

17. Inada A, Nienaber C, Katsuta H, *et al.* Carbonic anhydrase II-positive pancreatic cells are progenitors for both endocrine and exocrine pancreas after birth. Proc Natl Acad Sci US A. 2008;105:19915-19.

18. Criscimanna A, Speicher JA, Houshmand G, *et al.* Duct cells contribute to regeneration of endocrine and acinar cells following pancreatic damage in adult mice. Gastroenterology. 2011;141:1451-62.

19. Smukler SR, Arntfield ME, Razavi R, *et al.* The adult mouse and human pancreas contain rare multipotent stem cells that express insulin. Cell Stem Cell. 2011;8:281-93.

20. Li WC, Rukstalis JM, Nishimura W, *et al.* Activation of pancreatic-duct-derived progenitor cells during pancreas regeneration in adult rats. J Cell Sci. 2010;123:2792-802.

21. Zhou Q, Brown J, Kanarek A, *et al*. *In vivo* reprogramming of adult pancreatic exocrine cells to beta-cells. Nature. 2008;455:627-32.
22. Pan FC, Bankaitis ED, Boyer D, *et al*. Spatiotemporal patterns of multipotentiality in Ptf1a-expressing cells during pancreas organogenesis and injury-induced facultative restoration. Development. 2013;40: 751-64.
23. Thorel F, NeÂpote V, Avril I, *et al*. Conversion of adult pancreatic alpha cells to beta-cells after extreme beta-cell loss. Nature. 2010;464:1149-54.
24. Dor Y, Brown J, Martinez OI, *et al*. Adult pancreatic beta-cells are formed by self-duplication rather than stem-cell differentiation. Nature. 2004;429:41-6.
25. Ota S, Nishimura M, Murakami Y, *et al*. Involvement of Pancreatic Stellate Cells in Regeneration of Remnant Pancreas after Partial Pancreatectomy. PLoS ONE. 2016;11:e0165747.
26. Ziv O, Glaser B, Dor Y. The plastic pancreas. Dev Cell. 2013;26:3-7.
27. Migliorini A, Bader E, Lickert H. Islet cell plasticity and regeneration. Mol Metab. 2014;3:268-74.
28. Zha M, Xu W, Jones PM, *et al*. Isolation and characterization of human islet stellate cells. Exp Cell Res. 2016;34:61-6.
29. Lee E, Ryu GR, Ko SH, *et al*. Antioxidant treatment may protect pancreatic beta cells through the attenuation of islet fibrosis in an animal model of type 2 diabetes. BBRC. 2011;414:397-402.
30. Saito R, Yamada S, Yamamoto Y, *et al*. Conophyllin suppresses pancreatic stellate cells and improves islet fibrosis in Goto-Kakizaki rats. Endocrinology. 2012;153:621-30.
31. Datar SP, and Bhonde RR. Islet-derived stellate-like cells as a novel source for islet neogenesis in chicks. Poultry Science. 2009;88:654-60.
32. Yang J, Waldron RT, Su HY, *et al*. Insulin promotes proliferation and fibrosing responses in activated pancreatic stellate cells. AJP Gastrointestinal and Liver Physiology. 2016;311: G675-G687.
33. Habisch H, Zhou S, Siech M, *et al*. Interaction of Stellate Cells with Pancreatic Carcinoma Cells. Cancers. 2010;2:1661-82.
34. Phillips PA, McCarroll JA, Park S, *et al*. Rat pancreatic stellate cells secrete matrix metalloproteinases: implications for extracellular matrix turnover. Gut. 2003;52:275-82.
35. Omary MB, Lugea A, Lowe AW, *et al*. The pancreatic stellate cell: a star on the rise in pancreatic diseases. J Clin Invest. 2007;117:50-59.
36. Öhlund D, Handly-Santana A, Biffi G, *et al*. Distinct populations of inflammatory fibroblasts and myofibroblasts in pancreatic cancer. J Exp Med. 2017;214:579-96.
37. Mato E, Lucas M, Petriz L, *et al*. Identification of pancreatic stellate cell population with properties of progenitor cells: new role for stellate cells in the pancreas. Biochem J. 2009;421:181-91.
38. Zimmermann A, Gloor B, Kappeler A, *et al*. Pancreatic stellate cells contribute to regeneration early after acute necrotising pancreatitis in humans. Gut. 2002;51:574-8.
39. Bayan JA, Peng Z, Zeng N, *et al*. Crosstalk between activated myofibroblasts and β-cells in injured mouse pancreas. Pancreas. 2015;44:1111-20.

40. Fujiwara K, Ohuchida K, Mizumoto K, *et al.* CD271⁺ subpopulation of pancreatic stellate cells correlates with prognosis of pancreatic cancer and is regulated by interaction with cancer cells. PLoS One. 2012;7:e52682.

41. Hammad AY, Ditillo M, Castanon L. Pancreatitis. Surg Clin North Am. 2018;98:895-913.

42. Domínguez Muñoz JE, Lucendo Villarín AJ, Carballo Álvarez LF, *et al.* Spanish multicenter study to estimate the incidence of chronic pancreatitis. Rev Esp Enferm Dig. 2016;108:411-6.

43. Bosman FT, Carneiro F, Hruban RH & Theise ND. (2010). World Health Organization & International Agency for Research on Cancer. (4th ed.,). *WHO classification of tumours of the digestive system*. Lyon: International Agency for Research on Cancer.

44. Levi F, Bosetti C, Fernandez E, *et al.* Trends in lung cancer among young European women: the rising epidemic in France and Spain. Int J Cancer. 2007;121:462-5.

45. Iodice S, Gandini S, Maisonneuve P, *et al.* Tobacco and the risk of pancreatic cancer: a review and meta-analysis. Langenbecks Arch Surg. 2008;393:535-45.

46. Tramacere I, Scotti L, Jenab M, *et al.* Alcohol drinking and pancreatic cancer risk: a metaanalysis of the dose-risk relation. Int J Cancer. 2009;126:1474-86.

47. World Cancer Research Fund / American Institute for Cancer Research. Food, Nutrition, Physical Activity and the Prevention of Cancer: A global Perspective. Washington, DC: AICR, 2007.

48. Lowenfels AB, Maisonneuve P, Dimagno, *et al.* Hereditary pancreatitis and the risk of pancreatic cancer. International Herediary Pancreatitis Study Group. J Natl Cancer Inst. 1997;89:442-6.

49. Hruban RH, Pitman MB & Klimstra DS eds. (2007). *Tumors of the Pancreas*. Armed Forces Institute of Pathology: Washington, DC.

50. Solcia E, Capella C, & Klöppel G eds. (1997). *Tumours of the Pancreas*. Armed Forces Institute of Pathology: Washington, DC.

51. Holly EA, Chaliha I, Bracci PM, *et al.* Signs and symptoms of pancreatic cancer: a population-based case-control study in the San Francisco Bay area. Clin Gastroenterol Hepatol. 2004;2:510-17.

52. Chari ST, Leibson CL, Rabe KG, *et al.* Probability of pancreatic cancer following diabetes: a population-based study. Gastroenetrology. 2005;129:504-11.

53. Greenberg RE, Bank S, Stark B. Adenocarcinoma of the pancreas producing pancreatitis and pancreatic abscess. Pancreas. 1990;5:108-13.

54. Sohn TA, Yeo CJ, Cameron JL, *et al.* Resected adenocarcinoma of the pancreas-616 patients: results, outcomes, and prognostic indicators. J Gastrointest Surg. 2000;4:567-79.

55. Kayahara M, Nakagawara H, Kitagawa H, *et al.* The nature of neural invasion by pancreatic cancer. Pancreas. 2007;35:218-23.

56. Nagakawa T, Kayahara M, Ueno K, *et al.* Clinicopathological study on neural invasion to the extrapancreatic nerve plexus in pancreatic cancer. Hepatogastroenterology. 1992;39:51-5.

57. Fletcher CDM. (2013) *Diagnostic Histopathology of Tumors* (Volume 1) 4th ed. Philadelphia, US: Elsevier.

58. Edge BN, Byrd DR, Carducc MA, *et al.* (2010) *AJCC Cancer Staging Manual*, 7th ed. New York, US: Springer.

59. Klöppel G, Hruban RH, Longnecker DS, *et al.* (2000). Pathology and genetics of tumours of the digestive system. In: Hamilton SR, Aaltonen LA (Eds.). *Ductal adenocarcinoma of the pancreas*. (pp. 221-30). World Health Organization classification of tumours. Lyon, France: IARC Press.

60. Amin, MB, Edge SB, Greene FL, *et al.* (Eds.). (2017) *AJCC Cancer Staging Manual*. 8th ed. NY, US: Springer.

61. Urayama S. Pancreatic cáncer early detection: expanding higher-risk group with clinical and metabolomics parameters. World J Gastroenterol. 2015;21:1707-17.

62. Makhlouf HR, Almeida JL, Sobin LH. Carcinoma in jejunal pancreatic heterotropia. Arch Pathol Lab Med. 1999;123:707-11.

63. Carpelan-Holmström M, Nordling S, Pukkala E, *et al*. Does anyone survive pancreatic ductal adenocarcinoma? A nationwide study re-evaluating the data of the Finnish Cancer Registry. Gut. 2005;54:385-7.

64. Nagakawa T, Nagamori M, Futakami F, *et al.* Results of extensive surgery for pancreatic carcinoma. Cancer. 1996;77:640-5.

65. Morris JP, Wang SC, Hebrok M. KRAS, Hedgehog, Wnt and the twisted developmental biology of pancreatic ductal adenocarcinoma. Nat Rev Cancer. 2010;10:683-95.

66. Brat DJ, Lillemoe KD, Yeo CJ, *et al*. Progression of pancreatic intraductal neoplasias to infiltrating adenocarcinoma of the pancreas. Am J Surg Pathol. 1998;22:163-9.

67. Basturk O, Hong SM, Wood LD, *et al.* A revised classification system and recommendations from the Baltimore consensus meeting for neoplastic precursor lesions in the pancreas. Am J Surg Pathol. 2015;39:1730-41.

68. Li JB, Asakawa A, Cheng KC, *et al*. Biological effects of obestatin. Endocr. 2011;39:205-11.

69. Camina JP. Cell biology of the ghrelin receptor. J Neuroendocrinol. 2006;18:65-76.

70. McKee KK, Palyha OC, Feighner SD, *et al*. Molecular analysis of rat pituitary and hypothalamic growth hormone secretagogue receptors. Mol Endocrinol. 1997;11:415-23.

71. Ma X, Lin L, Qin G, *et al.* Ablations of Ghrelin and Ghrelin Receptor Exhibit Differential Metabolic Phenotypes and Thermogenic Capacity during Aging. PLoS ONE. 2011;6:e16391.

72. Zhang JV, Ren PG, Avsian-Kretchmer O, *et al*. Obestatin, a peptide encoded by the ghrelin gen, opposes ghrelin´s effects on food intake. Science. 2005;310:996-9.

73. Tang SQ, Jiang QY, Zhang YL, *et al*. Obestatin: Its physicochemical characteristics and physiological functions. Peptides. 2008;29:639-45.

74. Green BD, Grieve DJ. Biochemical properties and biological actions of obestatin and its relevance in type 2 diabetes. Peptides. 2018;100:249-59.

75. Alén BO, Nieto L, Gurriarán-Rodríguez U, *et al*. The NMR structure of human obestatin in membrane-like environments: insights into the structure-bioactivity relationship of obestatin. PLoS ONE. 2012;7:e45434.

76. Seoane LM, Al-Massadi O, Pazos Y, *et al*. Central obestatin administration does not modify either spontaneous or ghrelin-induced food intake in rats. J Endocrinol Invest. 2006;29:RC13-5.

77. Nogueiras R, Pfluher P, Tovar S, *et al*. Effects of obestatin on energy balance and growth hormone secretion in rodents. Endocrinology. 2007;148:21-6.

78. Sibilia V, Bresciani E, Lattuada N, *et al*. Intracerebroventricular acute and chronic administration of obestatin minimally affect food intake but not weight gain in the rat. J Endocrinol Invest. 2006;29:RC31-4.

79. Beasley MJ, Ange BA, Anderson CAM *et al*. Characteristics associated with fasting appetite hormones (obestatin, ghrelin, and leptin). Obesity (Silver Spring). 2009;17:349-54.

80. Harada T, Nakahara T, Yasuhara D, *et al*. Obestatin, acyl ghrelin, and des-acyl ghrelin responses to an oral glucose tolerance test in the restricting type of anorexia nervosa. Biol Psychiatry. 2008;63:245-7.

81. Camiña JP, Campos JF, Caminos JE, *et al*. Obestatin-mediated proliferation of human retinal pigment epithelial cells: regulatory mechanisms. J Cell Physiol. 2007;211:1-9.

82. Santos-Zas I, Gurriarán-Rodríguez U, Cid-Díaz T, *et al*. β-Arrestin scaffolds and signalling elements essential for the obestatin/GPR39 system that determine the myogenic program in human myoblast cells. Cell Mol Life Sci. 2016;73:617-35.

83. Santos-Zas I, Negroni E, Mamchaoui K, *et al*. Obestatin increases the regenerative capacity of human myoblasts transplanted intramuscularly in an immunodeficient mouse model. Mol Ther. 2017;25:345-59.

84. Alloatti G, Arnoletti E, Bassino E, *et al*. Obestatin affords cardioprotection to the ischemic-reperfused isolated rat heart and inhibits apoptosis in cultures of similarly stressed cardiomyocytes. Am J Physiol Heart Circ Physiol. 2010;299:H470-81.

85. Zhang MY, Li F, Wang JP. Correlation analysis of serum obestatin expression with insulin resistance in childhood obesity. Genet Mol Res. 2017;16(2) gmr16029210.

86. Zhang Q, Dong XW, Xia JY, *et al*. Obestatin plays beneficial role in cardiomyocyte injury induced by ischemia-reperfusion *in vivo* and *in vitro*. Med Sci Monit. 2017;23:2127-36.

87. Penna C, Tullio F, Femminò S, *et al*. Obestatin regulates cardiovascular function and promotes cardioprotection through the nitric oxide pathway. J Cell Mol Med. 2017;21:3670-8.

88. Li HQ, Wu YB, Yin CS, *et al*. Obestatin attenuated doxorubicin-induced cardiomyopathy via enhancing long noncoding Mhrt RNA expression. Biomed Pharmacother. 2016;81:474-81.

89. Sazdova IV, Ilieva BM, Minkov IB, *et al*. Obestatin as contractile mediator of excised frog heart. Cent Eur J Biol. 2009;4:327-34.

90. Unpublished results. Digestive Disease Week (DDW). Chicago, IL, US. MAY 06-09, 2017. Otero-Alen B, Leal-Lopez S, Estévez LS, *et al*.. The Obestatin/G Protein-Coupled Receptor 39 (GPR39) System in Human Stomach: Its Role on Pepsinogen I Secretion. Gastroenterology. 2017;152(5-S1):S911.

91. Unpublished results. Semana de las Enfermedades Digestivas. Valencia, Spain, 2018. Leal-Lopez S, Otero-Alen B, Estévez LS, *et al*. Papel del sistema obestatina/receptor acoplado a proteínas G 39 (GPR39) en la secreción de lipasa gástrica en estómago humano. Rev Esp Enferm Dig. 2018;110(Supl.1):239-240.

92. Chanoine JP, Wong AC, Barrios V: Obestatin, acylated and total ghrelin concentrations in the perinatal rat pancreas. Horm Res. 2006;66:81-88.

93. Granata R, Settanni F, Gallo D, *et al.* Obestatin promotes survival of pancreatic beta-cells and human islets and induces expression of genes involved in the regulation of beta-cell mass and function. Diabetes. 2008;57:967-79.
94. Pradhan G, Wu CS, Han Lee J, *et al.* Obestatin stimulates glucose-induced insulin secretion through ghrelin receptor GHS-R. Sci Rep. 2017;7:979.
95. Green BD, Irwin N, Flatt PR, et al. Direct and indirect effects of obestatin peptides on food intake and the regulation of glucose homeostasis and insulin secretion in mice. Peptides. 2007;28:981-7.
96. Qader SS, Håkanson R, Rehfeld, JF, *et al.* Proghrelin-derived peptides influence the secretion of insulin glucagon, pancreatic polypeptide and somatostatin: a study on isolated islets from mouse and rat pancreas. Regul Pept. 2008;146:230-7
97. Ren A, Guo Z, Wang YK, *et al.* Inhibitory effect of obestatin on glucose-induced insulin secretion in rats. Biochem Biophys Res Commun. 2008;369:969-72.
98. Egido EM, Hernández R, Marco J, *et al.* Effect of obestatin on insulin: glucagon and somatostatin secretion in the perfused rat pancreas. Regul Pept. 2009;152:61-6.
99. Favaro E, Granata R, Miceli I, *et al.* The ghrelin gene products and exendin-4 promote survival of human pancreatic islet endothelial cells in hyperglycaemic conditions, through phosphoinositide 3-kinase/ Akt, extracellular signal-related kinase (ERK)1/2 and cAMP/protein kinase A (PKA) signalling pathways. Diabetologia. 2012;55:1058-70.
100. Kapica M, Zabielska M, Puzio I, *et al.* Obestatin stimulates the secretion of pancreatic juice enzymes through a vagal pathway in anaesthetized rats - preliminary results. J Physiol Pharmacol. 2007;58:123-30.
101. Baragli L, Grande C, Gesmundo I, *et al.* Obestatin enhances *in vitro* generation of pancreatic islets through regulation of developmental pathways. PLoS One. 2013;8:e64374.
102. Kanat BH, Ayten R, Aydin S, *et al.* Significance of appetite hormone ghrelin and obestatin levels in the assessment of the severity of acute pancreatitis. Turk J Gastroenterol. 2014;25:309-13.
103. Ceranowicz P, Warzecha Z, A. Dembinski A, *et al.* Pretreatment with obestatin inhibits the development of cerulean induced pancreatitis. J PhysioL Pharmacol. 2009;60:95-101.
104. Bukowczan J, Warzecha Z, Ceranowicz P, *et al.* Pretreatment with obestatin reduces the severity of ischemia/reperfusion- induced acute pancreatitis in rats. Eur J Pharmacol. 2015;760:113-21.
105. Bukowczan J, Warzecha Z, Ceranowicz P, *et al.* Obestatin accelerates the recovery in the course of ischemia/reperfusion- induced acute pancreatitis in rats. PLoS ONE. 2015;10:E0134380.
106. Álvarez CJ, Lodeiro M, Theodoropoulou M, *et al.* Obestatin stimulates Akt signalling in gastric cancer cells through b-arrestin-mediated epidermal growth factor receptor transactivation. Endocr-Relat Cancer. 2009;16:599-611.
107. Manning BD, Cantley LC. Akt/PKB signalling: navigating downstream. Cell. 2007;129:1261-74.
108. Tremblay F, Perreault M, Klaman LD, *et al.* Normal food intake and body weight in mice lacking the G protein-coupled receptor GPR39. Endocrinology. 2007;148:501-6.

109. Egerod KL, Holst B, Petersen PS, *et al.* GPR39 splice variants versus antisense gene LYPD1: expression and regulation in gastrointestinal tract, endocrine pancreas, liver and white adipose tissue. Mol Endocrinol. 2007;21:1685-98.

110. Pacheco-Pantoja EL, Ranganath LR, Gallagher JA, *et al.* Receptors and effects of gut hormones in three osteoblastic cell lines. BMC Physiol. 2011;11:12-52.

111. Fontenot E, DeVente JE, Seidel ER. Obestatin and ghrelin in obese and in pregnant women. Peptides. 2007;28:1937-44.

112. Gurriarán-Rodríguez U, Al-Massadi O, Crujeiras AB, *et al.* Preproghrelin expression is a key target for insulin action on adipogenesis. J Endocrinol. 2011;210:R1-7.

113. Gurriarán-Rodríguez U, Santos-Zas I, Al-Massadi O, *et al.* The obestatin/GPR39 system is up-regulated by muscle injury and functions as an autocrine regenerative system. J Biol Chem. 2012;287:38379-89.

114. Gurriarán-Rodríguez U, Santos-Zas I, González-Sánchez J, *et al.* Action of obestatin in skeletal muscle repair: stem cell expansion, muscle growth, and microenvironment remodeling. Mol Ther. 2015;23:1003-21.

115. Holst B, Egerod KL, Jin C, *et al.* G-protein-coupled receptor 39 deficency is associated with pancreatic islet dysfunction. Endocrinology. 2009;150:2477-585.

116. McKee KK , Tan CP, Palyha OC, *et al.* Cloning and characterization of two human G protein-coupled receptor genes (GPR38 and GPR39) related to the growth hormone secretagogue and neurotensin receptors. Genomics. 1997;46:426-34.

117. Alén BO, Leal-López S, Otero Alén M, *et al.* The role of the obestatin/GPR39 system in human gastric adenocarcinomas. Oncotarget. 2015;7:5957-71.

118. Zhao H, Qiao J, Zhang S. GPR39 marks specific cells within the sebaceous gland and contributes to skin wound healing. Mol Endocr. 2007;7:1685-98.

119. Volante M, Rosas R, Ceppi P, *et al.* Obestatin in human neuroendocrine tissues and tumours: expression and effect on tumour growth. J Pathol. 2009;218:458-66.

120. Markowska A, Ziółkowska A, Jaszczyńska-Nowinka K, *et al.* Elevated blood plasma concentrations of active ghrelin and obestatin in benign ovarian neoplasms and ovarian cancers. Eur J Gynaecol Oncol. 2009;30:518-22.

121. Malendowicz W, Ziolkowska A, Szyszka M, *et al.* elevated blood active ghrelin and unaltered totalghrelin and obestatin concentrations in prostate carcinoma. Urol Int. 2009;83:471-5.

122. Xie F, Liu H, Zhu YH, *et al.* Overexpression of GPR39 contributes to malignant development of human esophageal squamous cell carcinoma. BMC Cancer. 2011;11:86.

123. Edge SB, Byrd DR, Compton CC, *et al.*, editors. AJCC cancer staging manual. 7th ed. New York: Springer-Verlag; 2009; 117-126.

124. Raghay K, Garcia-Caballero T, Bravo S, *et al.* Ghrelin localization in the medulla of rat and human adrenal gland and in pheochromocytomas. Histol Histopathol. 2008;23:57-65.

125. Gao Z, Wang X, Wu K, *et al.* Pancreatic stellate cells increase the invasion of human pancreatic cancer cells through the stromal cell-derived factor-1/CXCR4 axis. Pancreatology. 2010;10:186-193.

126. Almahariq M, Tsalkova T, Me F.C *et al.* A novel EPAC-specific inhibitor suppresses pancreatic cancer cell migration and invasion. Mol. Pharmacol. 83:122-128.

127. Gur S, Sikka SC, Abdel-Mageed AB, *et al.* Imatinib mesylate (Gleevec) induces human corpus cavernosum relaxation by inhibiting receptor tyrosine kinases (RTKs): identification of new RTK targets. Urology. 2013;82:745.

128. Jesnowski R, Fürst D, Ringel J, *et al.* Immortalization of pancreatic stellate cells as an *in vitro* model of pancreatic fibrosis: deactivation is induced by matrigel and N-acetylcysteine. Lab Invest. 2005;85:1276-91.

129. Wehr AY, Furth EE, Sangar V, *et al.* Analysis of the human pancreatic stellate cell secreted proteome. Pancreas. 2011;40:557-66.

130. Futterman S, Swanson D, Kalina RE. A new, rapid fluorometric determination of retinol in serum. Invest Ophthalmol. 1975;14:125.

131. Gronberg M, Tsolakis AV, Magnusson L, *et al.* Distribution of obestatin and ghrelin in human tissues: immunoreactive cells in the gastrointestinal tract, pancreas, and mammary glands. Journal of Histochemistry and Cytochemistry. 2008;56:793-801.

132. Nielsen MFB, Mortensen MB, Detlefsen S. Identification of markers for quiescent pancreatic stellate cells in the normal human pancreas. Histochem Cell Biol. 2017;148:359-380.

133. Apte MV, Haber PS, Applegate TL, *et al.* Periacinar stellate shaped cells in rat pancreas: identification, isolation, and culture. Gut. 1998;43:128-33.

134. Xu Z, Vonlaufen A, Phillips PA, *et al.* Role of Pancreatic Stellate Cells in Pancreatic Cancer Metastasis. Am J Pathol. 2010;177:2585-96.

135. Brown KE, Broadhurst KA, Mathahs MM, *et al.* Expression of HSP47, a collagen-specific chaperone, in normal and diseased human liver. Lab Invest. 2005;85:789-97.

136. Hruban RH, Maitra A, Goggins M. Update on pancreatic intraepithelial neoplasia. Int J Clin Exp Pathol. 2008;1:306-16.

137. Schlüter C, Duchrow M, Wohlenberg C, *et al.* The cell proliferation-associated antigen of antibody Ki-67: a very large, ubiquitous nuclear protein with numerous repeated elements, representing a new kind of cell cycle-mantaining proteins. J Cell Biol. 1993;123:513-22.

138. Klein WM, Hruban RH, Klein-Szanto AJ, *et al.* Direct correlation between proliferative activity and dysplasia in pancreatic intraepithelial neoplasia (PanIN): additional evidence for a recently proposed model of progression. Mod Pathol. 2002;15:441-7.

139. Gurriarán-Rodríguez U, Al-Massadi O, Roca-Rivada A, *et al.* Obestatin as a regulator of adipocyte metabolism and adipogenesis. J Cell Mol Med. 2011;15:1927-40.

140. Lieber M, Mazzetta J, Nelson-Rees W, *et al.* Establishment of a continuous tumor-cell line (panc-1) from a human carcinoma of the exocrine pancreas. Int. J. Cancer. 1975;15:741-7.

141. Dexter DL, Matook GM, Meitner PA, *et al.* Establishment and characterization of two human pancreatic cancer cell lines tumorigenic in athymic mice. Cancer Res. 1982;42:2705-14.

142. Alén BO. Fundamental structural and biochemical features for the obestatin/GPR39 system mitogenic action. Thesis dissertation. Univesdad de Santiago de Compostela, Santiago de Compostela, Spain. 2016. http://hdl.handle.net/10347/14993.

143. Marshall JC, Collins J, Marino N, *et al*. The Nm23-H1 metastasis suppressor as a translational target. Eur J Cancer. 2010;46:1278-82.

144. Tee YT, Chen GD, Lin LY, *et al*. Nm23-H1: a metastasis-associated gene. Taiwan J Obstet Gynecol. 2006;45:107-13.

145. Iizuka N, Tangoku A, Hazama S, *et al*. Nm23-H1 gene as a molecular switch between the free-floating and adherent states of gastric cancer cells. Cancer Lett. 2001;174:65-71.

146. Friess H, Guo XZ, Tempia-Caliera AA, *et al*. Differential expression of metastasis-associated genes in papilla of vater and pancreatic cancer correlates with disease stage. J Clin Oncol. 2001;19:2422-32.

147. De Wever O, Pauwels P, Craene B*, et al*. Molecular and pathological signatures of epithelial-mesenchymal transitions at the cancer invasion front. Histochem Cell Biol 2008;130:481-94.

148. Oyanagi J, Ogawa T, Sato H, *et al*. Epithelial-mesenchymal transition stimulates human cancer cells to extend microtubule-based invasive protrusions and suppresses cell growth in collagen gel. PLoS One. 2012;7:e53209.

149. Gradiz R, Silva HC, Carvalho L, *et al*. MIA PaCa-2 and PANC-1 - pancreas ductal adenocarcinoma cell lines with neuroendocrine differentiation and somatostatin receptors. Sci Rep. 2016;6:21648.

150. Aiello NM, Bajor DL, Norgard RJ, *et al*. Metastatic progression is associated with dynamic changes in the local microenvironment. Nat Commun. 2016;7:12819.

151. Ceausu AR, Ciolofan A, Cimpean AM, *et al*. The mesenchymal-epithelial and epithelial-mesenchymal cellular plasticity of liver metastases with digestive origin. Anticancer Res. 2018;38:811-6.

152. Grupp K, Melling N, Bogoevska V, et al. Expression of ICAM-1, E-cadherin, periostin and midkine in metastases of pancreatic ductal adenocarcinomas. Exp Mol Pathol. 2018;104:109-13.

153. Zetter BR. Angiogenesis and tumour metastasis. Annu Rev Med. 1998;49:407-24.

154. Wang, Z. Transactivation of epidermal growth factor receptor by G protein-coupled receptors: Recent progress, challenges and future research. Int J Mol Sci. 2016;17.pii:E95.

155. Park SJ, Gu MJ, Lee DS, *et al*. EGFR expression in pancreatic intraepithelial neoplasia and ductal adenocarcinoma. Int J Clin Exp Pathol. 2015;8:8298-304.

156. Halle C, Lando M, Svendsrud DH, *et al*. Membranous expression of ectodomain isoforms of the epidermal growth factor receptor predicts outcome after chemoradiotherapy of lymph node-negative cervical cancer. Clin Cancer Res. 201;17:5501-12.

157. Gan HK, Cvrljevic AN, Johns TG. The epidermal growth factor receptor variant III (EGFRvIII): where wild things are altered. FEBS J. 2013;280:5350-70.

158. Cunningham, PS. 2010. The ghrelin receptor isoforms (GHS-R1a and GHS-R1b) and GPR39: an investigation into receptor dimerization. University of Technology, Queensland, Australia. Doctoral dissertation. Queensland.
https://eprints.qut.edu.au/39443/1/Peter_Cunningham_Thesis.pdf

159. Zhang S, Yu D. Targeting Src family kinases in anti-cancer therapies: turning promise into triumph. Trends Pharmacol Sci. 2012;33:122-8.

160. Pazos Y, Alvarez CJ, Camiña JP, *et al.* Stimulation of extracellular signal-regulated kinases and proliferation in the human gastric cancer cells KATO-III by obestatin. Growth Factors. 2007;25:373-381.

161. Leconet W, Larbouret C, Chardès T, *et al.* Preclinical validation of AXL receptor as a target for antibody-based pancreatic cancer immunotherapy. Oncogene. 2014;33:5405-14.

162. Green J, Nusse R, van Amerongen R. The role of Ryk and Ror receptor tyrosine kinases in Wnt signal transduction. Cold Spring Harb Perspect Biol. 2014;6: pii: a009175.

163. Mahajan K, Coppola D, Chen YA, *et al.* Ack1 tyrosine kinase activation correlates with pancreatic cancer progression. Am J Pathol. 2012;180:1386-93.

164. Je DW, O YM, Ji YG, *et al.* The inhibition of SRC family kinase suppresses pancreatic cancer cell proliferation, migration, and invasion. Pancreas. 2014;43:768-76.

165. Layton T, Stalens C, Gunderson F, *et al.* Syk tyrosine kinase acts as a pancreatic adenocarcinoma tumor suppressor by regulating cellular growth and invasion. Am J Pathol. 2009;175:2625-36.

166. Takahashi R, Hirata Y, Sakitani K, *et al.* Therapeutic effect of c-Jun N-terminal kinase inhibition on pancreatic cancer. Cancer Sci. 2013;104:337-44.

167. Taniuchi K, Furihata M, Naganuma S, *et al.* BCL7B, a predictor of poor prognosis of pancreatic cancers, promotes cell motility and invasion by influencing CREB signalling. Am J Cancer Res. 2018;8:387-404.

168. Korc M. p38 MAPK in pancreatic cancer: finding a protective needle in the haystack. Clin Cancer Res. 2014;20:5866-8.

169. Del Reino P, Alsina-Beauchamp D, Escós A, *et al.* Pro-oncogenic role of alternative p38 mitogen-activated protein kinases p38γ and p38δ, linking inflammation and cancer in colitis-associated colon cancer. Cancer Res. 2014;74:6150-60.

170. Cicenas J, Kvederaviciute K, Meskinyte I, *et al.* KRAS, TP53, CDKN2A, SMAD4, BRCA1, and BRCA2 mutations in pancreatic cancer. Cancers (Basel). 2017;9:pii: E42.

171. Yoo SM, Cho SJ, Cho YY. Molecular targeting of ERKs/RSK2 signalling axis in cancer prevention. J Cancer Prev. 2015;20:165-71.

172. New M, Van Acker T, Long JS, *et al.* Molecular pathways controlling autophagy in pancreatic cancer. Front Oncol. 2017;7:28.

173. Lehv M, Fitzgerald PJ. Pancreatic acinar cell regeneration. IV. Regeneration after resection. Am J Pathol. 1977;53:513-35.

174. Pearson KW, Scott D, Torrance B. Effects of partial surgical pancreatectomy in rats. I. Pancreatic regeneration. Gastroenterology. 1997;72:469-73.

175. Masamune A, Shimosegawa T. Pancreatic stellate cells-multi-functional cells in the pancreas. Pancreatology. 2013;13:102-5.

176. Kordes C, Sawitza I, Götze S, *et al.* Hepatic stellate cells contribute to progenitor cells and liver regeneration. J Clin Invest. 2014;124:5503-15.

177. Ceranowicz P, Warzecha Z, Dembinski A, *et al.* Pretreatment with obestatin inhibits the development of cerulein-induced pancreatitis. J Physiol Pharmacol. 2009;60:95-101.

178. Forte E, Chimenti I, Rosa P, *et al*. EMT/MET at the Crossroad of Stemness, Regeneration and Oncogenesis: The Ying-Yang Equilibrium Recapitulated in Cell Spheroids. Cancers (Basel). 2017;9:98pii: E98.

179. Saghiri M.A, Asatourian A, Sorenson CM, *et al*. Role of Angiogenesis in Endodontics: Contributions of Stem Cells and Proangiogenic and Antiangiogenic Factors to Dental Pulp Regeneration. J Endod. 2015;41:797-803.

180. Lowery J, Kuczmarski ER, Herrmann H, *et al*. Intermediate Filaments Play a Pivotal Role in Regulating Cell Architecture and Function. J Biol Chem. 2015;290:17145-53.

181. Kopito RR, Sitia R. Aggresomes and Russell bodies. Symptoms of cellular indigestion? EMBO Rep. 2000;1:225-31.

182. Hyttinen JM, Amadio M, Viiri J, *et al*. Clearance of misfolded and aggregated proteins by aggrephagy and implications for aggregation diseases. Ageing Res Rev. 2014;18:16-28.

183. Bang Y, Kang BY, Choi HJ. Preconditioning stimulus of proteasome inhibitor enhances aggresome formation and autophagy in differentiated SH-SY5Y cells. Neurosci Lett. 2014;566:263-8.

184. Cid-Díaz T, Santos-Zas I, González-Sánchez J, *et al*. Obestatin controls the ubiquitin-proteasome and autophagy-lysosome systems in glucocorticoid induced muscle cell atrophy. Journal of Cachexia, Sarcopenia and Muscle 2017;8:974-90.

185. Sun Y, Liu WZ, Liu T, *et al*. Signalling pathway of MAPK/ERK in cell proliferation, differentiation, migration, senescence and apoptosis. J Recept Signal Transduct Res. 2015;35:600-4.

186. Keefe MD, Wang H, De La O JP, *et al*. β-catenin is selectively required for the expansion and regeneration of mature pancreatic acinar cells in mice. Dis Model Mech. 2012;5:503-14.

187. Reya T, Duncan AW, Ailles L, *et al*. A role for Wnt signalling in self-renewal of haematopoietic stem cells. Nature. 2003;423:409-14.

188. Kalani MY, Cheshier SH, Cord BJ, *et al*. Wnt-mediated self-renewal of neural stem/progenitor cells. Proc Natl Acad Sci USA. 2008;105:16970-75.

189. Potten CS, Loeffler M. Stem cells: Attributes, cycles, spirals, pitfalls and uncertainties. Lessons for and from the crypt. Development. 1990;110:1001-20.

190. Troy A, Cadwallader AB, Fedorov Y, *et al*. Coordination of satellite cell activation and self-renewal by par-complex-dependent asymmetric activation of p38a/b MAPK. Cell Stem Cell. 2012;11:541-53.

191. Kapica M, Puzio I, Kato I, *et al*. Exogenous obestatin affects pancreatic enzyme secretion in rat through two opposite mechanisms, direct inhibition and vagally-mediated stimulation. J Anim Feed Sci. 2018;27:155-62.

192. McKelvey ST, Toner D, Connell AM, *et al*. Coeliac and hepatic nerve function following selective vagotomy. Br J Surg. 1973;60:219-21.

193. Beasley JM, Ange BA, Anderson CA, *et al*. Characteristics associated with fasting appetite hormones (obestatin, ghrelin, and leptin). Obesity (Silver Spring). 2009;17:349-54.

194. Dolenšek J, Rupnik MS, Stožer A. Structural similarities and differences between the human and the mouse pancreas. Islets. 2015;7:e1024405.

195. Skelin Klemen M, Dolenšek J, Slak Rupnik M, *et al*. The triggering pathway to insulin secretion: Functional similarities and differences between the human and the mouse β cells and their translational relevance. Islets. 2017;9:109-39.

196. Russell RC, Thomson JP, Bloom SR. The effect of truncal and selective vagotomy on the release of pancreatic glucagon, insulin and enteroglucagon. Br J Surg. 1974;61:821-4.

197. Apte MV, Pirola RC, Wilson JS. Battle-scarred pancreas: role of alcohol and pancreatic stellate cells in pancreatic fibrosis. J Gastroenterol Hepatol. 2006;3:S97-S101.

198. McCarroll JA, Phillips PA, Santucci N, *et al*. Vitamin A inhibits pancreatic stellate cell activation: implications for treatment of pancreatic fibrosis. Gut. 2006;55:79-89.

199. Lieber M, *et al*. Establishment of a continuous tumor-cell line (PANC-1) from a human carcinoma of the exocrine pancreas. Int. J. Cancer. 1975;15:741-7.

200. Tan MH, Nowak NJ, Loor R, *et al*. Characterization of a new primary human pancreatic tumor line. Cancer Invest. 1986;4:15-23.

201. Sato K. Cellular functions regulated by phosphorylation of EGFR on Tyr845. Int J Mol Sci. 2013;14:10761-90.

202. Chen HY, White E. Role of autophagy in cancer prevention. Cancer Prev Res. 2011;4:973-83.

203. Ikenaga N, Ohuchida K., Mizumoto K., *et al*. CD10+ pancreatic stellate cells enhance the progression of pancreatic cancer. Gastroenterology. 2010;139:1041-51.

204. Birtolo C, Pham H, Morvaridi S, *et al*. Cadherin-11 is a cell surface marker up-regulated in activated pancreatic stellate cells and is involved in pancreatic cancer cell migration. Am. J. Pathol. 2017;187:146-55.

205. Thiery JP, Acloque H, Huang RYJ, *et al*. Epithelial-mesenchymal transitions in development and disease. Cell. 2009;25,139:871-90.

206. Yue Z, Jin S, Yang C, *et al*. Beclin 1, an autophagy gene essential for early embryonic development, is a haploinsufficient tumor suppressor. Proc Natl Acad Sci US. 2003;100:15077-82

207. Koukourakis MI, *et al*. Autophagosome proteins LC3A, LC3B and LC3C have distinct subcellular distribution kinetics and expression in cancer cell lines. PLoS One. 2015;10:e0137675.

208. Zaarur N, *et al*. Proteasome failure promotes positioning of lysosomes around the aggresome via local block of microtubule-dependent transport. Mol. Cell. Biol. 2014;34:1336-48.

209. Wiche G, Winter L. Plectin isoforms as organizers of intermediate filament cytoarchitecture. Bioarchitecture 2011;1:14-20.

210. Wiche G, Osmanagic-Myers S, Castañon MJ. Networking and anchoring through plectin: a key to IF functionality and mechanotransduction. Curr. Opin. Cell Biol. 2015;32:21-29.

211. Gao C, Chen YG. Dishevelled: The hub of Wnt signalling. Cell Signal. 2010;22:717-27.

212. Louie SH, Yang XY, Conrad WH, *et al*. Modulation of the beta-catenin signalling pathway by the dishevelled-associated protein Hipk1. PLoS One. 2009;4:e4310.

213. Miyakoshi A, Ueno N, Kinoshita N. Rho guanine nucleotide exchange factor xNET1 implicated in gastrulation movements during Xenopus development. Differentiation. 2004;72:48-55.

214. Schwarz-Romond T, Merrifield C, Nichols BJ, *et al*. The Wnt signalling effector Dishevelled forms dynamic protein assemblies rather than stable associations with cytoplasmic vesicles. J. Cell Sci. 2005;118:5269-77.

215. Logan CY, Nusse R. The Wnt signalling pathway in development and disease. Annu Rev Cell Dev Biol. 2004;20:781-810.

216. Angers S, Moon RT. Proximal events in Wnt signal transduction. Nat Rev Mol Cell Biol. 2009;10:468-77.

217. Corbett L, Mann J, Mann DA. Non-canonical Wnt predominates in activated rat hepatic stellate cells, influencing HSC survival and paracrine stimulation of kupffer cells. PLoS ONE 2015;10:e0142794.